



**Universiteit
Leiden**
The Netherlands

A balanced clock: network plasticity in the central mammalian clock

Olde Engberink, A.H.O.

Citation

Olde Engberink, A. H. O. (2022, June 30). *A balanced clock: network plasticity in the central mammalian clock*. Retrieved from <https://hdl.handle.net/1887/3421086>

Version: Publisher's Version

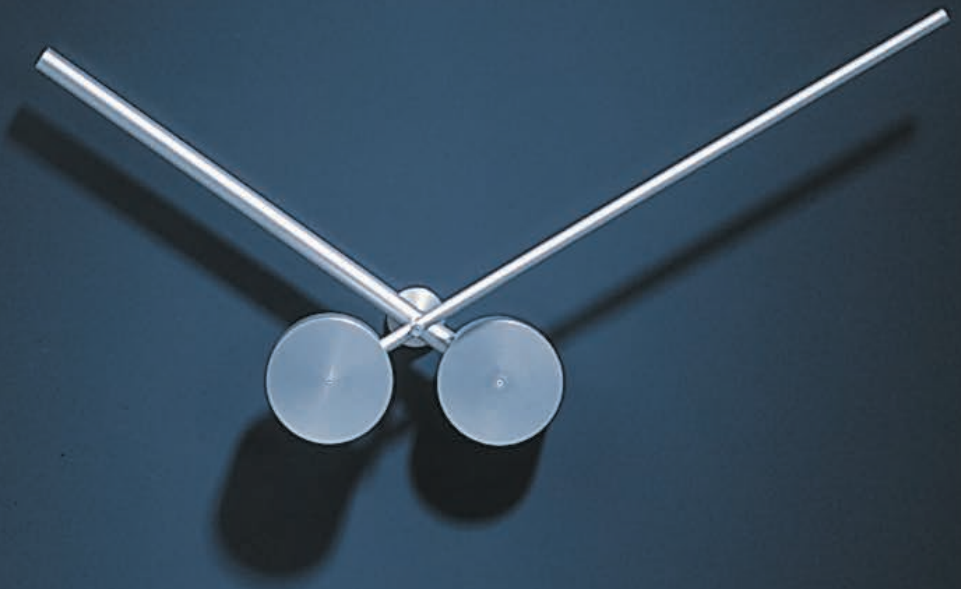
License: [Licence agreement concerning inclusion of doctoral thesis in the Institutional Repository of the University of Leiden](#)

Downloaded from: <https://hdl.handle.net/1887/3421086>

Note: To cite this publication please use the final published version (if applicable).

A BALANCED CLOCK

Network plasticity
in the central mammalian clock



Anneke H.O. Olde Engberink

A BALANCED CLOCK
Network plasticity in the central mammalian clock

Anneke H.O. Olde Engberink

The research described in this thesis was partly financially supported by the Velux Stiftung, Switzerland

ISBN: 978-94-93278-09-7

Cover picture: clock designed and created by WK Design, Veendam

Layout & Printing by Off Page, Amsterdam

Copyright © 2022 by Anneke H.O. Olde Engberink

No parts of this thesis may be reproduced in any form without prior permission of the author

A BALANCED CLOCK
Network plasticity in the central mammalian clock

Proefschrift

ter verkrijging van
de graad van doctor aan de Universiteit Leiden,
op gezag van rector magnificus prof.dr.ir. H. Bijl,
volgens besluit van het college voor promoties
te verdedigen op donderdag 30 juni 2022
klokke 13:45 uur

door

Anneke Hermina Octavia Olde Engberink
geboren te Eindhoven
in 1986

PROMOTOR

Prof. Dr. J.H. Meijer

CO-PROMOTOR

Dr. S. Michel

PROMOTIECOMMISSIE

Prof. Dr. O.C. Meijer

Dr. E.A. Tolner

Prof. Dr. H.W. Slabbekoorn

Prof. Dr. A. Kalsbeek [Amsterdam UMC]

Prof. Dr. C.S. Colwell [UCLA]

TABLE OF CONTENTS

Chapter 1	General introduction	7
Chapter 2	Brief light exposure at dawn and dusk can encode day length in the neuronal network of the mammalian circadian pacemaker	29
Chapter 3	Aging affects the capacity of photoperiodic adaptation downstream from the molecular clock	51
Chapter 4	Aging affects GABAergic function and calcium levels in mammalian central clock	79
Chapter 5	Chloride cotransporter KCC2 is essential for GABAergic inhibition in the SCN	99
Chapter 6	General discussion	117
Chapter 7	Summary	133
	Nederlandse samenvatting	139
	Dankwoord	145
	List of publications	147
	Curriculum vitae	149



one

GENERAL INTRODUCTION

From the earliest emergence of life, organisms have been exposed to a dynamic and constantly changing environment. Through evolutionary processes, species were able to adapt to these changes in order to survive and reproduce. One environmental factor that has hardly changed in time is the rotation of the earth around its axis and its annual orbit around the sun, generating daily and seasonal cycles, respectively. These rather constant environmental time cues in the geophysical environment allowed organisms to develop a clock that could time important events, like feeding and reproduction. Circadian timing mechanisms have a deep evolutionary history, first arising in prokaryotes such as cyanobacteria and (co-)evolved in almost all living species. These timing mechanisms comprise of endogenous circadian rhythms as well as an adaptive, time-measuring system.

Until the 18th century it was generally assumed that all behavioral rhythms were caused by environmental cues, like day light, temperature, and the magnetic field of the earth. In 1729 Jean-Jacques de Mairan observed, for the first time, an internal timekeeping mechanism in the mimosa plant. The plant followed the sunlight with its branches and leaves throughout the day. When de Mairan transferred the plant to constant darkness, the rhythmic movement of the plant continued. This surprising finding showed that external light is not necessary to maintain circadian rhythmicity (de Mairan, 1729). Two hundred years later, Maynard Johnson presented observations that mice showed a sustained activity rhythm with a period that deviated slightly from 24 hours when placed in constant darkness (Johnson, 1926). Johnson was the first researcher who established that mice are able to intrinsically regulate a rhythmicity of about 24 h. Since then, many researchers documented that organisms, ranging from unicellular to mammals, exhibit endogenous circadian rhythms (Pittendrigh, 1960; Cohen & Golden, 2015).

1. CIRCADIAN RHYTHMS

1.1. Entrainment

As mentioned above, without external timing cues circadian rhythms in behavior persist, thereby demonstrating the existence of an endogenous timing system. The period of this internal rhythm deviates slightly between individuals, and also between species, and is approximately one day (hence “circa”-“dian”). For instance, when a mouse is placed in a cage equipped with a running wheel in constant darkness, the wheel running rhythm will remain, but the mouse will start and stop running a few minutes earlier every cycle. This “free-running” rhythm displays the internal period of the mouse, which is often shorter than 24 h and referred to as “tau” (Figure 1). Despite their endogenous nature, circadian rhythms are responsive to light and darkness. Under natural conditions there is adaptation of the organisms circadian clock to the environmental cycle, thus matching internal time to the solar time. This is a key property of the circadian system and is known as “entrainment” (Pittendrigh & Daan, 1976), for review: (Golombek & Rosenstein, 2010).

The adaptive characteristic of the circadian system enables organisms to survive under changing conditions by anticipating periodic events, such as the availability of food. Light is the most important timing signal (“zeitgeber”) for keeping the internal circadian rhythms synchronized to the environmental 24 h cycle. There are, however, additional non-photoc

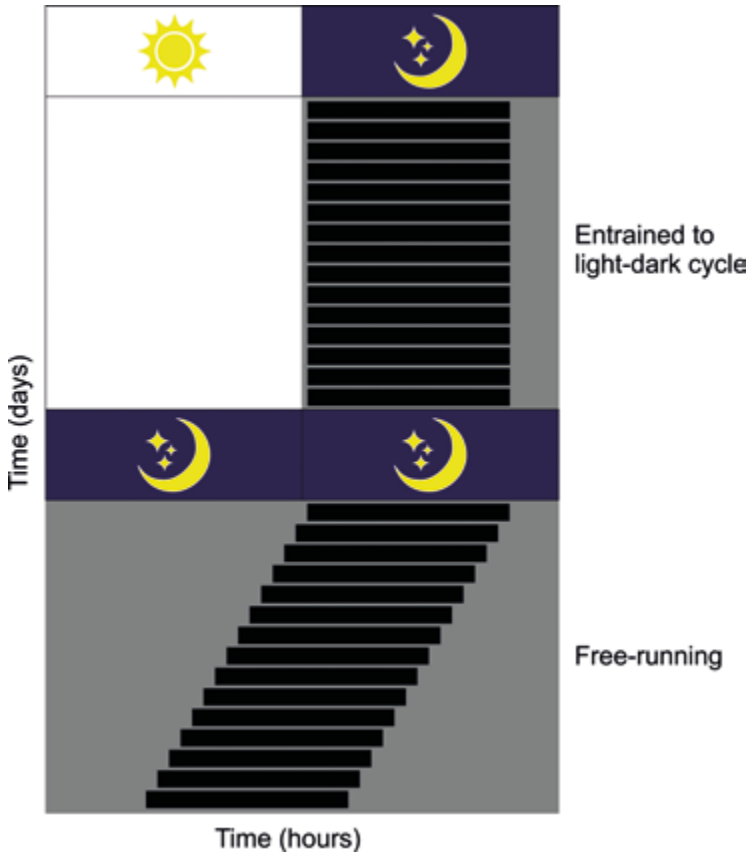


Figure 1. Circadian rhythm in behavioral activity of the mouse. Schematic representation of an actogram of the behavioral wheel running activity of a mouse. Consecutive days are plotted below each other. The black bars represent wheel running activity. In the upper half (first 15 days), the mouse is entrained to a light-dark cycle of LD 12:12. In the lower half (days 16-30), the mouse is placed in constant darkness and starts its “free-running” behavioral activity ~ 0.5 h earlier every day due to its internal period of 23.5 h.

zeitgebers, like environmental temperature, feeding cycles, and behavioral activity that provide input to the circadian clocks and can modulate its function (Hughes & Piggins, 2012; Lewis *et al.*, 2020). In contrast to the photic stimuli, non-photic zeitgebers generally have the opposite effect on the phase of the circadian clock. The generation of a timing signal by the mammalian clock is thus a complex interplay between photic and non-photic stimuli (Challet & Pevet, 2003).

1.2. Molecular clock

Circadian rhythmicity is driven by numerous clock genes that are expressed with a period of about 24 h. In 2017, the award of the Nobel Prize in Physiology or Medicine was awarded to Jeffrey C. Hall, Michael Rosbash, and Michael W. Young for their “discoveries of molecular mechanisms controlling the circadian rhythm” which is an acknowledgement of the fundamental importance

of circadian clocks (Callaway & Ledford, 2017). These three investigators unraveled the molecular pathway that controls the internal circadian rhythms in fruit flies (Bargiello *et al.*, 1984; Zehring *et al.*, 1984; Price *et al.*, 1998). Since that discovery, many studies were carried out to also identify the mammalian version of these genes (Shearman *et al.*, 1997; Gekakis *et al.*, 1998; Sangoram *et al.*, 1998). The unifying principle of cellular circadian timekeeping, in all organisms investigated, is based on self-sustained transcriptional-translational feedback loops (TTFLs).

In mammalian cells, the main loop starts when CLOCK proteins binds to BMAL1 proteins to form a dimer that binds to the E-box regions in the promotor of clock genes and thereby drive the daytime transcription of period (*Per1*, *Per2*, and *Per3*) and cryptochrome (*Cry1* and *Cry2*) genes (Buhr & Takahashi, 2013). Over the course of the day, the products of these genes, PER and CRY, accumulate and form dimers. These dimers translocate back into the nucleus of the cell where they suppress CLOCK-BMAL1 activity at their own E-boxes. During the night, subsequent degradation of PER and CRY allows the CLOCK-BMAL1 dimers to eventually start the cycle again. This core TTFL is stabilized and enhanced by additional negative and positive feedback loops. For instance, CLOCK and BMAL1 drive E-box mediated circadian expression of the nuclear receptors ROR α , REV-ERB α , and REV-ERB β which in turn act via REV response element (RRE) sequences to activate and suppress BMAL1 transcription, respectively (Lowrey & Takahashi, 2004; Hastings *et al.*, 2018). In addition, oscillations in cytosolic signaling molecules, like cAMP and Ca²⁺, interact with the different TTFLs to further stabilize and tune the cellular molecular clocks (Hastings *et al.*, 2008). The TTFL is highly conserved across species and present in almost all mammalian cell types providing local timing systems in most tissues (Reppert & Weaver, 2001). However, these peripheral clocks are like instruments in an orchestra, which are directed by a conductor. In mammals, this conductor is the central circadian clock which is located in the brain.

2. CENTRAL CIRCADIAN CLOCK IN MAMMALS: THE SUPRACHIASMATIC NUCLEUS

First evidence for the location of the mammalian biological clock was found independently in 1972 by two laboratories. Both research groups lesioned the brain region in the anterior hypothalamus, directly above the optic chiasm; the suprachiasmatic nucleus (SCN), which caused the disappearance of behavioral rhythms in drinking and running activity (Stephan & Zucker, 1972) and in corticosterone production by the adrenal gland (Moore & Eichler, 1972). Although these studies demonstrated that an intact SCN was necessary for the expression of circadian rhythms, they did not fully prove that the SCN was the location of the central mammalian pacemaker. Actual evidence came a few years later when another important study performed *in vivo* electrophysiological recordings in the SCN. The electrical activity in the SCN appeared rhythmic with high activity during the day and low during the night while surrounding tissue was oscillating in antiphase. When the SCN was completely isolated from the rest of the tissue, the surrounding tissue lost their rhythmicity, while the SCN remained rhythmic (Inouye & Kawamura, 1979). After this pivotal study that drove neurophysiological studies in the SCN, three different research groups demonstrated in 1982 that the SCN could be isolated in brain slices and that the rhythmicity in electrical activity remained

(Green & Gillette, 1982; Groos & Hendriks, 1982; Shibata *et al.*, 1982). These findings indicated that the SCN does not require rhythmic input, but remains oscillating endogenously, also when kept in constant conditions. The most conclusive evidence that the SCN are indeed the site of the mammalian circadian pacemaker came more than a decade later by transplantation studies in which restoration of circadian rhythmicity was observed after transplantation of fetal SCN tissue in arrhythmic hamsters whose own SCN had been ablated. Moreover, using tau mutant hamster as donors, the free running period length of the host wild type hamster (ca 24 h) was changed to the one of the donor (20 h) (Ralph *et al.*, 1990; Silver *et al.*, 1996).

2.1. Anatomical and functional organization of the SCN

The SCN is located in the anterior hypothalamus, directly above the optic chiasm and bilateral to the third ventricle, and consists of two connected nuclei. Each nucleus consists of about 10,000 neurons and is subdivided into a “core” and “shell” based on the distribution of peptide phenotypes and efferent and afferent connectivity (Moore, 1996).

The ventrolateral core contains vasoactive intestinal polypeptide (VIP) and gastrin releasing peptide (GRP) and receives direct light input through the retinohypothalamic tract (RHT). The dorsomedial shell contains a large number of arginine vasopressin (AVP) producing cells and receives input from the SCN core, and limbic, hypothalamic, and brainstem nuclei (Abrahamson & Moore, 2001). Additionally, almost all SCN neurons express γ -aminobutyric acid (GABA) receptors. Anatomical studies generally support a neuropeptide-based classification of the SCN subtypes (Leak *et al.*, 1999; Abrahamson & Moore, 2001; Masumoto *et al.*, 2006). However, the functional heterogeneity within the SCN network is more complicated (Morin, 2007). New SCN cell types were discovered by studying single cell transcriptional heterogeneity, which led to new interpretations of the functional variability and connectivity of SCN neurons (Park *et al.*, 2016). The majority of VIP and AVP neurons co-express the neuropeptide neuromedin S (NMS), which has shown to dictate circadian period length and is required for the generation of behavioral rhythms. The detection of NMS cells as a population of pacemaking neurons allows for better targeting of treatment of circadian dysfunction (Lee *et al.*, 2015).

The SCN exhibits precise and high-amplitude rhythms in electrical activity and communicates this time information to the rest of the brain and body. Regardless of whether an organism is diurnal (day-active) or nocturnal (night-active), the ensemble electrical discharge in the SCN is high during the day and low during the night (Meijer *et al.*, 1997; Caldelas *et al.*, 2003). When the retina is exposed to light, the membrane potential of retinorecipient SCN cells are sufficiently depolarized to generate action potentials. Apart from these light-induced potential changes, SCN cells exhibit circadian rhythms in spontaneous firing frequencies (Webb *et al.*, 2009). The neurons of the SCN have this unique property of generating spontaneous action potentials for about 4-6 hours each day, usually during the daytime (Schaap *et al.*, 2003; Brown *et al.*, 2006; VanderLeest *et al.*, 2007). Several currents account for this daily rhythm in action potential generation, like persistent Na^+ currents, L-type Ca^{2+} currents, hyperpolarization-activated currents (I_h), large-conductance Ca^{2+} activated K^+ (BK) currents, and fast delayed rectifier (FDR) K^+ currents (Brown & Piggins, 2007; Colwell, 2011; Harvey *et al.*, 2020). The electrical activity of the individual SCN neurons will together

generate an ensemble electrical signal, which will be corrected in phase by the retinorecipient cells in order to align the SCN output signal to the external zeitgeber cycles.

2.2. The SCN as a neuronal network

When dispersed in culture, individual SCN neurons can maintain cell-autonomous circadian cycles in gene expression, intracellular calcium concentration, and neuronal firing rate (Noguchi *et al.*, 2017). However, these cells often form only erratic networks. As a result the rhythms are more sloppy and the isolated neurons show independent free-running rhythms with a large variation in period length (Welsh *et al.*, 1995; Herzog *et al.*, 2004). When the network maintains more intact, like in organotypic slices (Tominaga *et al.*, 1994), the ensemble rhythmic output of the SCN is more precise and the phases of individual cells are better synchronized. Communication and synchronization between SCN cells are key for generating a coherent, stable, and high amplitude output rhythm and enable the circadian system to adapt to environmental changes. Some SCN neurons are electrically coupled by gap junctions (Colwell, 2000; Long *et al.*, 2005), but all cells communicate via transmissions of action potentials after which neurochemicals like VIP and GABA are released. In addition, neuroendocrine signaling, i.e. the release of neurohormones like GRP and AVP, is an important communication factor in the SCN (Mohawk & Takahashi, 2011; Maywood, 2018; Astiz *et al.*, 2019).

VIP signaling is critically important for synchronization among the SCN neurons as loss of VIP (VIP/PHI^{-/-}) or the gene encoding its receptor in the SCN, VPAC2 (*Vipr2*^{-/-}), leads to weakened circadian rhythmicity in electrical activity and amplitude, gene expression, and metabolism (Vosko *et al.*, 2007). Moreover, the SCN loses its synchrony to environmental light cues and behavioral rhythms in VIP/PHI^{-/-} and *Vipr2*^{-/-} mice are disrupted (Harmar *et al.*, 2002; Colwell *et al.*, 2003; Aton *et al.*, 2005; Maywood *et al.*, 2006; Brown *et al.*, 2007; Sheward *et al.*, 2007; Lucassen *et al.*, 2012).

Almost all SCN neurons contain GABA as a neurotransmitter (Moore & Speh, 1993; Abrahamson & Moore, 2001; Belenky *et al.*, 2008), but in contrast to the advanced knowledge of the role of VIP in SCN synchronization, the role of GABAergic signaling in the SCN is still subject of debate (Ono *et al.*, 2018). GABA was initially reported to synchronize rhythms in electrical activity in dispersed clock cells by daily application of GABA (Liu & Reppert, 2000). Moreover, GABAergic signaling proved to be necessary for coupling between the ventral and dorsal part of the SCN after a shift in the light-dark cycle (Albus *et al.*, 2005). But, on the other hand, GABA antagonist have shown to increase the amplitude of PER2::LUC rhythms by reducing the phase distribution of the individual SCN cells (Aton *et al.*, 2006). Additionally, inhibition of GABA_A signaling using gabazine decreased period variability in cultured SCN slices, suggesting that GABA has a rather destabilizing effect on the SCN rhythms (Freeman *et al.*, 2013). Other work suggested that the role of GABA in synchronization depends on the state of the SCN neuronal network. GABA_A signaling promoted re-synchronization when the dorsal and ventral SCN rhythms were 6-12 h apart, but opposed synchronization when the SCN was in a steady-state (Evans *et al.*, 2013).

It should be noted that the role of GABA in coupling might depend on the polarity of the neuronal response, as GABAergic signaling can be inhibitory as well as excitatory in the SCN (Wagner *et al.*, 1997). Several studies have found that the polarity of the GABAergic response depends on

the circadian phase, regional localization, and even the length of the day (i.e. photoperiod) (De Jeu & Pennartz, 2002; Albus *et al.*, 2005; Choi *et al.*, 2008; Farajnia *et al.*, 2014b).

The GABAergic response is based on the chloride (Cl^-) flow across the cell membrane through a GABA-gated chloride channel. The direction of the Cl^- flow (in or out of the cell), and thus the polarity of the GABAergic signal, depends in part on the intracellular concentration of chloride ($[\text{Cl}^-]_i$) and the relationship between the chloride equilibrium potential (E_{Cl^-}) and the membrane potential (V_m) (Kaila, 1994; Ben-Ari, 2002). Low levels of $[\text{Cl}^-]_i$ lead to a Cl^- influx through the GABA receptor mediated channel and subsequent hyperpolarization of the membrane potential, and thus to an inhibitory action of GABA (Figure 2A). Under certain conditions, however, $[\text{Cl}^-]_i$ can be higher and E_{Cl^-} can be more depolarized relative to the resting membrane potential. This causes an outward flow of Cl^- when the GABA channel opens and leads consequently to depolarization and excitatory action of GABA (Figure 2B). Different classes of cation-chloride-cotransporters (CCCs) regulate $[\text{Cl}^-]_i$. The SCN expresses at least two of the CCC transporters that regulate $[\text{Cl}^-]_i$ and determine the chloride equilibrium potential (Choi *et al.*, 2008; Belenky *et al.*, 2010); the $\text{Na}^+\text{-K}^+\text{-2Cl}^-$ cotransporter 1 (NKCC1) transporting Cl^- out of the cell and the $\text{K}^+\text{-Cl}^-$ cotransporter 2 (KCC2) which activation leads to Cl^- accumulation in the cell (Blaesse *et al.*, 2009; Rohr *et al.*, 2019). In the immature brain, the E_{Cl^-} and $[\text{Cl}^-]_i$ are high due to early expression of NKCC1, leading to excitatory actions of GABA. During development there is a switch in the expression of NKCC1 and KCC2 and in mature neurons higher expression levels of KCC2 lead to Cl^- influx and hyperpolarization, upon GABA_A receptor activation (Ben-Ari, 2002). However, even in the mature brain, GABAergic depolarization and excitation has been reported for multiple brain areas, including the SCN (Chung, 2012). Recently, it was demonstrated that indeed a switch in regulation of KCC2 and NKCC1 expression corresponds with plasticity in GABA_A signaling in the SCN (Rohr *et al.*, 2019). In the SCN, the KCCs are the primary regulators of $[\text{Cl}^-]_i$, whereas the chloride uptake NKCC1 contributes moderately to regulating $[\text{Cl}^-]_i$ (Klett & Allen, 2017). The polarity of the GABAergic response, being excitatory or inhibitory, consequently determines the E/I balance in the SCN. The right balance between excitation and inhibition is crucial for proper information processing and thus brain functioning (Zhou & Yu, 2018). Since GABA is the principle neurotransmitter in the SCN, it is also the main contributor to the E/I balance. Both GABA and the E/I balance are thought to play important roles in synchronization and communication within the SCN network (Farajnia *et al.*, 2014b; Myung *et al.*, 2015; Kim *et al.*, 2019; Rohr *et al.*, 2019) which are needed for proper adjustment to external light-dark cycles.

2.3. Entrainment of circadian rhythms by the SCN

Communication and coupling within the SCN network are important to generate a robust output signal to the periphery, but also to synchronize the SCN to the environmental conditions. Synchronizing the internal timing to the outside world is achieved by “phase shifting” actions of the SCN. SCN cells can adjust the phase of their circadian rhythm in response to zeitgeber signals, of which light is the most important one. This phase shifting capacity of the SCN is based on a time-dependent responsiveness of the network to light. When animals are kept under constant conditions, like constant darkness, and are exposed to a short light pulse, they will shift their rhythms

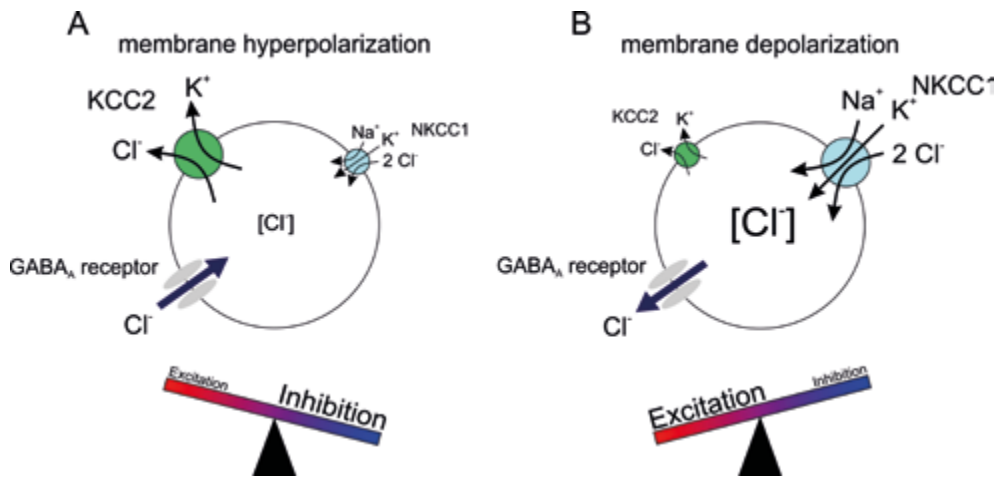


Figure 2. GABAergic activity in SCN cells. A. When there is relatively more expression of the Cl^- extruder KCC2, the intracellular Cl^- concentration will be low. If the GABA receptor is activated, the GABA-gated Cl^- channel will open and there will be an inward flow of the negatively charged Cl^- ions. This will hyperpolarize the membrane and result in an inhibitory action. B. In case there is relatively more NKCC1 expression, the intracellular Cl^- levels will be high. When the GABA-gated Cl^- channel opens, Cl^- flows out of the cell causing a depolarization of the membrane potential and consequently an excitatory response.

depending on the timing of the light pulse. Light pulses presented during the “subjected” early night will phase delay the rhythms, whereas at the end of the “subjected” night, the light exposure will induce phase advances (Daan & Pittendrigh, 1976). This phase dependent responsiveness of the SCN is essential for proper entrainment to the surrounding environment and a common response property of all living organisms. Phase shifting capacity is diminished when the SCN is in a more desynchronized state with low amplitude (vanderLeest *et al.*, 2009), emphasizing the importance of coupling within the SCN.

2.4. Encoding day length by the SCN

As described above, the SCN uses coupling mechanisms, on the one hand, to synchronize the rhythms of the individual cells resulting in a coherent signal to the periphery, and on the other hand, to adjust the phase of the SCN rhythm to the environmental conditions. The rotation of the earth on its axis causes day-night changes in light exposure. In addition, the SCN encodes for seasonal changes due to the earth’s annual revolution around the sun. Seasonal changes in the environment, like fluctuations in photoperiod, light intensity, temperature, and food availability, have great impact on the physiology of all organisms. Although daily timekeeping is a property at the level of the SCN neurons, the SCN network is needed to measure the annual changes in day length.

Ex vivo electrophysiological recordings from single cells shows that the activity patterns of single SCN cells do not change with photoperiod. As under a 12 h photoperiod, individual SCN cells

are electrically active for a relatively short amount of time (4 – 6 h) when exposed to a short or long photoperiod (Schaap *et al.*, 2003; Brown & Piggins, 2009). The SCN is able to encode for different photoperiods by adjusting waveform changes of the ensemble electrical activity. The distribution of single-cell patterns of electrical activity are compressed, meaning that the peak in their activity is clustered, when mice are entrained to a short day photoperiod (Figure 3A), whereas the activity patterns are more dispersed when exposed to a long day photoperiod (Figure 3B). The change in distribution of phases within the SCN causes the sinusoidal waveform of the ensemble electrical activity to change, both *in vivo* as *ex vivo*, resulting in a more narrow peak width with high amplitude in short days and a wider peak width with low amplitude in long days (Mrugala *et al.*, 2000; VanderLeest *et al.*, 2007). Accordingly, the phase relationship between the SCN neurons determines the multiunit electrical activity pattern, and the ensemble waveform change is responsible for photoperiodic encoding in the SCN.

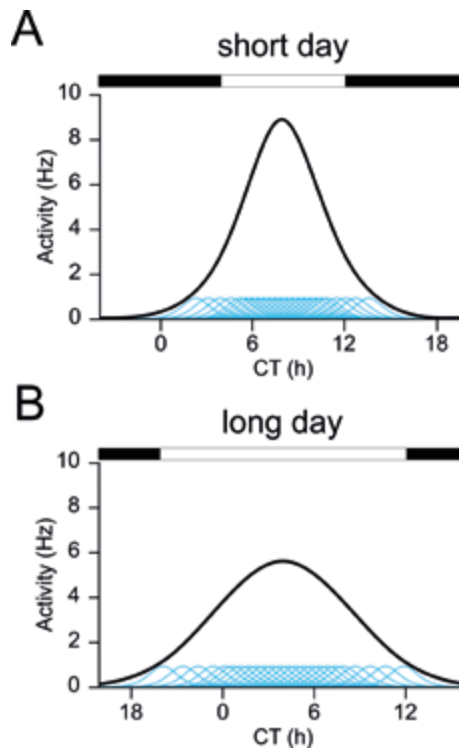


Figure 3. The distribution of single cell electrical activity patterns determine the multiunit electrical activity waveform in long and short photoperiod. The shape of the multiunit electrical activity waveform (shown as a thick black line) is derived from the summation of single-unit activity patterns (blue lines) that are distributed over the 24 h cycle according to a Gaussian distribution. This distribution is narrow in a short day (LD 8:16) photoperiod (A) and broad in a long day (LD 16:8) photoperiod (B). Above the figures, the light-dark schedule for each photoperiod is shown. White bars represent daytime, and black bars represent nighttime. Adapted from Meijer *et al.*, 2012

In vivo electrophysiological recordings in freely moving mice show that the transitions in behavior – i.e. the onset and offset of behavioral activity – occur at half maximal levels of the SCN's electrical activity (Houben *et al.*, 2009). When mice are exposed to long and short day photoperiods, the electrical output signal regulates the duration of behavioral activity in a similar manner. Indeed, exposure to long and short photoperiods has significant effects on the behavioral patterns in wheel-running activity in mice, with compressed and expanded durations of the activity period, respectively (Refinetti, 2002; VanderLeest *et al.*, 2007). Thus, the expanded and compressed waveform in multiunit electrical activity correspond to compressed and expanded durations of nocturnal behavioral activity, under a long and short day photoperiod, respectively (Houben *et al.*, 2009). The photoperiod-induced changes in behavioral activity and in the waveform of electrical activity retain for several days in rodents, after release into constant conditions. In other words, the SCN has a “memory” for photoperiod. This memory is of importance when using *ex vivo* methods to study photoperiodic encoding in the SCN tissue.

Similar to the electrophysiological studies, molecular studies have shown that differences in day length do not influence single-cell gene expression profiles, but rather affect the SCN at the network level (Naito *et al.*, 2008). The phase distribution of several clock genes, like *Per1* and 2, *Cry1* and 2, *Bmal1*, *Rev-erb* and *Dbp*, changes when exposed to different photoperiods (Sumová *et al.*, 2002; Sumová *et al.*, 2003; Hazlerigg *et al.*, 2005; Johnston *et al.*, 2005; Inagaki *et al.*, 2007; Naito *et al.*, 2008; Sosniyenko *et al.*, 2009; Buijink *et al.*, 2016).

Accordingly, photoperiodic encoding by the SCN is a neuronal network property, rather than a capability of the single neurons. Plasticity, coupling strength, and communication within the SCN network is therefore crucial for proper seasonal encoding and allows for changes in phase distribution. However, the exact mechanisms responsible for photoperiodic phase alterations are still not completely understood. As discussed earlier this chapter, several neurotransmitters, like VIP and GABA, are good candidates for coupling mechanisms within the SCN (Maywood *et al.*, 2006; Vosko *et al.*, 2007; Rohr *et al.*, 2019) and thus also for seasonal encoding. When neurons are desynchronized in phase, like under an extreme (long) photoperiod, the SCN neurons resynchronize via coupling processes mediated by both VIP and GABA_A signaling (Evans *et al.*, 2013). Accordingly, VIP knock out mice lose the ability to adapt to either long or short photoperiods (Lucassen *et al.*, 2012). The polarity of GABAergic responses also changes under the influences of different day lengths, with more GABAergic inhibition in SCN slices of mice exposed to short photoperiod and more GABAergic excitation under long photoperiod. These results suggest that the mechanisms that contribute to the degree of synchronization might partly depend on the E/I ratio (Farajnia *et al.*, 2014b).

3. AGING

The degree of synchronization and the strength of intercellular coupling may, potentially irreversibly, be influenced by aging or disease. Aging inevitably affects many aspects of (brain) physiology and behavior, including the circadian system (Buijink & Michel, 2020). At the behavioral level, age-related changes often lead to a reduction in behavioral activity levels and fragmented

sleep-wake rhythms in both humans and animal models (Valentinuzzi *et al.*, 1997; Dijk & Duffy, 1999; Hofman & Swaab, 2006; Farajnia *et al.*, 2012). Older mice show longer latencies to re-entrain their locomotor activity rhythms after phase shifts (Biello, 2009). Exposure to repeated abrupt changes in the phase of the light-dark cycle can even lead to higher mortality rate in old mice (Davidson *et al.*, 2006). These behavioral deficits are likely the consequence of a weakened timing signal generated by the SCN (Oster *et al.*, 2003; Farajnia *et al.*, 2014a).

Both *in vivo* and *ex vivo* studies showed a significant reduction in the amplitude of the ensemble electrical activity rhythm of the aged SCN (Satinoff *et al.*, 1993; Watanabe *et al.*, 1995; Nakamura *et al.*, 2011; Farajnia *et al.*, 2012). Surprisingly, there is no, or only limited, age-related neuronal cell loss in the SCN (Roozendaal *et al.*, 1987; Miller *et al.*, 1989; Fernandez *et al.*, 2021). The reduction in output signal is more likely the consequence of decreased synchronization within the SCN network (Watanabe *et al.*, 1995; Farajnia *et al.*, 2012). In addition, there are studies that showed significant deficits in circadian modulation of the physiology of individual SCN neurons (Aujard *et al.*, 2001; Farajnia *et al.*, 2012).

Ex vivo electrophysiological recordings showed changes in the phase distribution of single cell neuronal activity rhythms in SCN slices of aged mice. Subpopulations of neurons had their peak in electrical activity during the middle of the night, so in antiphase to the peak in electrical activity of most subpopulations. In contrast, SCN activity in young control slices clustered around the middle of the day (Farajnia *et al.*, 2012). These anti-phase oscillations cause reduced synchronization within the network which is likely responsible for the diminished amplitude of the SCN output signal.

The neurotransmitters VIP and GABA contribute to synchronization mechanisms in the SCN network and are both affected by aging. The number of VIP expressing neurons within the SCN declined in very old rats (Chee *et al.*, 1988) and humans (Zhou *et al.*, 1995). Also, the VIP and VPAC2 receptor mRNA expression rhythm was altered during the aging process (Kawakami *et al.*, 1997; Krajnak *et al.*, 1998; Kalló *et al.*, 2004). The number of GABAergic synaptic terminals in the SCN are diminished by 26% due to aging (Palomba *et al.*, 2008) and GABAergic postsynaptic currents are reduced in frequency and amplitude (Nygard *et al.*, 2005; Farajnia *et al.*, 2012). These age-associated alterations in neurotransmitter functionality could account for the reduced phase coherence between SCN neurons.

Besides the changes at the network level, there is also evidence for age-related deteriorations at the level of the single cell (Aujard *et al.*, 2001; Farajnia *et al.*, 2012). Among these cellular deficits are changes in membrane properties of SCN neurons. Aging was shown to diminish the circadian regulation and function in a number of ion channels. For instance, the FDR channel and the transient K⁺ channel exhibited a loss in circadian rhythmicity in channel activity in old mice, which could contribute to a change in firing frequency (Farajnia *et al.*, 2012). Also, the circadian rhythms in the BK current are impaired in SCN neurons during aging which caused significant changes in action potential waveform (Farajnia *et al.*, 2015). These age-related changes in SCN ion channels and currents are likely to contribute to the lack of circadian modulation of membrane potential and membrane conductance observed in the aged SCN neurons (Farajnia *et al.*, 2012). The cellular deficits possibly lead to dysregulation of SCN calcium (Ca²⁺) rhythms, since the levels of intracellular Ca²⁺ concentration ([Ca²⁺]_i) were found to be reversed in aged mice, with high [Ca²⁺]_i at night and

normal levels during the day, when compared to the SCN of young mice (Farajnia *et al.*, 2015). Ca^{2+} ions are important for regulating molecular mechanisms of rhythm generation (Lundkvist *et al.*, 2005) and play an important role in photic responses (Irwin & Allen, 2007). A possibly disrupted Ca^{2+} homeostasis will affect neuronal communication, but also basic rhythm generation, and is therefore an interesting target for restoring age-related clock dysfunction.

4. OUTLINE OF THIS THESIS

The experimental research in this thesis aims to gain more understanding of how the SCN network is organized and what is needed for network changes. More specifically, this work focused on the potential role of GABA and the GABAergic E/I balance in SCN network plasticity. Communication and synchronization in the SCN are important for the generation of a strong and coherent output signal. Under certain conditions, like long photoperiod, the phases of the individual SCN cells are more dispersed over the 24 hour cycle as evidenced by measurements of electrical activity and clock gene expression. Aging is also known to affect the network organization of the SCN with deterioration in synchronization among the individual SCN neurons. In this thesis, I present work that contributes to research questions regarding the effect of light exposure and/or aging on several characteristics of SCN network plasticity.

Chapter 2 describes a series of studies that examine whether exposure to light for the full length of the day was needed to achieve cellular reorganization within the SCN network as demonstrated after entrainment to long or short photoperiod. In other words, is reception of the full photoperiod needed for photoperiodic encoding in the SCN, or does exposure to short light pulses at the beginning and end of the day suffice? To examine this, mice were exposed to “skeleton photoperiods” that mimicked long summer days of 16 hours or short winter days of 8 hours. Skeleton photoperiods consist of two brief light exposures of 30 minutes that mark the beginning and end of the day. Early studies have shown that nocturnal rodents are very well capable to behaviorally adapt to these skeleton photoperiods (Pittendrigh & Daan, 1976; Stephan, 1983). In **chapter 2** multiple behavioral, cellular, and molecular experiments were conducted to examine the level of SCN network adaptations after entrainment to skeleton photoperiods.

Photoperiodic phase adjustment in the SCN network is a good example of SCN network plasticity. As described in this introduction, previous research has shown that aging affects the circadian clock at different levels, among which the network level. In **chapters 3 and 4** we further investigated the effect of aging on several cellular, network, and behavioral properties of the circadian system. In **chapter 3**, the plasticity of the circadian clock in old mice was examined at the behavioral level by recording activity while mice were exposed to different photoperiods. After the behavioral recordings, measurements of single-cell bioluminescence imaging of the clock gene *per2* were made. The aim was to investigate if, and how, the molecular clock adapts to changing day lengths with aging. Measuring the phase distribution of clock gene expression under different conditions allowed to explore the level of plasticity in the old SCN network.

The effect of aging on GABAergic function, the concomitant E/I balance, and on Ca^{2+} homeostasis was investigated in **chapter 4**. During aging, the SCN network becomes less synchronized and

chapter 4 assessed whether the E/I balance could play a potential mechanistic role. To address this question, the polarity of Ca^{2+} transients in response to exogenous GABA stimulation was determined in SCN slices of old (20-24 months) mice and young controls. From these results, the E/I balance was established in the old and young SCN. Moreover, the baseline Ca^{2+} transients provided information on the $[\text{Ca}^{2+}]_i$ of old and young SCN neurons and thus on the effect of aging on calcium homeostasis.

The research described in this thesis, and results from other studies, suggest that the balance between GABAergic excitation and inhibition plays a role in synchronization and/or plasticity of the SCN network. However, the exact role or mechanism remains topic for future studies. Pharmacological manipulations of GABAergic signaling, or chloride levels, are important tools in both in vivo and in vitro research regarding the E/I balance. In **chapter 5** experiments with a newly developed blocker – ML077 – of the KCC2 channel were conducted to investigate the efficiency of this blocker and the role of KCC2 in the GABAergic responses in SCN slices. Using calcium imaging, GABA-induced single-cell Ca^{2+} transients were recorded before and after blocking KCC2 with ML077 in SCN slices of mice entrained to different photoperiods. ML077 proved to be able to shift previously GABAergic inhibitory responses to excitatory ones and promises to be a powerful tool in researching the effect of E/I balance on the level of synchronization in the SCN network.

REFERENCES

1. Abrahamson, E.E. & Moore, R.Y. (2001) Suprachiasmatic nucleus in the mouse: retinal innervation, intrinsic organization and efferent projections. *Brain Res.*, 916, 172-191.
2. Albus, H., Vansteensel, M.J., Michel, S., Block, G.D. & Meijer, J.H. (2005) A GABAergic mechanism is necessary for coupling dissociable ventral and dorsal regional oscillators within the circadian clock. *Curr. Biol.*, 15, 886-893.
3. Astiz, M., Heyde, I. & Oster, H. (2019) Mechanisms of Communication in the Mammalian Circadian Timing System. *Int. J. Mol. Sci.*, 20.
4. Aton, S.J., Colwell, C.S., Hahner, A.J., Waschek, J. & Herzog, E.D. (2005) Vasoactive intestinal polypeptide mediates circadian rhythmicity and synchrony in mammalian clock neurons. *Nat. Neurosci.*, 8, 476-483.
5. Aton, S.J., Huettnner, J.E., Straume, M. & Herzog, E.D. (2006) GABA and Gi/o differentially control circadian rhythms and synchrony in clock neurons. *Proc. Natl. Acad. Sci. U. S. A.*, 103, 19188-19193.
6. Aujard, F., Herzog, E.D. & Block, G.D. (2001) Circadian rhythms in firing rate of individual suprachiasmatic nucleus neurons from adult and middle-aged mice. *Neuroscience*, 106, 255-261.
7. Bargiello, T.A., Jackson, F.R. & Young, M.W. (1984) Restoration of circadian behavioural rhythms by gene transfer in *Drosophila*. *Nature*, 312, 752-754.
8. Belenky, M.A., Sollars, P.J., Mount, D.B., Alper, S.L., Yarom, Y. & Pickard, G.E. (2010) Cell-type specific distribution of chloride transporters in the rat suprachiasmatic nucleus. *Neuroscience*, 165, 1519-1537.
9. Belenky, M.A., Yarom, Y. & Pickard, G.E. (2008) Heterogeneous expression of gamma-aminobutyric acid and gamma-aminobutyric acid-associated receptors and transporters in the rat suprachiasmatic nucleus. *J. Comp. Neurol.*, 506, 708-732.
10. Ben-Ari, Y. (2002) Excitatory actions of gaba during development: the nature of the nurture. *Nature reviews. Neuroscience*, 3, 728-739.
11. Biello, S.M. (2009) Circadian clock resetting in the mouse changes with age. *Age (Dordrecht, Netherlands)*, 31, 293-303.
12. Blaesse, P., Airaksinen, M.S., Rivera, C. & Kaila, K. (2009) Cation-chloride cotransporters and neuronal function. *Neuron*, 61, 820-838.
13. Brown, T.M., Banks, J.R. & Piggins, H.D. (2006) A novel suction electrode recording technique for monitoring circadian rhythms in single and multiunit discharge from brain slices. *J. Neurosci. Methods*, 156, 173-181.
14. Brown, T.M., Colwell, C.S., Waschek, J.A. & Piggins, H.D. (2007) Disrupted neuronal activity rhythms in the suprachiasmatic nuclei of vasoactive intestinal polypeptide-deficient mice. *J. Neurophysiol.*, 97, 2553-2558.
15. Brown, T.M. & Piggins, H.D. (2007) Electrophysiology of the suprachiasmatic circadian clock. *Prog. Neurobiol.*, 82, 229-255.
16. Brown, T.M. & Piggins, H.D. (2009) Spatiotemporal heterogeneity in the electrical activity of suprachiasmatic nuclei neurons and their response to photoperiod. *J. Biol. Rhythms*, 24, 44-54.
17. Buhr, E.D. & Takahashi, J.S. (2013) Molecular Components of the Mammalian Circadian Clock. In Kramer, A., Mrosovsky, M. (eds) *Circadian Clocks*. Springer Berlin Heidelberg, Berlin, Heidelberg, pp. 3-27.
18. Buijink, M.R., Almog, A., Wit, C.B., Roethler, O., Olde Engberink, A.H., Meijer, J.H., Garlaschelli, D., Rohling, J.H. & Michel, S. (2016) Evidence for Weakened Intercellular Coupling in the Mammalian Circadian Clock under Long Photoperiod. *PLoS One*, 11, e0168954.
19. Buijink, M.R. & Michel, S. (2020) A multi-level assessment of the bidirectional relationship between aging and the circadian clock. *J. Neurochem.*
20. Caldelas, I., Poirel, V.-J., Sicard, B., Pvet, P. & Challet, E. (2003) Circadian profile and photic regulation of clock genes in the suprachiasmatic nucleus of a diurnal mammal *Arvicaptus ansorgei*. *Neuroscience*, 116, 583-591.
21. Callaway, E. & Ledford, H. (2017) Medicine Nobel awarded for work on circadian clocks. *Nature*, 550, 18.
22. Challet, E. & Pevet, P. (2003) Interactions between photic and nonphotic stimuli to synchronize the master circadian clock in mammals. *Front. Biosci.*, 8, s246-257.

23. Chee, C.A., Roozendaal, B., Swaab, D.F., Goudsmit, E. & Mirmiran, M. (1988) Vasoactive intestinal polypeptide neuron changes in the senile rat suprachiasmatic nucleus. *Neurobiol. Aging*, 9, 307-312.
24. Choi, H.J., Lee, C.J., Schroeder, A., Kim, Y.S., Jung, S.H., Kim, J.S., Kim, D.Y., Son, E.J., Han, H.C., Hong, S.K., Colwell, C.S. & Kim, Y.I. (2008) Excitatory actions of GABA in the suprachiasmatic nucleus. *J. Neurosci.*, 28, 5450-5459.
25. Chung, L. (2012) Recent progress in GABAergic excitation from mature brain. *Arch. Pharm. Res.*, 35, 2035-2044.
26. Cohen, S.E. & Golden, S.S. (2015) Circadian Rhythms in Cyanobacteria. *Microbiol. Mol. Biol. Rev.*, 79, 373-385.
27. Colwell, C.S. (2000) Rhythmic coupling among cells in the suprachiasmatic nucleus. *J. Neurobiol.*, 43, 379-388.
28. Colwell, C.S. (2011) Linking neural activity and molecular oscillations in the SCN. *Nat. Rev. Neurosci.*, 12, 553-569.
29. Colwell, C.S., Michel, S., Itri, J., Rodriguez, W., Tam, J., Lelievre, V., Hu, Z., Liu, X. & Waschek, J.A. (2003) Disrupted circadian rhythms in VIP- and PHI-deficient mice. *Am. J. Physiol. Regul. Integr. Comp. Physiol.*, 285, R939-949.
30. Daan, S. & Pittendrigh, C.S. (1976) A Functional analysis of circadian pacemakers in nocturnal rodents. *Journal of comparative physiology*, 106, 253-266.
31. Davidson, A.J., Sellix, M.T., Daniel, J., Yamazaki, S., Menaker, M. & Block, G.D. (2006) Chronic jet-lag increases mortality in aged mice. *Curr. Biol.*, 16, R914-916.
32. De Jeu, M. & Pennartz, C. (2002) Circadian modulation of GABA function in the rat suprachiasmatic nucleus: excitatory effects during the night phase. *J. Neurophysiol.*, 87, 834-844.
33. de Mairan, J.-J. (1729) Observation botanique. *Histoire de l'Académie Royale des Sciences Paris*.
34. Dijk, D.J. & Duffy, J.F. (1999) Circadian regulation of human sleep and age-related changes in its timing, consolidation and EEG characteristics. *Ann. Med.*, 31, 130-140.
35. Evans, J.A., Leise, T.L., Castanon-Cervantes, O. & Davidson, A.J. (2013) Dynamic Interactions Mediated by Nonredundant Signaling Mechanisms Couple Circadian Clock Neurons. *Neuron*, 80, 973-983.
36. Farajnia, S., Deboer, T., Rohling, J.H., Meijer, J.H. & Michel, S. (2014a) Aging of the suprachiasmatic clock. *Neuroscientist*, 20, 44-55.
37. Farajnia, S., Meijer, J.H. & Michel, S. (2015) Age-related changes in large-conductance calcium-activated potassium channels in mammalian circadian clock neurons. *Neurobiol. Aging*, 36, 2176-2183.
38. Farajnia, S., Michel, S., Deboer, T., vanderLeest, H.T., Houben, T., Rohling, J.H., Ramkisoensing, A., Yassenkov, R. & Meijer, J.H. (2012) Evidence for neuronal desynchrony in the aged suprachiasmatic nucleus clock. *J. Neurosci.*, 32, 5891-5899.
39. Farajnia, S., van Westering, T.L.E., Meijer, J.H. & Michel, S. (2014b) Seasonal induction of GABAergic excitation in the central mammalian clock. *Proc. Natl. Acad. Sci. USA*, 111, 9627-9632.
40. Fernandez, F.-X., Kaladchibachi, S. & Negelspach, D.C. (2021) Resilience in the suprachiasmatic nucleus: Implications for aging and Alzheimer's disease. *Exp. Gerontol.*, 147, 111258.
41. Freeman, G.M., Krock, R.M., Aton, S.J., Thaben, P. & Herzog, E.D. (2013) GABA networks destabilize genetic oscillations in the circadian pacemaker. *Neuron*, 78, 799-806.
42. Gekakis, N., Staknis, D., Nguyen, H.B., Davis, F.C., Wilsbacher, L.D., King, D.P., Takahashi, J.S. & Weitz, C.J. (1998) Role of the CLOCK protein in the mammalian circadian mechanism. *Science*, 280, 1564-1569.
43. Golombek, D.A. & Rosenstein, R.E. (2010) Physiology of Circadian Entrainment. *Physiol. Rev.*, 90, 1063-1102.
44. Green, D.J. & Gillette, R. (1982) Circadian rhythm of firing rate recorded from single cells in the rat suprachiasmatic brain slice. *Brain Res.*, 245, 198-200.
45. Groos, G. & Hendriks, J. (1982) Circadian rhythms in electrical discharge of rat suprachiasmatic neurones recorded in vitro. *Neurosci. Lett.*, 34, 283-288.
46. Harmar, A.J., Marston, H.M., Shen, S., Spratt, C., West, K.M., Sheward, W.J., Morrison, C.F., Dorin, J.R., Piggins, H.D., Reubi, J.C., Kelly, J.S., Maywood, E.S. & Hastings, M.H. (2002) The VPAC(2) receptor is essential for circadian function in the mouse suprachiasmatic nuclei. *Cell*, 109, 497-508.
47. Harvey, J.R.M., Plante, A.E. & Meredith, A.L. (2020) Ion Channels Controlling Circadian

- Rhythms in Suprachiasmatic Nucleus Excitability. *Physiol. Rev.*, 100, 1415-1454.
48. Hastings, M.H., Maywood, E.S. & Brancaccio, M. (2018) Generation of circadian rhythms in the suprachiasmatic nucleus. *Nat. Rev. Neurosci.*, 19, 453-469.
 49. Hastings, M.H., Maywood, E.S. & O'Neill, J.S. (2008) Cellular circadian pacemaking and the role of cytosolic rhythms. *Curr. Biol.*, 18, R805-r815.
 50. Hazlerigg, D.G., Ebling, F.J.P. & Johnston, J.D. (2005) Photoperiod differentially regulates gene expression rhythms in the rostral and caudal SCN. *Curr. Biol.*, 15, R449-450.
 51. Herzog, E.D., Aton, S.J., Numano, R., Sakaki, Y. & Tei, H. (2004) Temporal precision in the mammalian circadian system: a reliable clock from less reliable neurons. *J. Biol. Rhythms*, 19, 35-46.
 52. Hofman, M.A. & Swaab, D.F. (2006) Living by the clock: The circadian pacemaker in older people. *Ageing Research Reviews*, 5, 33-51.
 53. Houben, T., Deboer, T., van Oosterhout, F. & Meijer, J.H. (2009) Correlation with behavioral activity and rest implies circadian regulation by SCN neuronal activity levels. *J. Biol. Rhythms*, 24, 477-487.
 54. Hughes, A.T. & Piggins, H.D. (2012) Feedback actions of locomotor activity to the circadian clock. *Prog. Brain Res.*, 199, 305-336.
 55. Inagaki, N., Honma, S., Ono, D., Tanahashi, Y. & Honma, K.-i. (2007) Separate oscillating cell groups in mouse suprachiasmatic nucleus couple photoperiodically to the onset and end of daily activity. *Proc. Natl. Acad. Sci. USA*, 104, 7664-7669.
 56. Inouye, S.T. & Kawamura, H. (1979) Persistence of circadian rhythmicity in a mammalian hypothalamic "island" containing the suprachiasmatic nucleus. *Proc. Natl. Acad. Sci. U. S. A.*, 76, 5962-5966.
 57. Irwin, R.P. & Allen, C.N. (2007) Calcium response to retinohypothalamic tract synaptic transmission in suprachiasmatic nucleus neurons. *J. Neurosci.*, 27, 11748-11757.
 58. Johnson, M.S. (1926) Activity and distribution of certain wild mice in relation to biotic communities. *J. Mammal.*, 7, 245-277.
 59. Johnston, J.D., Ebling, F.J. & Hazlerigg, D.G. (2005) Photoperiod regulates multiple gene expression in the suprachiasmatic nuclei and pars tuberalis of the Siberian hamster (*Phodopus sungorus*). *Eur. J. Neurosci.*, 21, 2967-2974.
 60. Kaila, K. (1994) Ionic basis of GABAA receptor channel function in the nervous system. *Prog. Neurobiol.*, 42, 489-537.
 61. Kalló, I., Kalamatianos, T., Piggins, H.D. & Coen, C.W. (2004) Ageing and the diurnal expression of mRNAs for vasoactive intestinal peptide and for the VPAC2 and PAC1 receptors in the suprachiasmatic nucleus of male rats. *J. Neuroendocrinol.*, 16, 758-766.
 62. Kawakami, F., Okamura, H., Tamada, Y., Maebayashi, Y., Fukui, K. & Ibata, Y. (1997) Loss of day-night differences in VIP mRNA levels in the suprachiasmatic nucleus of aged rats. *Neurosci. Lett.*, 222, 99-102.
 63. Kim, Y.-B., Colwell, C.S. & Kim, Y.I. (2019) Long-term ionic plasticity of GABAergic signalling in the hypothalamus. *J. Neuroendocrinol.*, 31, e12753.
 64. Klett, N.J. & Allen, C.N. (2017) Intracellular Chloride Regulation in AVP+ and VIP+ Neurons of the Suprachiasmatic Nucleus. *Sci. Rep.*, 7, 10226.
 65. Krajncak, K., Kashon, M.L., Rosewell, K.L. & Wise, P.M. (1998) Aging alters the rhythmic expression of vasoactive intestinal polypeptide mRNA but not arginine vasopressin mRNA in the suprachiasmatic nuclei of female rats. *J. Neurosci.*, 18, 4767-4774.
 66. Leak, R.K., Card, J.P. & Moore, R.Y. (1999) Suprachiasmatic pacemaker organization analyzed by viral transynaptic transport. *Brain Res.*, 819, 23-32.
 67. Lee, I.T., Chang, A.S., Manandhar, M., Shan, Y., Fan, J., Izumo, M., Ikeda, Y., Motoike, T., Dixon, S., Seinfeld, J.E., Takahashi, J.S. & Yanagisawa, M. (2015) Neuromedin s-producing neurons act as essential pacemakers in the suprachiasmatic nucleus to couple clock neurons and dictate circadian rhythms. *Neuron*, 85, 1086-1102.
 68. Lewis, P., Oster, H., Korf, H.W., Foster, R.G. & Erren, T.C. (2020) Food as a circadian time cue — evidence from human studies. *Nature Reviews Endocrinology*, 16, 213-223.
 69. Liu, C. & Reppert, S.M. (2000) GABA synchronizes clock cells within the suprachiasmatic circadian clock. *Neuron*, 25, 123-128.
 70. Long, M.A., Jutras, M.J., Connors, B.W. & Burwell, R.D. (2005) Electrical synapses

- coordinate activity in the suprachiasmatic nucleus. *Nat. Neurosci.*, 8, 61-66.
71. Lowrey, P.L. & Takahashi, J.S. (2004) Mammalian circadian biology: elucidating genome-wide levels of temporal organization. *Annual review of genomics and human genetics*, 5, 407-441.
 72. Lucassen, E.a., van Diepen, H.C., Houben, T., Michel, S., Colwell, C.S. & Meijer, J.H. (2012) Role of vasoactive intestinal peptide in seasonal encoding by the suprachiasmatic nucleus clock. *The European journal of neuroscience*, 35, 1466-1474.
 73. Lundkvist, G.B., Kwak, Y., Davis, E.K., Tei, H. & Block, G.D. (2005) A calcium flux is required for circadian rhythm generation in mammalian pacemaker neurons. *J. Neurosci.*, 25, 7682-7686.
 74. Masumoto, K.H., Nagano, M., Takashima, N., Hayasaka, N., Hiyama, H., Matsumoto, S., Inouye, S.T. & Shigeyoshi, Y. (2006) Distinct localization of prokineticin 2 and prokineticin receptor 2 mRNAs in the rat suprachiasmatic nucleus. *Eur. J. Neurosci.*, 23, 2959-2970.
 75. Maywood, E.S. (2018) Synchronization and maintenance of circadian timing in the mammalian clockwork. *Eur. J. Neurosci.*
 76. Maywood, E.S., Reddy, A.B., Wong, G.K., O'Neill, J.S., O'Brien, J.A., McMahon, D.G., Harmar, A.J., Okamura, H. & Hastings, M.H. (2006) Synchronization and maintenance of timekeeping in suprachiasmatic circadian clock cells by neuropeptidergic signaling. *Curr. Biol.*, 16, 599-605.
 77. Meijer, J.H., Schaap, J., Watanabe, K. & Albus, H. (1997) Multiunit activity recordings in the suprachiasmatic nuclei: in vivo versus in vitro models. *Brain Res.*, 753, 322-327.
 78. Miller, M.M., Gould, B.E. & Nelson, J.F. (1989) Aging and long-term ovariectomy alter the cytoarchitecture of the hypothalamic-preoptic area of the C57BL/6J mouse. *Neurobiol. Aging*, 10, 683-690.
 79. Mohawk, J.a. & Takahashi, J.S. (2011) Cell autonomy and synchrony of suprachiasmatic nucleus circadian oscillators. *Trends Neurosci.*, 34, 349-358.
 80. Moore, R.Y. (1996) Entrainment pathways and the functional organization of the circadian system. *Prog. Brain Res.*, 111, 103-119.
 81. Moore, R.Y. & Eichler, V.B. (1972) Loss of a circadian adrenal corticosterone rhythm following suprachiasmatic lesions in the rat. *Brain Res.*, 42, 201-206.
 82. Moore, R.Y. & Speh, J.C. (1993) GABA is the principal neurotransmitter of the circadian system. *Neurosci. Lett.*, 150, 112-116.
 83. Morin, L.P. (2007) SCN organization reconsidered. *J. Biol. Rhythms*, 22, 3-13.
 84. Mrugala, M., Zlomanczuk, P., Jagota, A. & Schwartz, W.J. (2000) Rhythmic multiunit neural activity in slices of hamster suprachiasmatic nucleus reflect prior photoperiod. *Am. J. Physiol. Regul. Integr. Comp. Physiol.*, 278, R987-994.
 85. Myung, J., Hong, S., DeWoskin, D., De Schutter, E., Forger, D.B. & Takumi, T. (2015) GABA-mediated repulsive coupling between circadian clock neurons in the SCN encodes seasonal time. *Proc. Natl. Acad. Sci. USA*, 112, E3920-3929.
 86. Naito, E., Watanabe, T., Tei, H., Yoshimura, T. & Ebihara, S. (2008) Reorganization of the suprachiasmatic nucleus coding for day length. *J. Biol. Rhythms*, 23, 140-149.
 87. Nakamura, T.J., Nakamura, W., Yamazaki, S., Kudo, T., Cutler, T., Colwell, C.S. & Block, G.D. (2011) Age-related decline in circadian output. *J. Neurosci.*, 31, 10201-10205.
 88. Noguchi, T., Leise, T.L., Kingsbury, N.J., Diemer, T., Wang, L.L., Henson, M.A. & Welsh, D.K. (2017) Calcium Circadian Rhythmicity in the Suprachiasmatic Nucleus: Cell Autonomy and Network Modulation. *eNeuro*, 4.
 89. Nygard, M., Hill, R.H., Wikstrom, M.A. & Kristensson, K. (2005) Age-related changes in electrophysiological properties of the mouse suprachiasmatic nucleus in vitro. *Brain Res. Bull.*, 65, 149-154.
 90. Ono, D., Honma, K.I., Yanagawa, Y., Yamanaka, A. & Honma, S. (2018) Role of GABA in the regulation of the central circadian clock of the suprachiasmatic nucleus. *J. Physiol. Sci.*, 68, 333-343.
 91. Oster, H., Baeriswyl, S., Van Der Horst, G.T. & Albrecht, U. (2003) Loss of circadian rhythmicity in aging mPer1-/-mCry2-/- mutant mice. *Genes Dev.*, 17, 1366-1379.
 92. Palomba, M., Nygård, M., Florenzano, F., Bertini, G., Kristensson, K. & Bentivoglio, M. (2008) Decline of the Presynaptic Network, Including GABAergic Terminals, in the Aging Suprachiasmatic Nucleus of the Mouse. *J. Biol. Rhythms*, 23, 220-231.

93. Park, J., Zhu, H., O'Sullivan, S., Ogunnaike, B.A., Weaver, D.R., Schwaber, J.S. & Vadigepalli, R. (2016) Single-Cell Transcriptional Analysis Reveals Novel Neuronal Phenotypes and Interaction Networks Involved in the Central Circadian Clock. *Front. Neurosci.*, 10, 481.
94. Pittendrigh, C.S. (1960) Circadian rhythms and the circadian organization of living systems. *Cold Spring Harb. Symp. Quant. Biol.*, 25, 159-184.
95. Pittendrigh, C.S. & Daan, S. (1976) A Functional Analysis of Circadian Pacemakers in Nocturnal Rodents. IV. Entrainment. *Journal of Comparative Physiology A*, 106, 291--331.
96. Price, J.L., Blau, J., Rothenfluh, A., Abodeely, M., Kloss, B. & Young, M.W. (1998) double-time is a novel *Drosophila* clock gene that regulates PERIOD protein accumulation. *Cell*, 94, 83-95.
97. Ralph, M.R., Foster, R.G., Davis, F.C. & Menaker, M. (1990) Transplanted suprachiasmatic nucleus determines circadian period. *Science*, 247, 975-978.
98. Refinetti, R. (2002) Compression and expansion of circadian rhythm in mice under long and short photoperiods. *Integr. Physiol. Behav. Sci.*, 37, 114-127.
99. Reppert, S.M. & Weaver, D.R. (2001) Molecular analysis of mammalian circadian rhythms. *Annu. Rev. Physiol.*, 63, 647-676.
100. Rohr, K.E., Pancholi, H., Haider, S., Karow, C., Modert, D., Raddatz, N.J. & Evans, J. (2019) Seasonal plasticity in GABAA signaling is necessary for restoring phase synchrony in the master circadian clock network. *eLife*, 8.
101. Roozendaal, B., van Gool, W.A., Swaab, D.F., Hoogendijk, J.E. & Mirmiran, M. (1987) Changes in vasopressin cells of the rat suprachiasmatic nucleus with aging. *Brain Res.*, 409, 259-264.
102. Sangoram, A.M., Saez, L., Antoch, M.P., Gekakis, N., Staknis, D., Whiteley, A., Fruechte, E.M., Vitaterna, M.H., Shimomura, K., King, D.P., Young, M.W., Weitz, C.J. & Takahashi, J.S. (1998) Mammalian circadian autoregulatory loop: a timeless ortholog and mPer1 interact and negatively regulate CLOCK-BMAL1-induced transcription. *Neuron*, 21, 1101-1113.
103. Satinoff, E., Li, H., Tchong, T.K., Liu, C., McArthur, A.J., Medanic, M. & Gillette, M.U. (1993) Do the suprachiasmatic nuclei oscillate in old rats as they do in young ones? *Am. J. Physiol.*, 265, R1216-1222.
104. Schaap, J., Albus, H., VanderLeest, H.T., Eilers, P.H., Detari, L. & Meijer, J.H. (2003) Heterogeneity of rhythmic suprachiasmatic nucleus neurons: Implications for circadian waveform and photoperiodic encoding. *Proc. Natl. Acad. Sci. USA*, 100, 15994-15999.
105. Shearman, L.P., Zylka, M.J., Weaver, D.R., Kolakowski, L.F., Jr. & Reppert, S.M. (1997) Two period homologs: circadian expression and photic regulation in the suprachiasmatic nuclei. *Neuron*, 19, 1261-1269.
106. Sheward, W.J., Maywood, E.S., French, K.L., Horn, J.M., Hastings, M.H., Seckl, J.R., Holmes, M.C. & Hattar, A.J. (2007) Entrainment to feeding but not to light: circadian phenotype of VPAC2 receptor-null mice. *J. Neurosci.*, 27, 4351-4358.
107. Shibata, S., Oomura, Y., Kita, H. & Hattori, K. (1982) Circadian rhythmic changes of neuronal activity in the suprachiasmatic nucleus of the rat hypothalamic slice. *Brain Res.*, 247, 154-158.
108. Silver, R., LeSauter, J., Tresco, P.A. & Lehman, M.N. (1996) A diffusible coupling signal from the transplanted suprachiasmatic nucleus controlling circadian locomotor rhythms. *Nature*, 382, 810-813.
109. Sosniyenko, S., Hut, R.A., Daan, S. & Sumová, A. (2009) Influence of photoperiod duration and light-dark transitions on entrainment of Per1 and Per2 gene and protein expression in subdivisions of the mouse suprachiasmatic nucleus. *The European journal of neuroscience*, 30, 1802-1814.
110. Stephan, F.K. (1983) Circadian rhythms in the rat: constant darkness, entrainment to T cycles and to skeleton photoperiods. *Physiol. Behav.*, 30, 451-462.
111. Stephan, F.K. & Zucker, I. (1972) Circadian rhythms in drinking behavior and locomotor activity of rats are eliminated by hypothalamic lesions. *Proc. Natl. Acad. Sci. U. S. A.*, 69, 1583-1586.
112. Sumová, A., Jác, M., Sládek, M., Sauman, I. & Illnerová, H. (2003) Clock gene daily profiles and their phase relationship in the rat suprachiasmatic nucleus are affected by photoperiod. *J. Biol. Rhythms*, 18, 134-144.
113. Sumová, A., Sládek, M., Jác, M. & Illnerová, H. (2002) The circadian rhythm of Per1 gene product in the rat suprachiasmatic nucleus

- and its modulation by seasonal changes in daylength. *Brain Res.*, 947, 260-270.
114. Tominaga, K., Okamura, H. & Inouye, S.T. (1994) Organotypic slice culture of the suprachiasmatic nucleus. *Neurosci. Biobehav. Rev.*, 18, 601-604.
 115. Valentinuzzi, V.S., Scarbrough, K., Takahashi, J.S. & Turek, F.W. (1997) Effects of aging on the circadian rhythm of wheel-running activity in C57BL/6 mice. *Am. J. Physiol.*, 273, R1957-1964.
 116. VanderLeest, H.T., Houben, T., Michel, S., Deboer, T., Albus, H., Vansteensel, M.J., Block, G.D. & Meijer, J.H. (2007) Seasonal encoding by the circadian pacemaker of the SCN. *Curr. Biol.*, 17, 468-473.
 117. vanderLeest, H.T., Rohling, J.H.T., Michel, S. & Meijer, J.H. (2009) Phase shifting capacity of the circadian pacemaker determined by the SCN neuronal network organization. *PLoS One*, 4, e0004976.
 118. Vosko, A.M., Schroeder, A., Loh, D.H. & Colwell, C.S. (2007) Vasoactive intestinal peptide and the mammalian circadian system. *Gen. Comp. Endocrinol.*, 152, 165-175.
 119. Wagner, S., Castel, M., Gainer, H. & Yarom, Y. (1997) GABA in the mammalian suprachiasmatic nucleus and its role in diurnal rhythmicity. *Nature*, 387, 598-603.
 120. Watanabe, A., Shibata, S. & Watanabe, S. (1995) Circadian rhythm of spontaneous neuronal activity in the suprachiasmatic nucleus of old hamster in vitro. *Brain Res.*, 695, 237-239.
 121. Webb, A.B., Angelo, N., Huettner, J.E. & Herzog, E.D. (2009) Intrinsic, nondeterministic circadian rhythm generation in identified mammalian neurons. *Proc. Natl. Acad. Sci. U. S. A.*, 106, 16493-16498.
 122. Welsh, D.K., Logothetis, D.E., Meister, M. & Reppert, S.M. (1995) Individual neurons dissociated from rat suprachiasmatic nucleus express independently phased circadian firing rhythms. *Neuron*, 14, 697-706.
 123. Zehring, W.A., Wheeler, D.A., Reddy, P., Konopka, R.J., Kyriacou, C.P., Rosbash, M. & Hall, J.C. (1984) P-element transformation with period locus DNA restores rhythmicity to mutant, arrhythmic *Drosophila melanogaster*. *Cell*, 39, 369-376.
 124. Zhou, J.N., Hofman, M.A. & Swaab, D.F. (1995) VIP neurons in the human SCN in relation to sex, age, and Alzheimer's disease. *Neurobiol. Aging*, 16, 571-576.
 125. Zhou, S. & Yu, Y. (2018) Synaptic E-I Balance Underlies Efficient Neural Coding. *Front. Neurosci.*, 12



two

BRIEF LIGHT EXPOSURE AT DAWN AND DUSK CAN ENCODE DAY LENGTH IN THE NEURONAL NETWORK OF THE MAMMALIAN CIRCADIAN PACEMAKER

Anneke H.O. Olde Engberink¹, Job Huisman¹, Stephan Michel^{1*}, Johanna H. Meijer^{1*}

¹Department of Cellular and Chemical Biology, Laboratory for Neurophysiology, Leiden University Medical Center,
Einthovenweg 20, 2333 ZC, Leiden, the Netherlands.

*these authors share senior author

Published in FASEB J., 2020, 34, 13685-13695

ABSTRACT

The central circadian pacemaker in mammals, the suprachiasmatic nucleus (SCN), is important for daily as well as seasonal rhythms. The SCN encodes seasonal changes in day length by adjusting phase distribution among oscillating neurons thereby shaping the output signal used for adaptation of physiology and behavior. It is well-established that brief light exposure at the beginning and end of the day, also referred to as “skeleton” light pulses, are sufficient to evoke the seasonal behavioral phenotype. However, the effect of skeleton light exposure on SCN network reorganization, remains unknown. Therefore, we exposed mice to brief morning and evening light pulses, that mark the time of dawn and dusk in a short winter- or a long summer day. Single-cell PER2::LUC recordings, electrophysiological recordings of SCN activity, and measurements of GABA response polarity revealed that skeleton light-regimes affected the SCN network to the same degree as full photoperiod. These results indicate the powerful, yet potentially harmful effects of even relatively short light exposures during the evening or night for nocturnal animals.

1. INTRODUCTION

The rotation of the earth around its axis, combined with the earth orbiting the sun causes both daily and seasonal changes in photoperiod, light intensity, temperature, and food availability. Many organisms have evolved an intrinsic clock that produces circadian rhythms that help anticipate these changes in the environment. In mammals, the central circadian clock resides in the suprachiasmatic nucleus (SCN) of the ventral hypothalamus and provides daily signals to downstream tissues (Ralph *et al.*, 1990; Hastings *et al.*, 2018). Individual SCN neurons generate autonomous circadian rhythms by a genetic feedback loop of clock genes and their protein products (Buhr & Takahashi, 2013). Intercellular interactions synchronize and stabilize the rhythms of cells within the network (Mohawk & Takahashi, 2011) and cause the SCN to produce a coherent signal of the ensemble. This signal is in turn synchronized to the ambient light-dark cycle through light information perceived by the retina and projects to the SCN via the retinohypothalamic tract.

The SCN adapts to photoperiodic changes in day length, and thereby acts not only as a daily pacemaker, but also as a seasonal pacemaker. Seasonal encoding is achieved by a compression of the distribution of single-cell patterns of electrical activity in short winter days, and decompression in long summer days (VanderLeest *et al.*, 2007; Brown & Piggins, 2009). The readjustment of phases within the SCN leads to an alteration in the ensemble waveform of SCN electrical activity (MUA) with a wider peak width in long days and a more narrow peak width in short days (Mrugala *et al.*, 2000). This SCN waveform is thus an internal representation of the length of the day, and leads to the proper seasonal adjustments in mammals.

The studies on seasonal encoding by the SCN have been an excellent example of the ability of integrated networks to perform tasks that exceed the ability of individual neurons within the network; while individual SCN neurons have the cell-autonomous ability to produce circadian rhythms, they require a functioning network to recognize and encode the length of the day. Proper recognition of the season by the SCN is, therefore, an emerging property of the network, rather than a single-cell property.

However, there has been a major shortcoming in the study on seasonal encoding. In laboratory conditions, nocturnal animals are routinely exposed to light for the full length of the day. In contrast, in nature these animals experience environmental light conditions that are far from that: they spend most of their days in dark burrows and see the light usually only during dusk and dawn. We have, therefore, undertaken an investigation in which we question whether the reception of the full photoperiod is necessary to achieve the cellular reorganization within the SCN. Early studies have shown that these “skeleton” photoperiods are sufficient for adaptation of behavioral activity in nocturnal rodents, with shorter duration of activity during short summer nights and longer activity duration during the winter nights (Pittendrigh & Daan, 1976; Rosenwasser *et al.*, 1983; Stephan, 1983). Whether skeleton photoperiods will also affect the phase-shifting responses to light pulses – clearly present in full photoperiod – and are sufficient to evoke the molecular and electrophysiological adaptations of the central circadian clock has not been studied.

In this study, we use skeleton photoperiods consisting of 30 minutes light exposure at the beginning and end of each day to mimic long days of 16 hours and short days of 8 hours.

Exposure to the skeleton photoperiod affected the circadian clock in a strikingly similar manner as a full photoperiod. At different levels ranging from behavioral to electrophysiological (spike impulse frequency) and molecular rhythms (single-cell PER2 expression), neurotransmitter function (GABA-action) and phase-shifting capacity, the characteristic responses of adaptation to photoperiod could be reproduced with exposure to light pulses marking the beginning and end of the day.

2. MATERIALS AND METHODS

2.1. Animals and behavioral activity recordings

All experiments were performed using either male wild-type mice of 2 – 5 months old (C57BL/6J, Envigo, Horst, the Netherlands) or male homozygous PERIOD2::LUCIFERASE (PER2::LUC) mice of 3 – 6 months old, the latter were backcrossed to C57bl/6 and bred at the Leiden University Medical Center animal facility (Buijink *et al.*, 2016). All animals were housed in climate-controlled cabinets with full-spectrum diffused lighting with an intensity between 50 and 100 lux (Osram truelight TL), and *ad libitum* access to food and water throughout the experiment. The mice were entrained to either a skeleton long or short photoperiod according to the following protocol (see Figure 1A): all animals were first placed in 12 hours light – 12 hours dark (LD 12:12) for at least 1 week, and then 1 week in a skeleton photoperiod 12:12 (LDLD 0.5:11:0.5:12). For the skeleton long photoperiod, mice were thereafter exposed for 7 - 10 days to a skeleton photoperiod 14:10 (LDLD 0.5:13:0.5:10), and subsequently for at least 4 weeks to a skeleton photoperiod 16:8 (LDLD 0.5:15:0.5:8). For the skeleton short photoperiod, mice were exposed for 7 days to a skeleton photoperiod 10:14 (LDLD 0.5:9:0.5:14), and finally at least 4 weeks to a skeleton photoperiod 8:16 (LDLD 0.5:7:0.5:16). Not all animals were able to entrain to a skeleton long photoperiod. It is a well-known phenomenon in the skeleton long photoperiod entrainment that the final reduction in “night” length to 8 hours can lead to unstable entrainment, and the mice then “phase-jump” to a more stable phase angle of entrainment, which then represents entrainment to a short skeleton photoperiod (Pittendrigh & Daan, 1976; Stephan, 1983). We excluded all data from this study from animals with unstable entrainment leading to a phase jump. During entrainment to the skeleton photoperiod, mice were housed individually and their cages were equipped with a running wheel and a passive infrared sensor (PIR) for recording locomotor and home-cage activity, respectively. Both the number of wheel revolutions and PIR data were recorded using ClockLab software (ClockLab; Actimetrics, Wilmette, IL). The PIR data were used as an extra control, in addition to the running wheel recordings, for the determination of entrainment. Activity onsets and offsets were determined during the last 14 days of each photoperiod by visual inspection of the actogram by three investigators independently. The average onset and offset as well as the duration of activity (alpha) were calculated in ClockLab. All animal experiments were performed in accordance with the regulations of the Dutch law on animal welfare, and the institutional ethics committee for animal procedures of the Leiden University Medical Center (Leiden, the Netherlands) approved the protocol (DEC 13198 and PE.18.113.004).

2.2. Behavioral experiments

For the phase-shifting experiments, mice were either entrained to skeleton long or short photoperiod as described above or for at least 28 days to full long (LD 16:8) or short (LD 8:16) photoperiod after which the animals were released into constant darkness (DD). On day 4 in DD, the animals received a 30 minutes white light pulse around circadian time 15 (CT15). CT12 was routinely defined as the time of the onset of activity. From each animal in the cabinet, the onset of activity was calculated at day 4 in DD, and the timing of the light pulse was determined such that most animals would receive the light pulse closest to CT15 ($CT15 \pm 1$ h). The behavioral activity was recorded for another week after the light pulse. The phase shifts in the locomotor activity rhythm were calculated in ClockLab from the wheel running data by measuring the difference between fitted lines through the activity onsets in DD before and after the light pulse.

2.3. Bioluminescence imaging

PER2::LUC mice were entrained to skeleton long or short photoperiod as described above and were taken for experimentation after at least 28 days in the final photoperiod. Slice cultures of the SCN were prepared as previously described (Buijink *et al.*, 2016). In brief, mice were killed by decapitation within one to three hours before the projected night of the skeleton photoperiod. Decapitation and subsequent dissection of the brain took place in dim red light until the optic nerves were cut. The brain was dissected and placed in modified ice-cold artificial cerebrospinal fluid (ACSF), containing (in mM): NaCl 116.4, KCl 5.4, NaH_2PO_4 1.0, $MgSO_4$ 0.8, $CaCl_2$ 1, $MgCl_2$ 4, $NaHCO_3$ 23.8, glucose 15.1, and 5 mg/L of gentamycin (Sigma Aldrich, Munich, Germany) and saturated with 95% O_2 – 5% CO_2 . From each brain, two consecutive coronal slices (200 μ m thick) of the hypothalamus containing the SCN were made with a vibrating microtome (VT 1000S, Leica Microsystems, Wetzlar, Germany). The slice containing the anterior SCN was optically identified, the subsequent slice was considered to contain the posterior SCN. From these slices, the SCN was isolated and two explant cultures were maintained on a Millicell membrane insert (PICMORG50, Merck – Millipore, Burlington, MA, USA) in a 35 mm dish containing 1.2 mL of Dulbecco's Modified Eagle's Medium supplemented with 10 mM HEPES buffer (Sigma-Aldrich, Munich, Germany), 2% B-27 (Gibco, Landsmeer, The Netherlands), 5 U/mL of penicillin, 5 μ g/mL of streptomycin (0.1% penicillin-streptomycin; Sigma-Aldrich, Munich, Germany), and 0.2 mM D-luciferin sodium salt (Promega, Leiden, The Netherlands) and adjusted to pH 7.2 with NaOH. The dish containing the slices was sealed with a glass cover slip and transferred to a temperature-controlled (37 °C) and light-tight chamber (Life Imaging Services, Reinach, Switzerland), equipped with an upright microscope and a cooled CCD camera (ORCA –UU-BT-1024, Hamamatsu Photonics Europe, Herrsching am Ammersee, Germany). Bioluminescence images from the anterior and posterior SCN explants were acquired consecutively with an exposure time of 29 minutes resulting in image series with 1 hour time resolution.

Data analysis

The image time series were analyzed using a custom-made, MATLAB-based (Mathworks, Natick, MA, USA) program, as described in (Buijink *et al.*, 2016). In brief, groups of pixels that showed

characteristics of single-cells were identified and these regions of interest (ROIs) will be referred to as single-cells. Single-cells were only used if the time series contained at least three cycles with periods between 18 and 30 hours, and with peaks above and troughs below the trend line. The processed intensity traces from the single-cell rhythms were evaluated on sustained PER2::LUC signal and circadian rhythm characteristics, like peak time and period. Phase distribution was defined as the standard deviation (SD) of the peak time from all cells per explant, of the first cycle in vitro. Single-cell period variability was defined as the cycle-to-cycle time difference between the half-maximum of the rising edge of the PER2::LUC expression rhythm. The variability in period is defined as the standard deviation (SD) of the cycle interval of individual cells, calculated for the first three cycles in vitro, and averaged per slice.

2.4. Ex vivo electrophysiology

Mice were entrained to skeleton long or short photoperiod as described above and were taken for experimentation after at least 28 days in the final photoperiod. The SCN slices were prepared during the light pulse that marks the end of the day. Coronal brain slices (~450 μm thick) were prepared using a tissue chopper, and the slice containing the SCN was transferred to a laminar flow chamber. The tissue was submerged into and continuously perfused (1.5 mL/min) with oxygenated regular ACSF (CaCl_2 increased to 2 mM and without MgCl_2 , compared to modified ACSF, 35 °C, 95% O_2 and 5% CO_2). The slice was stabilized using an insulated tungsten fork and settled in the recording chamber for ~1 hour before the electrodes were placed in the center of the left and right SCN to obtain multiunit neuronal activity recordings from both nuclei. Action potentials were recorded using 75 μm 90% platinum/10% iridium electrodes. The signals were amplified ($\times 10,000$) by a high impedance amplifier (5112, Signal Recovery, Bracknell, UK) and bandpass filtered (0.3 Hz low-pass, 3 kHz high-pass). Action potentials were selected by a window discriminator and the ones that exceeded a predetermined threshold well above the noise (~5 μV) were counted in 10 seconds bins using a custom-made automated computer program.

Data analysis

The electrophysiological data were analyzed using a custom-made program in MATLAB as described previously (VanderLeest *et al.*, 2007). The time of maximum activity was used as a marker of the phase of the SCN and was determined as the first peak in multiunit activity. Multiunit recordings of at least 24 hours in duration that expressed a clear peak in multiunit activity were moderately smoothed using a least-squares algorithm (Eilers, 2003). Subsequently, the SCN peak time, the peak width, and the relative peak amplitude (peak-to-trough ratio) of the first cycle *ex vivo* were determined.

2.5. Ca^{2+} imaging

Mice were entrained to skeleton long or short photoperiod as described above and were taken for experimentation after at least 28 days in the final photoperiod. Decapitation and subsequent dissection of the brain were similar as described above for the bioluminescence experiments, with the exception that the slices made for Ca^{2+} imaging were 250 μm thick. Slices were sequentially

maintained in regular, oxygenated ACSF. The slices were incubated in a water bath (37°C) for 30 minutes and were then maintained at room temperature until the start of the recordings. Recordings were performed within a 4 hours interval centered around the middle of the projected day, referring to the previous light regime of the animal. Neurons in brain slices were bulk-loaded with the ratiometric, membrane permeable Ca²⁺ indicator dye fura-2-acetoxymethyl ester (Fura-2-AM) as described previously (Michel *et al.*, 2013). Briefly, the slices were submerged into a mix of regular ACSF containing 7 μM Fura-2-AM for 10 minutes at 37°C. The slices were then rinsed four times with fresh ACSF before being transferred to a recording chamber (RC-26G, Warner Instruments, Hamden, CT, USA) mounted on the fixed stage of an upright fluorescence microscope (Axioskop 2-FS Plus, Carl Zeiss Microimaging, Oberkochen, Germany) and constantly perfused with oxygenated ACSF (2.5 mL/min) at room temperature. The indicator dye was excited alternatively at wavelengths of 340 and 380 nm by means of a monochromator (Polychrome V, TILL Photonics; now FEI Munich GmbH, Munich, Germany). Emitted light (505 nm) was detected by a cooled CCD camera (Sensicam, TILL Photonics; now FEI Munich GmbH, Munich, Germany), and images were acquired at 2 seconds intervals. Using an eight-channel pressurized focal application system (ALA-VM8, ALA scientific instruments, NY, USA), GABA (200 μM, 15 s) was applied locally and neuronal responses were recorded as Ca²⁺ transients. After two GABA pulses, which were separated by 1 minute baseline recording, ACSF containing elevated levels of K⁺ (20 mM, 15 s) was applied to identify healthy, responding neurons. Cells with at least a 10% increase in [Ca²⁺]_i in response to high levels of K⁺ were considered healthy cells. Both experiments and analysis were accomplished using imaging software (TILLvision, TILL Photonics; now FEI Munich GmbH, Munich, Germany).

Data analysis

Single-wavelength images were background subtracted, and ratio images (340/380) were generated. Region of interest-defined cells and mean ratio values were determined, from which the intracellular Ca²⁺ concentration was calculated. Neuronal Ca²⁺ responses were further analyzed using IGOR Pro (WaveMetrics, Portland, OR, USA). The transient responses in Ca²⁺ concentration within the first seconds after the stimulation were evaluated, with responses smaller than ± 10% of baseline values defined as non-responding cells. GABA-evoked responses showing Ca²⁺ transients with a decrease in amplitude lower than 10% from baseline were considered inhibitory and responses with an increase higher than 10% from baseline were defined as excitatory. Cells that showed both excitatory and inhibitory responses after one GABA stimulation were defined as biphasic. Per animal, two to three SCN slices were analyzed and the Ca²⁺ responses to GABA application were measured in 50 – 80 cells. For each animal, the distribution of the different types of responses and the E/I ratio were determined. To calculate the E/I ratio, the number of cells that responded excitatory was divided by the number of cells that responded inhibitory for each animal and averaged per group.

2.6. Statistics

Statistical analysis was performed using GraphPad Prism (San Diego, CA, USA) and RStudio (RStudio Team (2020). RStudio: Integrated Development Environment for R. RStudio, PBC, Boston,

MA, USA). The behavioral data on alpha and phase shifts and the electrophysiological data were analyzed with two-tailed student's *t*-tests. The effect of the skeleton long and short photoperiod on the distribution of GABAergic responses was tested using chi square tests. E/I ratio was tested with a two-tailed student's *t*-test. The bioluminescence data were analyzed using two-way ANOVAs with factors "photoperiod" (long or short) and "type" (full or skeleton) and in case of significance followed by a Sidak's correction for multiple comparisons. Last, the differences between the skeleton photoperiod and full photoperiod for the alpha, phase shifts, peak width, and PER2::LUC peak time SD were analyzed using two-way ANOVAs, type III, with factors "photoperiod" (long or short) and "type" (full or skeleton) and in case of significance followed by a Bonferroni correction for multiple comparisons. Differences with $P \leq 0.05$ were considered significant. All data are shown as mean \pm SEM.

3. RESULTS

3.1. Exposure to a skeleton photoperiod changes behavioral activity patterns

We investigated whether C57BL/6 mice are able to adapt to different day lengths using only 30 minutes light pulses presented at the beginning and end of the day, so-called skeleton photoperiod. Wild-type mice were exposed to an entrainment paradigm in which they first were exposed to a 12:12 light-dark cycle, then to a 12:12 skeleton photoperiod, and next, the timing of the morning and evening light pulses shifted gradually until they were either representing a long (LD 16:8) or a short (LD 8:16) photoperiod. Exposure to skeleton photoperiods had a clear differential effect on the behavioral patterns of wheel-running activity in mice (Figure 1A and B). In both groups, mice continued to be active during the dark interval between the two light pulses in accordance with their previous night. Compressed and expanded durations of the active phase (α) were observed under skeleton long and short photoperiods, respectively (Figure 1A and B, LP: $\alpha = 8.21 \pm 0.16$ h, $n = 16$, SP: $\alpha = 12.20 \pm 0.15$ h, $n = 29$, $P < 0.0001$). The circadian pattern of wheel-running activity in mice adapted to skeleton photoperiods corresponded with the previous reports using other rodents (Pittendrigh & Daan, 1976; Rosenwasser et al., 1983; Stephan, 1983) and thereby confirmed our experimental protocol. We also entrained wild-type mice to a full long and short photoperiod and the extent to which animals compressed or expanded their locomotor activity under skeleton photoperiods was quantitatively similar to the adaptation seen under full photoperiods (Figure S1A and (Refinetti, 2002; 2004; VanderLeest et al., 2007), full LP: $\alpha = 8.04 \pm 0.06$ h, $n = 9$, full SP: $\alpha = 12.24 \pm 0.31$ h, $n = 10$).

3.2. Phase-shifting capacity is different in mice adapted to a skeleton long vs short photoperiod

We next questioned how mice, once they were adapted to the skeleton photoperiod, would respond to phase-shifting light stimuli, since the maximum phase-shifting capacity depends strongly on the photoperiod to which animals are exposed (Refinetti, 2002; Evans et al., 2004; vanderLeest et al., 2009). To confirm the phase-shifting responses under full photoperiod (vanderLeest et

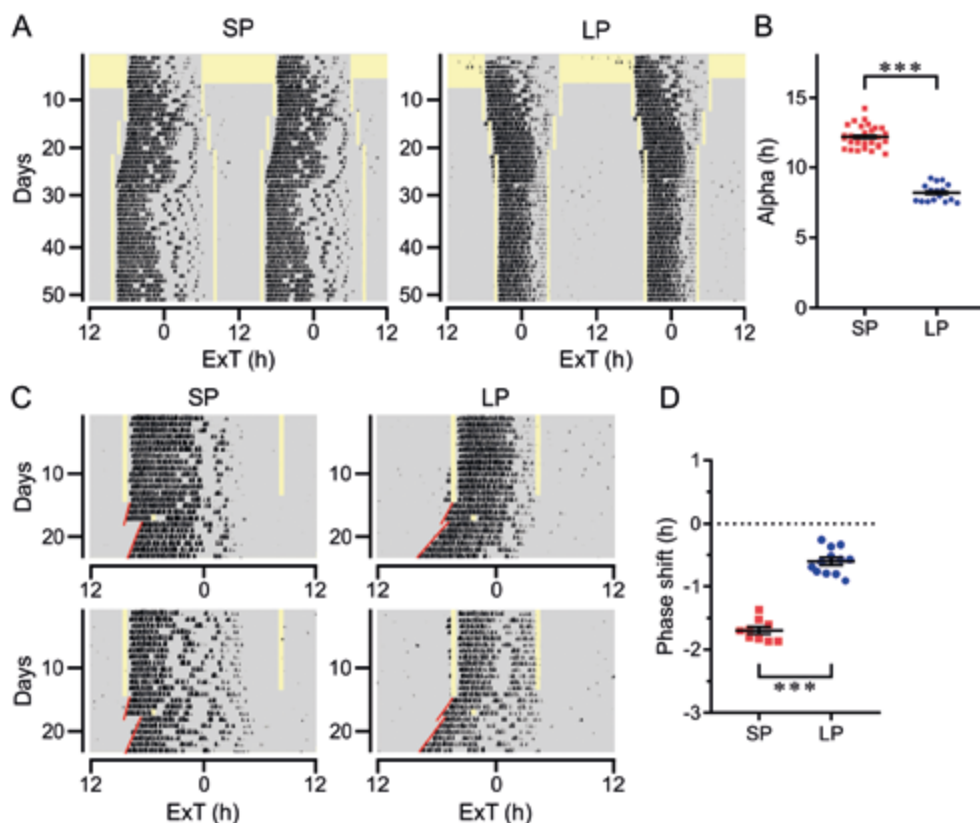


Figure 1. Behavioral responses of mice entrained to the skeleton photoperiod. A. Representative double-plotted actograms showing the locomotor wheel-running activity of a mouse during entrainment to skeleton short (left) and long (right) photoperiod. Grey areas represent darkness, yellow areas represent light. B. The duration of the activity phase (alpha) is higher in mice entrained to a skeleton short photoperiod compared to mice entrained to a skeleton long photoperiod. Data points shown are alphas calculated from all mice used for this study (both wild-type and *PER2::LUC* mice). C. Two representative single-plotted actograms showing the locomotor wheel-running activity in mice over the last 14 days of entrainment to a skeleton short (left) and long (right) photoperiod and the following DD period. On day 4 in DD, a light pulse was presented 3 hours after activity onset. Red lines are fitted through the activity onsets of the days in DD before and after the light pulse. Grey areas represent darkness, yellow areas represent light. D. The phase shift in response to a light pulse at \pm CT15 is higher in mice entrained to a skeleton short photoperiod compared to mice entrained to a skeleton long photoperiod. *** $P < 0.0001$, *t*-tests. Error bars, mean \pm SEM

et al., 2009), we first entrained mice to a full long and short photoperiod followed by three days in constant darkness and presented a light pulse at circadian time 15 (CT15) \pm 1 hour, a time point known to produce the maximum delay (vanderLeest *et al.*, 2009). In mice entrained to long days by full photoperiod, light-induced phase delays were attenuated in comparison to mice entrained to short days (Figure S1B, LP: -0.13 ± 0.26 h, $n = 7$ vs. SP: -1.92 ± 0.10 h, $n = 9$, $P < 0.0001$). Next, we investigated whether these characteristic differences would hold under skeleton photoperiods. Therefore, mice received a light stimulus at CT15 \pm 1 hour after entrainment to the skeleton photoperiod. Following

a skeleton short photoperiod, mice showed phase delays of ~ 1.7 hour in response to the light stimulus, whereas mice exhibited significantly smaller shifts of ~ 0.6 hour following adaptation to a skeleton long photoperiod (Figure 1C and D, LP: -0.60 ± 0.06 h, $n = 12$, SP: -1.69 ± 0.06 h, $n = 9$, $P < 0.0001$). The magnitude of the phase shifts is equal under a skeleton photoperiod compared to both long and short full photoperiod (Figure S1B, ns.). Both behavioral readouts of seasonal adaptation to full photoperiod, alpha and phase-shifting magnitude, are quite similar to our earlier studies ((VanderLeest et al., 2007) and (vanderLeest et al., 2009) respectively). The mechanisms underlying these behavioral changes are, therefore, only tested in skeleton photoperiods and compared with data from our previous studies generated under identical conditions. The phase-shifting capacity is intrinsic to the SCN and is explainable by the phase dispersal among SCN neurons, which is higher under a long photoperiod (vanderLeest et al., 2009). In full long photoperiod, phase dispersal of single-cell rhythms increases in the SCN and leads to a broader and more shallow waveform of the ensemble electrical activity (Mrugala et al., 2000; VanderLeest et al., 2007). Therefore, we next performed *ex vivo* experiments to test whether exposure to the skeleton photoperiod would suffice to encode day length in the SCN.

3.3. Waveform multiunit electrical activity (MUA) broadens under a skeleton long photoperiod

We measured the waveform and determined the peak width of the ensemble circadian MUA rhythm in SCN slices of mice entrained to a skeleton long or short photoperiod. A broader peak width corresponds with a wider phase distribution (Schaap et al., 2003; VanderLeest et al., 2007). Electrical recordings revealed high discharge rates during the projected day and low during the night, for both skeleton photoperiods. Peak time occurred about 1.5 hours before “midday”, at circadian time (CT) 6.60 ± 0.51 h ($n = 7$) for a skeleton short photoperiod and CT 2.74 ± 0.87 ($n = 7$) for a skeleton long photoperiod. The waveform of SCN ensemble electrical activity showed a significantly broader peak when mice were entrained to a skeleton long photoperiod compared to a short photoperiod (Figure 2, LP: 12.48 ± 0.49 h, $n = 7$, SP: 10.03 ± 0.77 h, $n = 7$, $P < 0.05$). These results show a photoperiodic effect on the waveform, that is peak width, of electrical activity that is similar for the skeleton and full photoperiod (VanderLeest et al., 2007).

3.4. Less GABAergic inhibition in mice entrained to a skeleton long photoperiod

We next investigated the effect of different skeleton photoperiods on GABAergic activity, by recording GABA-induced single-cell Ca^{2+} transients in SCN slices from mice adapted to either skeleton long or short photoperiod (Figure 3A). Ca^{2+} transients were categorized as inhibitory, excitatory, biphasic, or non-responder. The distribution of the different response types varied between recordings from animals entrained to skeleton long and short photoperiod. Adaptation to a skeleton long photoperiod decreased the GABA-induced inhibitory responses compared to short photoperiod (Figure 3B, 30% vs 37%, respectively; $P < 0.05$). Also, the percentage of GABAergic excitatory responses was higher than inhibitory responses in slices from a skeleton long photoperiod

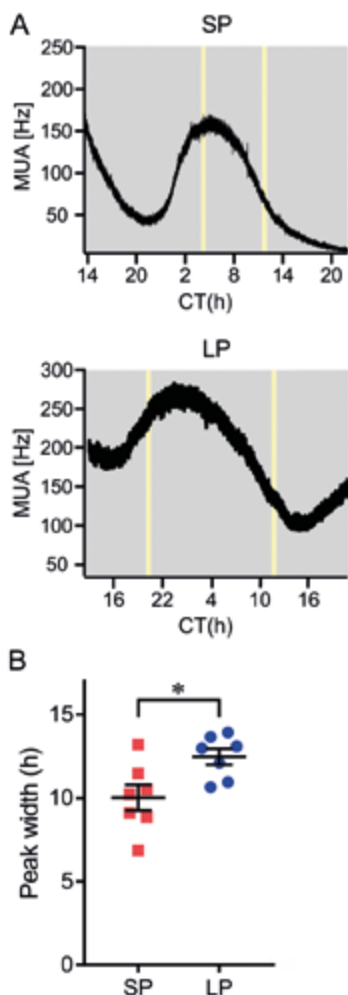


Figure 2. Skeleton long photoperiod causes broadening of the ensemble electrical activity pattern of the SCN. A. Example traces of ensemble electrical activity of the SCN in a slice from a mouse entrained to skeleton short (upper panel) and long (lower panel) photoperiod. The x-axis represents circadian time (CT 12 = onset of activity). Grey areas represent darkness, yellow areas represent light. B. The mean peak width of the ensemble electrical activity signal is higher in slices from mice entrained to a skeleton long photoperiod compared to slices from mice entrained to a skeleton short photoperiod. * $P < 0.05$, t-test. Error bars, mean \pm SEM

(Figure 3B, 39% vs. 30%, respectively; $P < 0.05$). The mean excitatory/inhibitory (E/I) ratio was not significantly different between the skeleton photoperiods (Figure 3C, n.s.), but especially following a skeleton long photoperiod, the E/I balance was remarkably high (increased excitation), similar to full long photoperiod (Farajnia *et al.*, 2014). Thus, our results show that just the timing of two light pulses affects the polarity of responses to GABA.

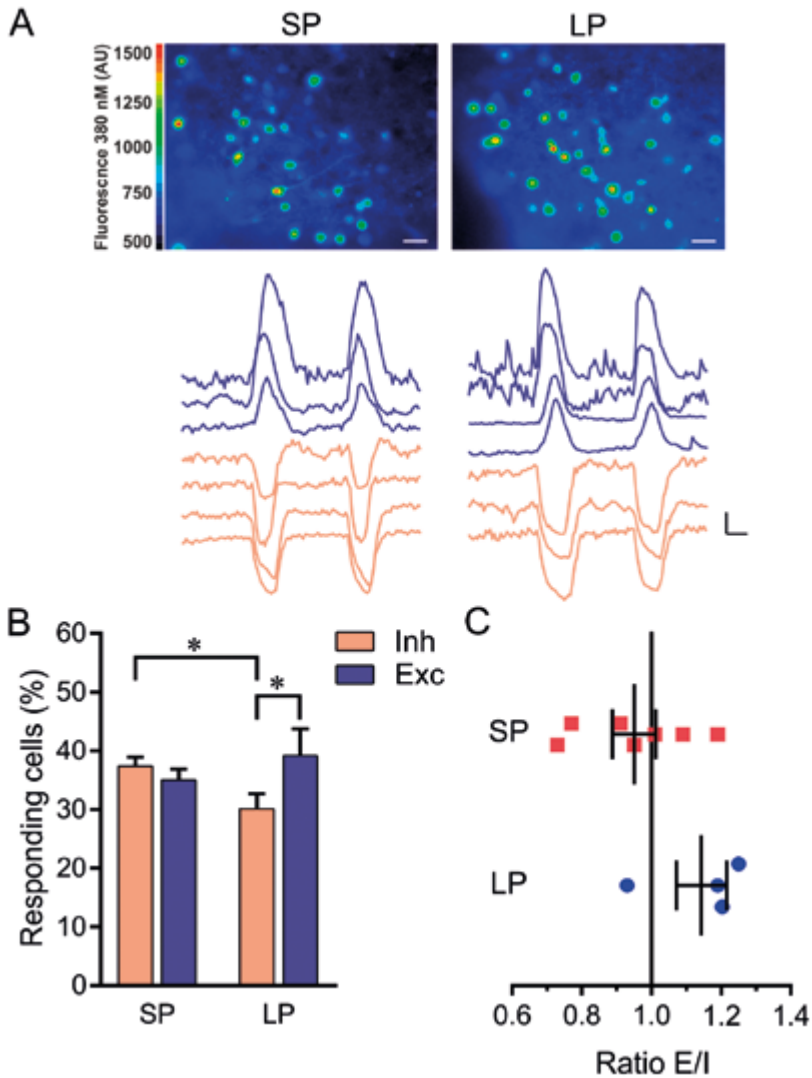


Figure 3. Less GABAergic inhibition after entrainment to a skeleton long photoperiod. **A.** Upper panels: examples of fura-2-AM loaded SCN neurons in slices from mice entrained to skeleton short (left) and long (right) photoperiod. Color scale indicates fluorescence at 380 nm excitation in arbitrary units (Scale bar, 20 μ m). Lower panels: example traces Ca²⁺ transients in response to two GABA pulses recorded from one slice adapted to skeleton short (left) or long (right) photoperiod. Excitatory responses are shown in blue and inhibitory responses in orange (Scale bars, 20 nM, 20 s). **B.** The percentage of inhibitory responding cells is lower in slices from a skeleton long photoperiod compared to short photoperiod. The percentage excitatory responding cells is higher than inhibitory responding cells in slices from a skeleton long photoperiod. * $P < 0.05$, χ^2 test. Error bars, mean \pm SEM. **C.** The mean ratios of excitatory to inhibitory GABAergic signaling for skeleton short and long photoperiod do not differ. Each value indicates the ratio of all cells measured from one animal. n.s., t-test

3.5. Phase distribution of PER2::LUC rhythms is higher in mice entrained to a skeleton long photoperiod.

To test whether a skeleton photoperiod leads to changes in phase synchrony as under full photoperiod, we next performed *ex vivo* experiments to establish the phase distribution of SCN neurons. We performed PER2::LUC bioluminescence imaging experiments and measured single-cell PER2::LUC expression rhythms over multiple days in cultured anterior and posterior SCN explants from mice entrained to either skeleton long or short photoperiod (Figure 4A). We determined peak time and period of PER2::LUC rhythms from smoothed bioluminescence intensity traces of single SCN neurons. After adaptation to a skeleton long photoperiod, both the anterior and posterior part of the SCN showed a wider phase distribution of peak times compared to a skeleton short photoperiod.

Moreover, the anterior part of the SCN of mice entrained to a skeleton long photoperiod showed a higher peak time dispersion when compared to the posterior part (Figure 4B, LP: anterior: 3.23 ± 0.20 h, posterior: 1.76 ± 0.22 h, $n = 6$, SP: anterior: 1.08 ± 0.03 h, posterior: 1.12 ± 0.08 h, $n = 7$, $P < 0.05$). Furthermore, single-cell period variability – measured as the standard deviation (SD) of the cycle intervals of the first three cycles – was higher in both the anterior and posterior part of the SCN of mice entrained to a skeleton long photoperiod, compared to short photoperiod (Figure 4C, LP: anterior: 1.42 ± 0.08 h, posterior: 0.97 ± 0.10 h, $n = 6$, SP: anterior: 0.94 ± 0.03 h, posterior: 0.75 ± 0.02 h, $n = 7$, $P < 0.05$). This suggests that the increase in phase distribution was achieved by an increase in period variability of single neurons. Distribution of PER2::LUC rhythms were remarkably similar in the SCN of mice entrained to skeleton and full long photoperiod (Buijink *et al.*, 2016).

4. DISCUSSION

Here, we show that exposure to a skeleton photoperiod affects the circadian clock in a similar manner as complete light exposure under a full photoperiod. At different levels ranging from behavioral to cellular and molecular, strikingly, nearly all characteristic responses to full photoperiod could be mimicked by just two 30 minutes pulses of light (Figure S1, (VanderLeest *et al.*, 2007; vanderLeest *et al.*, 2009; Farajnia *et al.*, 2014; Buijink *et al.*, 2016)). Exposure to a skeleton long photoperiod results in (a) complete adaptation of the behavioral activity pattern, (b) a reduction in the magnitude of phase delays in response to light pulses, (c) a broadening of the ensemble electrical activity pattern produced by the SCN *ex vivo*, (d) less GABAergic inhibitory responses in SCN neurons, and (e) desynchronization among oscillatory neurons, as revealed by single-cells *per2* clock gene expression. Moreover, the differences between a skeleton long photoperiod and skeleton short photoperiod were, for all parameters, concordant to the full photoperiods (see also Figure S1).

We entrained mice to full and skeleton long and short photoperiods and measured the extent to which animals compressed or expanded their duration of locomotor activity. The duration of wheel-running activity after adaptation to skeleton photoperiods is almost identical to our results obtained under full photoperiod (Figure S1A). Moreover, these results correspond qualitatively with those obtained in other rodent species and in *Drosophila* (Pittendrigh & Minis, 1964; Pittendrigh

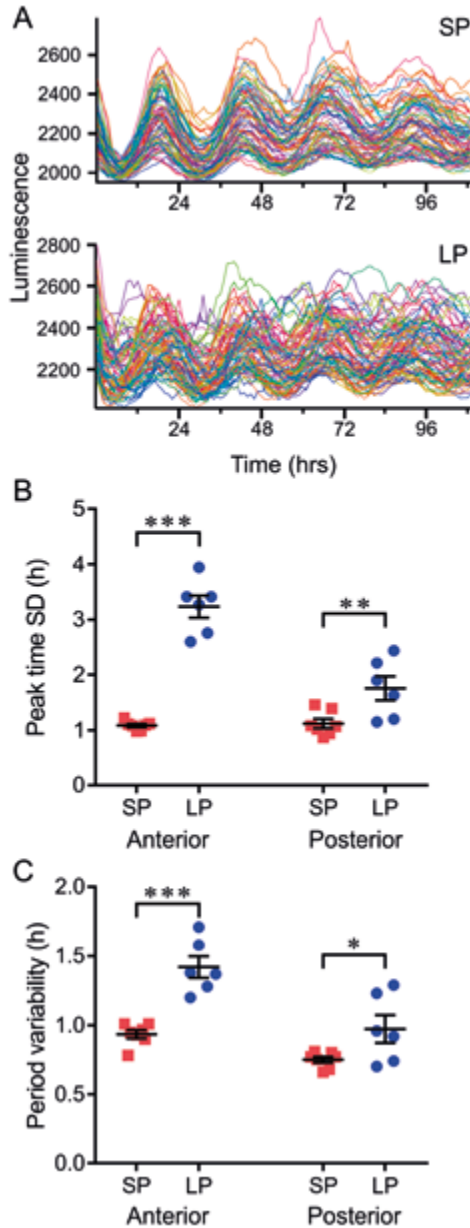


Figure 4. Phase distribution of PER2::LUC rhythms is higher in mice entrained to a skeleton long photoperiod. A. Examples of raw traces of bioluminescence intensity representing PER2::LUC expression from single cells in the anterior SCN of a mouse entrained to skeleton short (upper panel) and long (lower panel) photoperiod. The x-axis represents time in vitro after the start experiment. B. Phase distribution, defined by SD of peak times of the first cycle in vitro, is higher in both anterior and posterior SCN slices from mice entrained to a skeleton long photoperiod compared to short photoperiod. C. Period variability, defined as the SD of the cycle interval of individual cells over the first three cycles in vitro, is higher in both anterior and posterior SCN slices from mice entrained to a skeleton long photoperiod compared to short photoperiod. * $P < 0.05$, ** $P < 0.01$, *** $P < 0.0001$, two-way ANOVAs with Sidak multiple comparisons tests. Error bars, mean \pm SEM

& Daan, 1976; Rosenwasser *et al.*, 1983; Stephan, 1983). As under full photoperiod, we found that following adaptation to a skeleton photoperiod, the phase-shifting capacity is similarly reduced in short compared to long photoperiod (Figure S1B).

Behavioral adaptation to full photoperiods relies on a change in the degree of synchrony between the individual neurons (Quintero *et al.*, 2003; Schaap *et al.*, 2003; Yamaguchi *et al.*, 2003). Small neuronal subpopulations or single units in the SCN express only short durations of increased electrical activity and differ from one another in phase. The ensemble circadian waveform in electrical activity is composed of the sum of these neuronal activities (Mrugala *et al.*, 2000; Schaap *et al.*, 2003; Brown & Piggins, 2009). In full long photoperiod, the peak times in electrical activity in SCN neurons are more distributed over 24 hours, whereas the activity patterns from animals entrained to full short photoperiod are more synchronized (VanderLeest *et al.*, 2007; Brown & Piggins, 2009). Both *in vivo* and *ex vivo*, this results in a broad or narrow SCN multiunit activity pattern under long and short photoperiod, respectively (Mrugala *et al.*, 2000; Schaap *et al.*, 2003; VanderLeest *et al.*, 2007). We found that under skeleton photoperiods significant differences existed in the waveform of the SCN rhythm, with a compressed peak in a skeleton short photoperiod and a decompressed peak under a skeleton long photoperiod. As compared to results from previously published effects of a full long and short photoperiod on peak width, we show that the waveform of electrical activity is similarly affected by a skeleton and full photoperiod (skeleton LP: $12,48 \pm 0,49$ h, full LP: $11,76 \pm 0,37$ h, skeleton SP: $10,03 \pm 0,77$ h, full SP: $8,14 \pm 0,33$ h, factor “photoperiod” was significant: $P < 0.05$ for the skeleton and $P < 0.0001$ for full photoperiod, factor “type” [skeleton vs full] was ns both for LP and SP, two-way ANOVA followed by Bonferroni test (VanderLeest *et al.*, 2007)). Our data on waveform alterations suggest an underlying change in the phase distribution of SCN neurons.

We confirmed this by performing single-cell PER2::LUC bioluminescence recordings. A desynchronization of PER2 peak times was observed following a skeleton long photoperiod and more clustering in the phase following a skeleton short photoperiod. Responses of molecular rhythms to full photoperiodic exposure have also been shown for the clock genes *bmal1*, *per1*, and *per2* (Sumova *et al.*, 2004; Inagaki *et al.*, 2007; Naito *et al.*, 2008; Evans *et al.*, 2013; Myung *et al.*, 2015; Buijink *et al.*, 2016). It is well known that photoperiodic encoding at the molecular level relies on a different response of the anterior and the posterior SCN (Hazlerigg *et al.*, 2005; Inagaki *et al.*, 2007; Buijink *et al.*, 2016). We, therefore, tested whether a skeleton photoperiod leads to the same differential molecular response within the SCN. Indeed, we observed that the anterior SCN shows a significant higher phase dispersal under a skeleton long photoperiod compared to the posterior SCN, consistent with what we have shown earlier under full long photoperiod (skeleton LP: anterior: 3.23 ± 0.20 h, posterior: 1.76 ± 0.22 h, full LP: anterior: $3,42 \pm 0,19$ h, posterior: $1,81 \pm 0,15$ h, skeleton SP: anterior: 1.08 ± 0.03 h, posterior: 1.12 ± 0.08 h, full SP: anterior: $1,42 \pm 0,04$ h, posterior: $1,40 \pm 0,13$ h, factor “photoperiod” was significant: $P < 0.0001$ for skeleton and $P < 0.01$ for full photoperiod, factor “type” [skeleton vs full] was ns both for LP and SP, two-way ANOVA followed by Bonferroni test (Buijink *et al.*, 2016)). Specifically, we found a broad phase dispersal in the anterior SCN in response to light pulses at dawn and dusk similar to the responses measured in *per1* and PER2 after full long photoperiods (Inagaki *et al.*, 2007; Buijink *et al.*, 2016).

The mechanisms that regulate neuronal phase distribution are still unknown, but the main neurotransmitter in the SCN – γ -Aminobutyric acid (GABA) – plays a role in phase adjustment and synchronization of the SCN neuronal network (Liu & Reppert, 2000; Albus *et al.*, 2005; Evans *et al.*, 2013; DeWoskin *et al.*, 2015; Myung *et al.*, 2015). Besides its classical inhibitory function, GABA has shown to also act as an excitatory neurotransmitter within the SCN (Wagner *et al.*, 1997; De Jeu & Pennartz, 2002; Albus *et al.*, 2005; Choi *et al.*, 2008; Irwin & Allen, 2009; Farajnia *et al.*, 2014). When exposed to full long photoperiod, the GABAergic E/I ratio shifts toward more excitation, suggesting a role for the E/I ratio in phase synchronization of individual SCN neurons (Farajnia *et al.*, 2014; Rohr *et al.*, 2019). Adaptation to a skeleton long photoperiod decreased the GABA-induced inhibitory responses compared to a skeleton short photoperiod and the percentage of GABAergic excitatory responses was higher than inhibitory responses in slices from a skeleton long photoperiod. Thus, exposure to the skeleton photoperiod is sufficient to affect the polarity of the GABAergic response and sufficient to adjust phase synchronization in the SCN neuronal network. However, E/I ratio under skeleton short photoperiod is higher when compared to a full short photoperiod (skeleton SP: 0.95 ± 0.06 , full SP: 0.54), suggesting an additive effect of the full photoperiod light exposure on E/I balance. Given that the night-active rodents practically generate their own skeleton photoperiod by their behavior, it could be argued that the observed E/I balance and associated state of neuronal network is closer to their natural physiological conditions.

We conclude from our results that the continuous light-evoked neurotransmitter (ie, glutamate) release during the day is not required for coding photoperiod. Rather, we consider that the effects of light at the beginning and end of the animals' active period can be sufficient for photoperiodic adaptation by the SCN – from behavioral to cellular and molecular levels. This was unanticipated, because it is assumed that the characteristic of the SCN to respond tonically to light would be a prerequisite to adapt to the length of the day, thus requiring a full photoperiod (Yan & Silver, 2008). On the basis of the present results, our new hypothesis is that the phase delaying effect of light during dusk together with the phase advancing effect of light during dawn is sufficient to align the activity of SCN cells over the span of the day. This would agree with the concept of non-parametric entrainment, meaning that entrainment occurs on the basis of discrete phase shifts in response to pulses of light. The difference in the phase-shifting response that we observed between skeleton long and short photoperiod can accordingly be explained. Under a short photoperiod, when neurons are more synchronized in phase, a light pulse reaches all the single-cell oscillators at a similar phase leading the neurons to respond more coherent and resulting in a larger overall shift. In long day length, neurons are more desynchronized with a larger phase distribution, resulting in divergent phase-shifting responses and, as a consequence, a small overall shift (vanderLeest *et al.*, 2009).

The obvious question emerges whether the used skeleton light regime is merely an exotic paradigm used in laboratory research to unravel formal properties of clock cells, or whether there is also functional relevance. We argue that at least for nocturnal rodents the current protocol is possibly closer to the natural situation than full day light exposure. The behavior of many nocturnal animals sleeping underground during the day may already lead to a self-selected skeleton photoperiod with light exposures at the beginning and end of their active phase to mark the actual duration of the day.

And thus, exposure to full photoperiod, as is a general protocol in laboratory studies, may actually be less natural than exposure to a skeleton photoperiod. The results underscore the powerful effect of just brief pulses of light to achieve the full adjustment of the function of the SCN as a seasonal pacemaker.

Our findings are furthermore important given the use of electrical light at night, which is nowadays so abundantly present, especially in (sub)urban areas (Falchi *et al.*, 2016). This is particularly the case as the effects of long photoperiod can be completely mimicked by short pulses of light in the morning and evening, in about every single attribute of SCN organization and temporal behavior that we investigated. Even brief exposure to light, when animals get out of their burrows, can thus erroneously be interpreted as a sign for summer during winter time, leading to maladaptive physiological adaptation (such as the production of offspring at the wrong time of the year) (Russart & Nelson, 2018). There is mounting evidence that light at night disturbs the activity of nocturnal animal species including insects, showing the broad scale at which light pollution may be detrimental (Dominoni *et al.*, 2016; Knop *et al.*, 2017; Niepoth *et al.*, 2018; Sanders & Gaston, 2018). The fact that even brief light exposure can have physiological effects should be taken into consideration in light management programs aimed to preserve biodiversity.

ACKNOWLEDGEMENTS

We thank Gabriella Lundkvist for providing PER2::LUC knock-in mice and Mayke Tersteeg for her technical assistance and help with animal caretaking. We also thank Ruben Schalk and Tom de Boer for their help with the statistics. This study was supported by funding from Velux Stiftung (project grant 1029 to SM) and by funding from ERC (adv grant 834513 to JHM)

REFERENCES

2

1. Albus, H., Vansteensel, M.J., Michel, S., Block, G.D. & Meijer, J.H. (2005) A GABAergic mechanism is necessary for coupling dissociable ventral and dorsal regional oscillators within the circadian clock. *Curr. Biol.*, 15, 886-893.
2. Brown, T.M. & Piggins, H.D. (2009) Spatiotemporal heterogeneity in the electrical activity of suprachiasmatic nuclei neurons and their response to photoperiod. *J. Biol. Rhythms*, 24, 44-54.
3. Buhr, E.D. & Takahashi, J.S. (2013) Molecular Components of the Mammalian Circadian Clock. In Kramer, A., Mellow, M. (eds) *Circadian Clocks*. Springer Berlin Heidelberg, Berlin, Heidelberg, pp. 3-27.
4. Buijink, M.R., Almog, A., Wit, C.B., Roethler, O., Olde Engberink, A.H., Meijer, J.H., Garlaschelli, D., Rohling, J.H. & Michel, S. (2016) Evidence for Weakened Intercellular Coupling in the Mammalian Circadian Clock under Long Photoperiod. *PLoS One*, 11, e0168954.
5. Choi, H.J., Lee, C.J., Schroeder, A., Kim, Y.S., Jung, S.H., Kim, J.S., Kim, D.Y., Son, E.J., Han, H.C., Hong, S.K., Colwell, C.S. & Kim, Y.I. (2008) Excitatory actions of GABA in the suprachiasmatic nucleus. *J. Neurosci.*, 28, 5450-5459.
6. De Jeu, M. & Pennartz, C. (2002) Circadian modulation of GABA function in the rat suprachiasmatic nucleus: excitatory effects during the night phase. *J. Neurophysiol.*, 87, 834-844.
7. DeWoskin, D., Myung, J., Belle, M.D., Piggins, H.D., Takumi, T. & Forger, D.B. (2015) Distinct roles for GABA across multiple timescales in mammalian circadian timekeeping. *Proc. Natl. Acad. Sci. USA*, 112, E3911-3919.
8. Dominoni, D.M., Borniger, J.C. & Nelson, R.J. (2016) Light at night, clocks and health: from humans to wild organisms. *Biol. Lett.*, 12, 20160015.
9. Eilers, P.H. (2003) A perfect smoother. *Anal. Chem.*, 75, 3631-3636.
10. Evans, J.A., Elliott, J.A. & Gorman, M.R. (2004) Photoperiod differentially modulates photic and nonphotic phase response curves of hamsters. *Am. J. Physiol. Regul. Integr. Comp. Physiol.*, 286, R539-546.
11. Evans, J.A., Leise, T.L., Castanon-Cervantes, O. & Davidson, A.J. (2013) Dynamic Interactions Mediated by Nonredundant Signaling Mechanisms Couple Circadian Clock Neurons. *Neuron*, 80, 973-983.
12. Falchi, F., Cinzano, P., Duriscoe, D., Kyba, C.C., Elvidge, C.D., Baugh, K., Portnov, B.A., Rybnikova, N.A. & Furgoni, R. (2016) The new world atlas of artificial night sky brightness. *Sci. Adv.*, 2, e1600377.
13. Farajnia, S., van Westering, T.L.E., Meijer, J.H. & Michel, S. (2014) Seasonal induction of GABAergic excitation in the central mammalian clock. *Proc. Natl. Acad. Sci. USA*, 111, 9627-9632.
14. Hastings, M.H., Maywood, E.S. & Brancaccio, M. (2018) Generation of circadian rhythms in the suprachiasmatic nucleus. *Nat. Rev. Neurosci.*, 19, 453-469.
15. Hazlerigg, D.G., Ebling, F.J.P. & Johnston, J.D. (2005) Photoperiod differentially regulates gene expression rhythms in the rostral and caudal SCN. *Curr. Biol.*, 15, R449-450.
16. Inagaki, N., Honma, S., Ono, D., Tanahashi, Y. & Honma, K.-i. (2007) Separate oscillating cell groups in mouse suprachiasmatic nucleus couple photoperiodically to the onset and end of daily activity. *Proc. Natl. Acad. Sci. USA*, 104, 7664-7669.
17. Irwin, R.P. & Allen, C.N. (2009) GABAergic signaling induces divergent neuronal Ca²⁺ responses in the suprachiasmatic nucleus network. *Eur. J. Neurosci.*, 30, 1462-1475.
18. Knop, E., Zoller, L., Ryser, R., Gerpe, C., Horler, M. & Fontaine, C. (2017) Artificial light at night as a new threat to pollination. *Nature*, 548, 206-209.
19. Liu, C. & Reppert, S.M. (2000) GABA synchronizes clock cells within the suprachiasmatic circadian clock. *Neuron*, 25, 123-128.
20. Michel, S., Marek, R., Vanderleest, H.T., Vansteensel, M.J., Schwartz, W.J., Colwell, C.S. & Meijer, J.H. (2013) Mechanism of bilateral communication in the suprachiasmatic nucleus. *Eur. J. Neurosci.*, 37, 964-971.
21. Mohawk, J.A. & Takahashi, J.S. (2011) Cell autonomy and synchrony of suprachiasmatic nucleus circadian oscillators. *Trends Neurosci.*, 34, 349-358.
22. Mrugala, M., Zlomanczuk, P., Jagota, A. & Schwartz, W.J. (2000) Rhythmic multiunit neural activity in slices of hamster suprachiasmatic nucleus reflect prior

- photoperiod. *Am. J. Physiol. Regul. Integr. Comp. Physiol.*, 278, R987-994.
23. Myung, J., Hong, S., DeWoskin, D., De Schutter, E., Forger, D.B. & Takumi, T. (2015) GABA-mediated repulsive coupling between circadian clock neurons in the SCN encodes seasonal time. *Proc. Natl. Acad. Sci. USA*, 112, E3920-3929.
 24. Naito, E., Watanabe, T., Tei, H., Yoshimura, T. & Ebihara, S. (2008) Reorganization of the suprachiasmatic nucleus coding for day length. *J. Biol. Rhythms*, 23, 140-149.
 25. Niepoth, N., Ke, G., de Roode, J.C. & Groot, A.T. (2018) Comparing Behavior and Clock Gene Expression between Caterpillars, Butterflies, and Moths. *J. Biol. Rhythms*, 33, 52-64.
 26. Pittendrigh, C.S. & Daan, S. (1976) A functional analysis of circadian pacemakers in nocturnal rodents. *J. Comp. Physiol.*, 106, 291-331.
 27. Pittendrigh, C.S. & Minis, D.H. (1964) The Entrainment of Circadian Oscillations by Light and Their Role as Photoperiodic Clocks. *Am. Nat.*, 98, 261-294.
 28. Quintero, J.E., Kuhlman, S.J. & McMahon, D.G. (2003) The biological clock nucleus: a multiphasic oscillator network regulated by light. *J. Neurosci.*, 23, 8070-8076.
 29. Ralph, M.R., Foster, R.G., Davis, F.C. & Menaker, M. (1990) Transplanted suprachiasmatic nucleus determines circadian period. *Science*, 247, 975-978.
 30. Refinetti, R. (2002) Compression and expansion of circadian rhythm in mice under long and short photoperiods. *Integr. Physiol. Behav. Sci.*, 37, 114-127.
 31. Refinetti, R. (2004) Daily activity patterns of a nocturnal and a diurnal rodent in a seminatural environment. *Physiol. Behav.*, 82, 285-294.
 32. Rohr, K.E., Pancholi, H., Haider, S., Karow, C., Modert, D., Raddatz, N.J. & Evans, J. (2019) Seasonal plasticity in GABA(A) signaling is necessary for restoring phase synchrony in the master circadian clock network. *eLife*, 8.
 33. Rosenwasser, A.M., Boulos, Z. & Terman, M. (1983) Circadian feeding and drinking rhythms in the rat under complete and skeleton photoperiods. *Physiol. Behav.*, 30, 353-359.
 34. Russart, K.L.G. & Nelson, R.J. (2018) Artificial light at night alters behavior in laboratory and wild animals. *J. Exp. Zool. A. Ecol. Integr. Physiol.*, 329, 401-408.
 35. Sanders, D. & Gaston, K.J. (2018) How ecological communities respond to artificial light at night. *Journal of experimental zoology. Part A, Ecological and integrative physiology*, 329, 394-400.
 36. Schaap, J., Albus, H., VanderLeest, H.T., Eilers, P.H., Detari, L. & Meijer, J.H. (2003) Heterogeneity of rhythmic suprachiasmatic nucleus neurons: Implications for circadian waveform and photoperiodic encoding. *Proc. Natl. Acad. Sci. USA*, 100, 15994-15999.
 37. Stephan, F.K. (1983) Circadian rhythms in the rat: constant darkness, entrainment to T cycles and to skeleton photoperiods. *Physiol. Behav.*, 30, 451-462.
 38. Sumova, A., Bendova, Z., Sladek, M., Kovacicova, Z. & Illnerova, H. (2004) Seasonal molecular timekeeping within the rat circadian clock. *Physiol. Res.*, 53 Suppl 1, S167-176.
 39. VanderLeest, H.T., Houben, T., Michel, S., Deboer, T., Albus, H., Vansteensel, M.J., Block, G.D. & Meijer, J.H. (2007) Seasonal encoding by the circadian pacemaker of the SCN. *Curr. Biol.*, 17, 468-473.
 40. vanderLeest, H.T., Rohling, J.H.T., Michel, S. & Meijer, J.H. (2009) Phase shifting capacity of the circadian pacemaker determined by the SCN neuronal network organization. *PLoS One*, 4, e0004976.
 41. Wagner, S., Castel, M., Gainer, H. & Yarom, Y. (1997) GABA in the mammalian suprachiasmatic nucleus and its role in diurnal rhythmicity. *Nature*, 387, 598-603.
 42. Yamaguchi, S., Isejima, H., Matsuo, T., Okura, R., Yagita, K., Kobayashi, M. & Okamura, H. (2003) Synchronization of cellular clocks in the suprachiasmatic nucleus. *Science*, 302, 1408-1412.
 43. Yan, L. & Silver, R. (2008) Day-length encoding through tonic photic effects in the retinorecipient SCN region. *Eur. J. Neurosci.*, 28, 2108-2115.

SUPPLEMENTARY MATERIALS

2

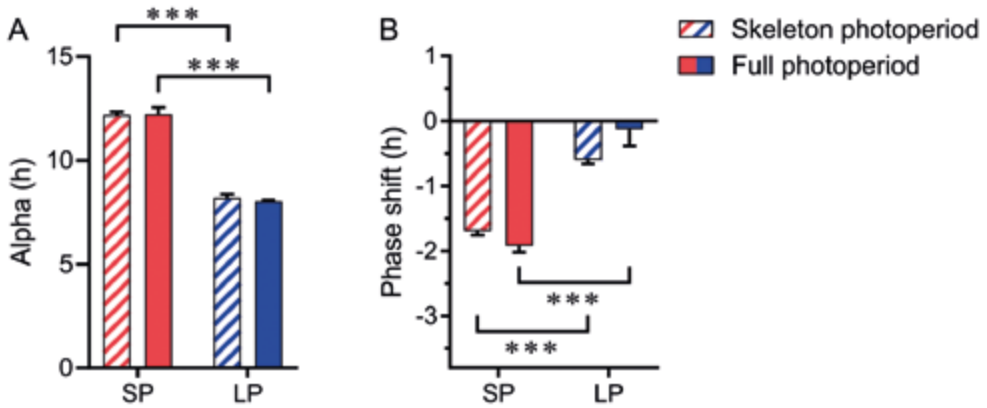


Figure S1. Exposure to skeleton long photoperiod affects the circadian clock in a similar manner as complete light exposure under full long photoperiod. A. The duration of activity phase (alpha) in mice entrained to skeleton and full, short and long photoperiod. Data for full photoperiod comes from animals that were used for phase shifting experiments. B. The mean phase shift in response to a light pulse at \pm CT15 in mice entrained to skeleton and full, short and long photoperiod. Striped red bars = skeleton short photoperiod, striped blue bars = skeleton long photoperiod, red bars = full short photoperiod, blue bars = full long photoperiod. *** $P < 0.0001$, two-way ANOVAs with Bonferroni multiple comparison tests. Error bars, mean \pm SEM.



three

AGING AFFECTS THE CAPACITY OF PHOTOPERIODIC ADAPTATION DOWNSTREAM FROM THE MOLECULAR CLOCK

Anneke H.O. Olde Engberink^{*1}; M. Renate Buijink^{*1}; Charlotte B. Wit¹; Assaf Almog²; Johanna H. Meijer¹; Jos H.T. Rohling¹; Stephan Michel¹.

¹Department of Cellular and Chemical Biology, Laboratory for Neurophysiology, Leiden University Medical Center, Einthovenweg 20, 2333 ZC, Leiden, the Netherlands.

²Lorentz Institute for Theoretical Physics, Leiden University, Leiden, the Netherlands.

* Authors contributed equally

Published in Journal of Biological Rhythms, 2020, 35, 167-179

ABSTRACT

3 Aging impairs circadian clock function, leading to disrupted sleep-wake patterns and a reduced capability to adapt to changes in environmental light conditions. This makes shift-work or the changing of time zones challenging for the elderly, and importantly, is associated with the development of age-related diseases. However, it is unclear what levels of the clock machinery are affected by aging, which is relevant for the development of targeted interventions. We found that naturally aged mice of >24 months had a reduced rhythm amplitude in behavior compared to young controls (3-6 months). Moreover, the old animals had strongly reduced ability to adapt to short photoperiods. Recording PER2::LUC protein expression in the suprachiasmatic nucleus revealed no impairment of the rhythms in PER2 protein under the three different photoperiods tested (LD: 8:16, 12:12 and 16:8). Thus, we observe a discrepancy between the behavioral phenotype and the molecular clock, and we conclude that the aging-related deficits emerge downstream of the core molecular clock. Since it is known that aging affects several intracellular and membrane components of the central clock cells, it is likely that an impairment of the interaction between the molecular clock and these components is contributing to the deficits in photoperiod adaptation.

1. INTRODUCTION

The continuing rise in life expectancy over the last decades has increased the attention for research on healthy aging. Even in healthy humans, aging is associated with fragmented sleep-wake patterns and declined circadian rhythms in eating patterns and hormone secretion, which in turn diminishes quality of life (Dijk and Duffy, 1999; Dijk et al., 1999; Carvalho-Bos et al., 2007; Froy, 2011). Aging reduces the capability of adapting to changes in light regimes, and exposure to abrupt changes in light-dark (LD) cycles even leads to a higher mortality rate in rodents (Davidson et al., 2006; Azzi et al., 2014). Aging humans show reduced season associated changes in behavior, and there is a seasonal effect on medical care needs and mortality in the elderly (Rolden et al., 2015; Cepeda et al., 2018). Moreover, several studies suggest a negative interaction between age-related neurodegenerative diseases and disturbances in circadian rhythmicity (Leng et al., 2019). It has been suggested that improving circadian rhythms in the elderly – for example with light therapy or melatonin treatment – can have beneficial effects on sleep-wake patterns. This will likely improve the quality of life, overall health and, moreover, could slow down the progression of neurodegenerative diseases (Most et al., 2010; Gaikwad, 2018).

The central circadian clock in mammals, the suprachiasmatic nucleus (SCN), is an interesting target for restoring circadian rhythms in the elderly. Age-related disruptions of rhythms in behavior and physiology can be restored by transplanting fetal SCN tissue near the hypothalamus of aged mice (Van Reeth et al., 1994; Cai et al., 1997). Moreover, it has been shown that disrupting circadian rhythms in the SCN (e.g. by knock-out of some core clock genes) induces various symptoms of premature aging in mice and rats (Kondratov et al., 2006; Dubrovsky et al., 2010). Knowledge on the functioning of the aging circadian clock will benefit the design of strategies for targeted interventions to enhance circadian rhythms in the elderly, improving their health and overall wellbeing.

A combination of molecular (e.g. clock gene expression), cellular (e.g. electrical activity), and network (e.g. neurotransmitters) elements underlie the proper functioning of the SCN. Electrical activity and neurotransmitters are important for synchronizing the SCN network, as well as for the output of the SCN to other brain areas. Aging is associated with reduced synchronization and amplitude of electrical activity rhythms in SCN neurons (Nakamura et al., 2011; Farajnia et al., 2012; Leise et al., 2013), partially due to the age-related decline in expression of important neurotransmitters, like vasoactive intestinal peptide (VIP) and γ -aminobutyric acid (GABA) (Kawakami et al., 1997; Nygard and Palomba, 2006; Palomba et al., 2008). Despite numerous studies, it is still unclear how aging affects the molecular clock in the SCN and to what extent core clock genes, like *Per2*, *Cry1*, and *Clock* are affected, while behavior is invariably been found to be affected (Asai et al., 2001; Weinert et al., 2001; Kolker et al., 2003; Wyse and Coogan, 2010; Nakamura et al., 2011; Chang and Guarente, 2013; Bonaconsa et al., 2014). Recent discoveries of small molecules with the potential to directly influence molecular clock components (Chen et al., 2018) increase the urgency to identify the best suitable components of the aging clock as targets for successful restoration of rhythmicity.

To study how aging affects circadian rhythms at the level of both the whole organism as well as the central circadian clock, we performed behavioral recordings of old (~24 months) and young (~5 months) PER2::LUC mice, and afterwards, recorded PER2::LUC gene expression characteristics in slices of the SCN. Under a 12:12 light-dark cycle (LD 12:12), we found that aging did not affect the molecular clock, as evidenced by unaltered PER2::LUC peak time and phase synchrony. Next, we investigated if challenging the circadian system by exposing mice to different photoperiods would induce differences at the behavioral level as well as the level of the molecular clock. We found that aging affected circadian behavior: old mice had reduced rhythm strength (LD 12:12) and were less able to adapt to short photoperiod (LD 8:16). However, old mice showed similar single-cell PER2::LUC rhythm characteristics after adaptation to long and short photoperiod as compared to young mice. These results suggest that the molecular clock of the aged SCN is still intact, while the behavioral phenotype is clearly affected.

2. MATERIALS AND METHODS

2.1. Animals and housing

The experiments performed in this study were conducted in accordance to the Dutch law on animal welfare. The permit (DEC 13198/PE. 16.039.001) was granted by the animal experiments committee Leiden. The homozygous PERIOD2::LUCIFERASE (PER2::LUC) mice were bred at the Leiden University Medical Center animal facility (see Buijink *et al.*, 2016). We have used young (4 – 8 months) and old (22 – 28 months) male PER2::LUC mice. The animals were kept in climate-controlled cabinets with full-spectrum diffused lighting with an intensity between 50-100 lux (Osram truelight TL), and *ad libitum* access to food and water throughout the experiment. Mice older than 20 months received, in addition to the regular food, hydration and nutritional gels as supportive care. Prior to behavioral assessment, mice were kept in groups of 2 – 5 mice in a 12h:12h light-dark (LD 12:12) cycle. During behavioral recordings, mice were kept in individual cages equipped with a passive infrared (PIR) sensor.

2.2. Behavioral analysis

Home cage activity was recorded with a PIR sensor throughout the experiment. First, behavior was recorded under LD 12:12 for at least 10 days. Then mice were exposed to either LD 16:8 or 8:16 for 28 days, which is referred to as photoperiod 1 (PP1). This was followed by a period of constant darkness (DD) for 11-14 days, before mice were exposed again to either LD 16:8 or 8:16 for at least 14 days referred to as photoperiod 2 (PP2), until the start of the bioluminescence recording of PER2::LUC. The photoperiod to which the mice were exposed was the same before and after DD. For the behavioral analysis we used: 1) the last 10 days of the LD 12:12 recordings, 2) the last 10 days of the first photoperiod exposure, 3) both 5 and 10 days from the second day of DD (marked in Figures) and 4) the last 10 days of the second photoperiod exposure, before the start of the Per2 recordings. For these time segments we determined the rhythm strength, the duration of activity (α) and resting (ρ), and relative activity level during α and ρ . Additionally, we determined the period

(τ) in DD over 10 days (free-running period). Time is expressed in projected external time (ExT), with ExT0 being the middle of the dark phase, and ExT12 the middle of the light phase.

We defined rhythm strength as the power of the F periodogram ($p = 0.05$ to peak). Alpha is defined by the interval between activity onset and offset. For this determination, activity recorded with the PIR sensors was averaged over 10 consecutive days (In DD, 5 days were used, and the period was corrected for τ , which was calculated over 10 days), and clustered in 10-minute bins. Activity onset and offset are less distinct in PIR recordings than in recordings of wheel running, on which standard methods for calculating alpha are developed. Therefore, we used the following characteristics to determine onset and offset for our recordings: the values of the highest average activity in a 10-hour bin of activity (M10), and lowest 5-hour bin (L5) was calculated (Witting *et al.*, 1990); activity was then smoothed for 2-hour bins; activity onset was defined as the first instance where the smoothed activity passed the $\frac{3}{4}$ value between L5 and M10 after the period with least activity; activity offset was defined as the last instance where the smoothed activity passed the $\frac{1}{2}$ value between L5 and M10 before the period with least activity (Figure S2).

To study the adaptation to photoperiod, we used the change in alpha from LD 12:12 to DD: Δ alpha. To obtain Δ alpha, the length of alpha for the period in LD 12:12 was subtracted from the length of alpha in DD (5 d).

2.3. Bioluminescence imaging and analysis

Slice cultures of the SCN were prepared as previously described (Buijink *et al.*, 2016). In brief, mice were killed by decapitation within one to three hours before lights off. The brain was dissected and placed in ice cold artificial cerebrospinal fluid (ACSF) with low Ca^{2+} and high Mg^{2+} . The ACSF contained (in mM): NaCl (116.4), KCl (5.4), NaH_2PO_4 (1.0), MgSO_4 (0.8), CaCl_2 (1.0), MgCl_2 (4.0), NaHCO_3 (23.8), D-glucose (15.1) and 5 mg/L gentamicin (Sigma-Aldrich, Munich, Germany), saturated with 95% O_2 -5% CO_2 and pH 7.4. From each brain, the hypothalamus, containing the SCN was isolated and sliced in 200 μm thick coronal slices with a VT 1000S vibrating microtome (Leica Microsystems, Wetzlar, Germany). The SCN was optically identified, cut out and both an anterior and posterior slice were placed on a Millicell membrane insert (PICMORG50, Merck – Millipore, Burlington, MA, USA) in a 35 mm petri dish. The dish contained 1.2 ml Dulbecco's Modified Eagle's Medium supplemented with 10 mM HEPES buffer (Sigma-Aldrich, Munich, Germany), 2% B-27 (Gibco, Landsmeer, The Netherlands), 5 U/ml penicillin, 5 $\mu\text{g}/\text{ml}$ streptomycin (0.1% penicillin-streptomycin; Sigma-Aldrich, Munich, Germany) and 0.2 mM D-luciferine sodium salt (Promega, Leiden, The Netherlands) and adjusted to pH 7.2 with NaOH.

The dish containing the slices was sealed with a glass cover slip and transferred to a temperature controlled (37 °C) and light-tight chamber (Life Imaging Services, Reinach, Switzerland), equipped with an upright microscope and a cooled CCD camera (ORCA –UU-BT-1024, Hamamatsu Photonics Europe, Herrsching am Ammersee, Germany). Bioluminescence images from the anterior and posterior slices were acquired consecutively with exposure time of 29 minutes resulting in image series with 1 h time resolution.

The bioluminescence image series were analyzed using a custom-made, MATLAB-based (Mathworks, Natick, MA, USA) program, as described in (Buijink *et al.*, 2016). In brief, we identified groups of pixels (ROIs) that showed characteristics of single-cells. Therefore, these ROI's are referred to as single-cells. The average bioluminescence was calculated for all pixels comprising the ROI's, for the image- series, resulting in bioluminescence traces representing PER2::LUC expression for each single-cell ROI. The raw traces were smoothed for further analysis of rhythm characteristics, like peak time and period. Phase distribution is defined as the standard deviation (SD) of peak time per slice, of the first cycle *in vitro*. The cycle-to-cycle interval is defined as the time difference between two consecutive half-maximum values of the rising edge of the PER2::LUC expression rhythm. The period variability is defined as the standard deviation (SD) of the cycle interval of individual cells, calculated for the first three cycles *in vitro*, and averaged per slice.

2.4. Community detection

We employed the community detection method we previously used for the identification of neuronal clusters in the SCN (Buijink *et al.*, 2016; Almog *et al.*, 2019). In short, a cross-correlation matrix was constructed from the multiple time series of PER2::LUC bioluminescence intensity traces. Followed by filtering out the local (neuron-specific) noise and global (SCN-wide) dependencies from the correlation matrix, using random matrix theory. The resulting communities have positive overall correlation within communities and negative overall correlation between communities, relative to the overall SCN activity. From a few slices the cluster locations could not be determined, this was the case for three slices in LP and one in SP (too few cells) in the anterior SCN and one slice in the posterior SCN in LP.

2.5. Statistical analysis

For the analysis of the data we used GraphPad Prism (San Diego, CA, USA). For comparing data from old and young mice we used a two-way ANOVA, followed by a Tukey's post hoc test. For the analysis of the data where we compared both old and young mice as well as LP and SP exposure, we used a one-way ANOVA, followed by a Sidak's multiple comparisons correction. Differences with $p < 0.05$ were considered significant.

3. RESULTS

3.1. PER2::LUC expression is not altered with aging under LD 12:12

Circadian rhythms in single-cell PER2::LUC expression were measured in slice cultures from old (21-28 months) and young (4-8 months) PER2::LUC mice maintained in LD 12:12 (for an example, see Figure 1A). We determined peak times and period of PER2::LUC rhythms from smoothed bioluminescence intensity traces of single SCN neurons. The average peak time was similar in slices from the SCN of young and old mice. Moreover, for both groups, peak time and period length did not differ between anterior and posterior slices (Figure 1B and C; Tukey's test, n.s.; table S1). Next, we tested whether aging affects the synchronization of PER2::LUC rhythms between SCN cells by using the standard deviation (SD) of peak times as a measure of phase distribution within slices.

In slices of the SCN from both young and old mice, PER2::LUC rhythms were synchronized to a similar degree (Figure 1D; Tukey's test, n.s.; table S1). The fluctuation of the cycle-to-cycle period was higher in the anterior SCN compared to the posterior SCN, both in slices from young and old mice (Figure 1E; Tukey's test, young: anterior vs posterior: $P < 0.05$, old: anterior vs posterior: $P < 0.05$; table S1). Combined, these results show that the PER2 expression in the SCN is unaltered by aging in the LD 12:12 light regime. Therefore, we sought to challenge the SCN in old mice using different photoperiods.

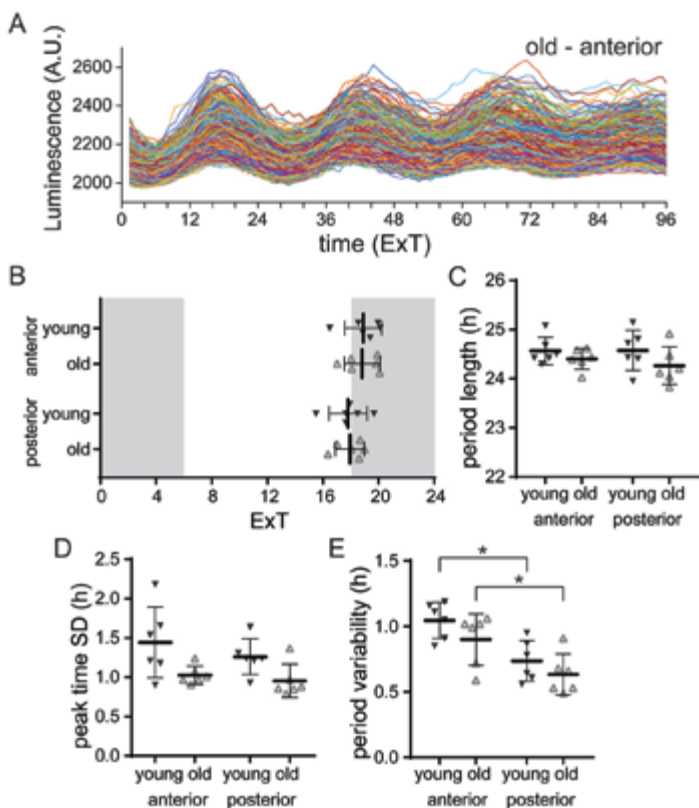


Figure 1. PER2::LUC expression is not altered with aging under LD 12:12. A. Examples of raw traces of bioluminescence intensity representing PER2::LUC expression from single cells in the anterior SCN of an old mouse (anterior, $n = 242$ cells; other examples in Suppl. Figure. S3). B. Average peak time of PER2::LUC rhythms per slice of the anterior and posterior SCN from young and old mice, plotted as external time (ExT). Shaded areas represent the projected dark phase. C. The average period length of the first 3 cycles in vitro is shown for the anterior and posterior SCN from young and old mice. D. Phase distribution is defined as the standard deviation (SD) of peak time of the first cycle in vitro and was calculated per slice. Phase distribution is shown for the anterior and posterior SCN from young and old mice. E. Period variability of single cells, averaged per slice from the anterior and posterior SCN from young and old mice. Filled triangles represent young mice ($n = 6$), and open triangles represent old mice ($n = 6$). Bars indicate mean \pm SD. * $P < 0.05$, 2-way analysis of variance, corrected for multiple comparison with Tukey's test.

3.2. Ability to behaviorally adapt to photoperiod is compromised in old mice

Both young and old mice were exposed to a seasonal adaptation protocol for either long or short photoperiod (LP and SP, respectively; Figure 2A and S2). Activity patterns in old mice were more fragmented, showing more activity during the day and a lower activity/rest-ratio, compared to young mice (Figure S1C). As a consequence, the behavioral rhythm strength in old mice was reduced in LD 12:12 when compared to young mice (Figure 2B; t-test: $P < 0.05$; table S2). Moreover, the free-running period in DD was longer after exposure to SP than after LP for young mice and this known after-effect of photoperiod (Pittendrigh and Daan, 1976) was absent in old mice (Figure 2C; Sidak's test, young: LP vs SP, $P < 0.01$, old: LP vs SP, n.s.; table S2). To examine if the mice were able to adapt to either long or short photoperiod, we determined the duration of locomotor activity (alpha) for the different light regime segments (Figure 2D) and subtracted the length of alpha in DD from its length in LD 12:12 as a measure for photoperiod-induced change in alpha (Δ alpha; Figure 2E). As expected, young mice showed an expansion of their activity profile under SP and a compression under LP, with an after-effect in the subsequent DD period (Figure 2D and S1; Refinetti, 2002). Old mice, however, were less capable of adapting to a different photoperiod. The alpha of old mice did not change after transition from LD 12:12 to SP nor from SP to DD, suggesting that old mice do not adapt to SP (Figure 2D and E, table S2). In contrast to the SP condition, old mice did show adaptation to LP, with their average alpha in DD following LP being lower than in LD 12:12 (Figure 2E and S1). The level of adaptation to LP – Δ alpha – did not significantly differ between old and young mice (Figure 2E and S1; Sidak's test, LP: young vs old, n.s.; table S2), however, the data from the old mice show a high variation, with some mice displaying no change of alpha in DD. This suggests that some old individuals were less able to adapt to LP. Taken together, the ability to adapt locomotor behavioral patterns to changing photoperiods is reduced in old mice.

3.3. Response of the molecular clock-network to photoperiod is unaltered in the aged SCN

We next investigated whether the reduced capability for seasonal adaptation in old mice is the result of a more rigid, less adaptive, molecular clock. Therefore, we measured PER2::LUC expression in SCN cultured slices of old and young mice after the mice were re-exposed for at least two weeks to either LP or SP following the DD period. We have previously shown that exposing young mice to a long photoperiod (LD 16:8) causes a wider phase distribution of peak times and a higher cycle-to-cycle period variability of single-cell PER2::LUC rhythms in the anterior part of the SCN, compared to short photoperiod (LD 8:16; Buijink et al., 2016). Since we see deficits in behavioral adaptation to photoperiod in old mice, and photoperiod can affect PER2 rhythm distribution, we may expect that the reduction in the capability to adapt to photoperiod is also seen at the molecular level.

Surprisingly, the PER2::LUC rhythms were remarkably similar in the SCN of young and old mice. The average peak time was about two hours later in the anterior slice, compared to the posterior slice, for all photoperiods in the SCN of both young and old mice (Figure 3B; Sidak's test, young vs old: n.s.; table S3). After adaptation to SP, we observed in the SCN of young mice a significantly shorter period length of PER2::LUC rhythms in the posterior part, compared to anterior part

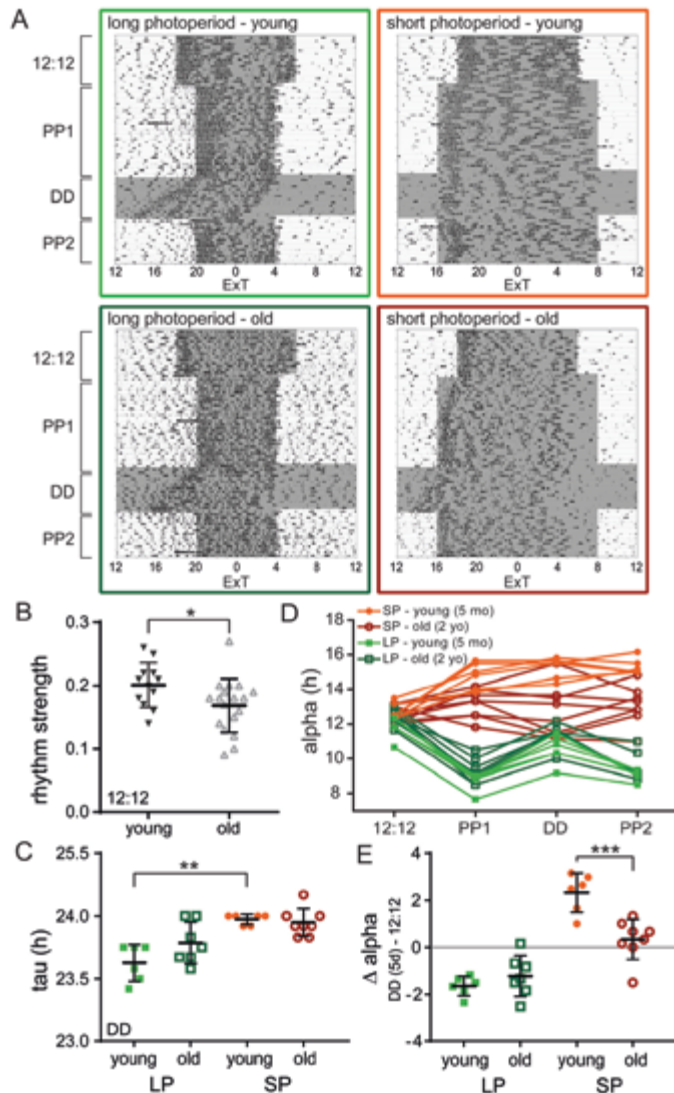


Figure 2. The ability to behaviorally adapt to photoperiod is reduced in old mice. A. Single-plotted actograms showing representative passive infrared recordings from activity of young (upper panels) and old (lower panels) mice, adapted to long photoperiod (LP; left) and short photoperiod (SP; right). Shaded areas represent the dark period. The time on the x-axis is given in external time (ExT). B. Rhythm strength of the LD 12:12 period for young (filled triangles; $n = 12$) and old (open triangles; $n = 18$) mice. C. Period (τ) of free-running behavioral rhythm during the period of constant darkness (DD; first 10 days) for young and old mice after adaptation to LP and SP. D. Activity period (α) for each segment of the entrainment protocol: LD 12:12, photoperiod 1 (PP1; LP or SP), constant darkness (DD; first 5 days), and PP2 (LP or SP), with each trace representing 1 mouse. E. Degree of adaptation to photoperiod represented by $\Delta \alpha$, which is determined by calculating the difference in α between LD 12:12 and the DD (5-day) period. $\Delta \alpha$ is given for young and old mice adapted to LP and SP. Filled circles represent SP, young ($n = 6$); open circles represent SP, old ($n = 8$); filled squares represent LP, young ($n = 6$); and open squares represent LP, old ($n = 7$). Bars indicate mean \pm SD. * $P < 0.05$, ** $P < 0.01$, *** $P < 0.001$, 1-way analysis of variance, corrected for multiple comparison with Sidak's test.

(Figure 3C; Sidak's test, young SP: anterior vs posterior, $P < 0.01$; table S3), and this was similar in the SCN of aged mice (Figure 3C; Sidak's test, posterior SCN SP: young vs old, n.s.; table S3). Consistent with previous studies, the anterior SCN of young mice adapted to LP showed a wider phase distribution of peak times, compared to SP condition (Figure 3D; Sidak's test, young anterior SCN: LP vs SP, $P < 0.001$; table S3). This difference between LP and SP was also present in SCN slices from old mice (Figure 3D; Sidak's test, old anterior SCN: LP vs SP, $P < 0.001$; table S3). Furthermore, in both the anterior and posterior part there was no significant difference in phase distribution between SCN slices from young and old mice (Figure 3D; Sidak's test, LP anterior: young vs old, n.s., LP posterior: young vs old, n.s., SP anterior: young vs old, n.s., SP posterior: young vs old, n.s.; table S3). Thus, even in the SCN of old mice, photoperiod still had a clear effect on the phase distribution of peak times.

We analyzed the fluctuations in period from cycle-to-cycle of individual cells in SCN slices from old and young mice as a measure for coupling strength (Herzog et al., 2015). The standard deviation (SD) of the cycle intervals of the first three cycles of PER2::LUC rhythms was determined for individual cells, and averaged per slice. Consistent with our previous study (Buijink et al., 2016), the average variability in single-cell period in the SCN of young mice adapted to LP was increased in the anterior part, compared to the posterior part (Figure 3E; Sidak's test, young LP: anterior vs posterior, $P < 0.01$; table S3) as well as to the (anterior) SCN of mice adapted to SP (Figure 3E; Sidak's test, young anterior SCN: LP vs SP, $P < 0.01$; table S3). This increase in single-cell cycle-to-cycle variability in the anterior SCN was similar in slices from old mice (Figure 3E; Sidak's test, old LP: anterior vs posterior, $P < 0.001$, old anterior SCN: LP vs SP, $P < 0.01$; table S3). There was no difference in the magnitude of increase of single-cell period variability between SCN slices from young and old mice (Figure 3E; Sidak's test, LP anterior SCN: young vs old, n.s.; table S3).

3.4. Degree of behavioral adaptation to photoperiod is related to PER2 period variability.

So far, we have shown that old mice have a reduced ability to adapt to changing photoperiods, while on the other hand they are still capable to adjust their molecular clock as do young mice. However, there is a higher level of variability in both behavioral and PER2::LUC data from the old, compared to young mice (Figure 2E and 3D). We wondered whether old mice that showed little adaptation in their alpha to LP also exhibited a smaller distribution in PER2::LUC peak times. Therefore, we correlated PER2::LUC period variability in the anterior SCN with the adaptation to SP or LP (Δ alpha). For the individual groups there is not a clear correlation between behavior and PER2::LUC expression rhythms (Figure S4). However, when all groups are plotted together, there appears to be an association between period variability and the adaptation of alpha to photoperiod (Figure S4; $R^2 = 0,74$).

3.5. Small changes on the level of functional clusters of neurons in the aged SCN

We have previously shown that there is a difference in functional cluster characteristics between the SCN of mice exposed to short and long photoperiod (Buijink et al., 2016). We wondered if

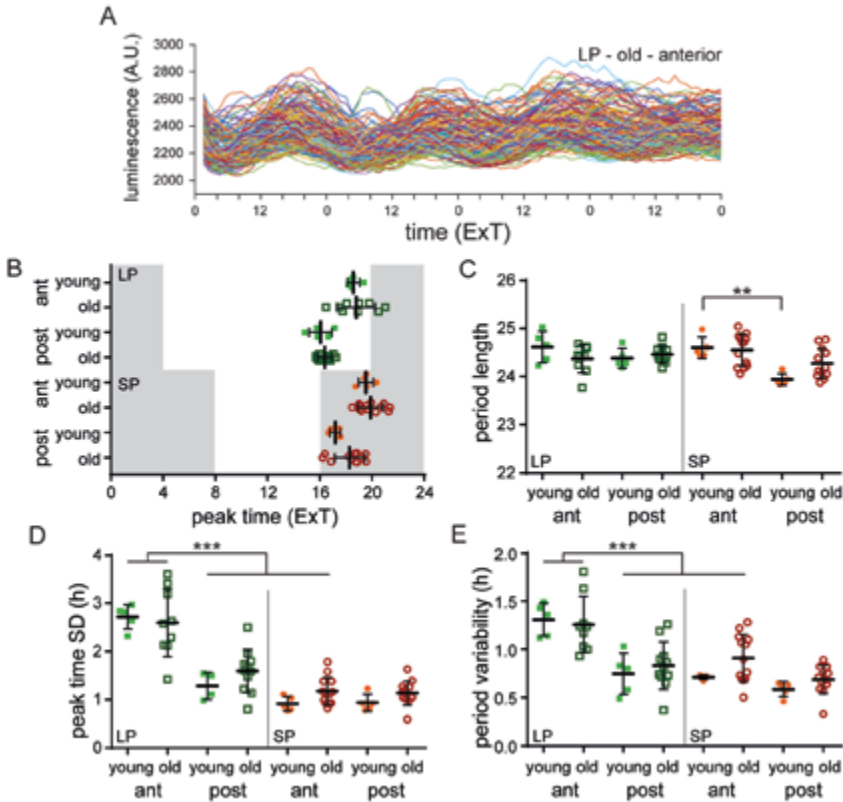


Figure 3. The molecular clock in the SCN of old mice can still adapt to different photoperiods. A. Examples of raw traces of bioluminescence intensity representing PER2::LUC expression from single cells from the anterior SCN of an old mouse ($n = 130$ cells). B. Average peak time of PER2::LUC rhythms per slice of the anterior and posterior SCN from young and old mice, adapted to long photoperiod (LP) and short photoperiod (SP) plotted as external time (ExT). Shaded areas represent the projected dark phase. C. Average period length of the first 3 cycles in vitro is shown for the anterior and posterior SCN from young and old mice entrained to LP and SP. D. Phase distribution of peak times per slice in the anterior and posterior SCN of young and old mice adapted to LP and SP. E. Single-cell period variability per slice in the anterior and posterior SCN of young and old mice adapted to LP and SP. LP: anterior: young: $n = 5$, old: $n = 9$, posterior: young: $n = 5$, old: $n = 11$; SP: anterior: young: $n = 5$, old: $n = 13$, posterior: young: $n = 5$, old: $n = 12$. Filled circles represent SP, young; open circles represent SP, old; filled squares represent LP, young; open squares represent LP, old. Bars indicate mean \pm SD. $**P < 0.01$, $***P < 0.001$, 1-way analysis of variance, corrected for multiple comparison with Sidak's test.

aging would affect any aspects of these clusters of SCN neurons, either in their spatial pattern, or their rhythm characteristics. Functional clusters were defined from time series data of PER2::LUC rhythm by an unbiased community detection algorithm (see Methods). We found that there is no difference in the location of the clustered cells in the SCN; there is a clear spatial distribution in the anterior and posterior SCN in both old and young mice, similar to that of our previous study. In LP, in both the young and old SCN, the VM/M cluster peaked earlier than the DL/L cluster, while in SP this was only the case in the old SCN (Figure 4B; Sidak's test, VM cluster vs DL cluster $P < 0.05$;

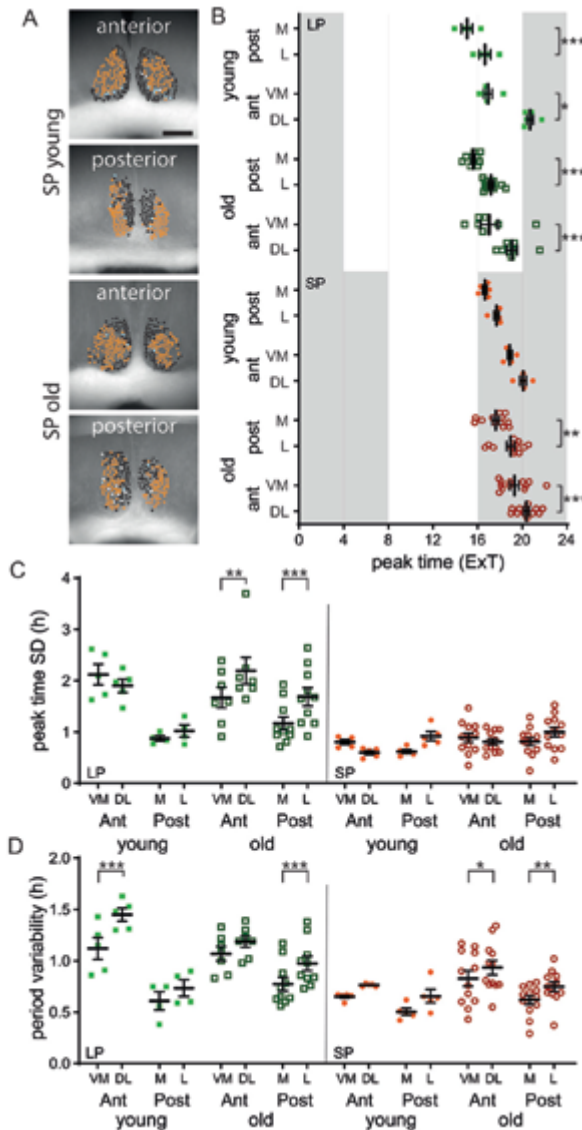


Figure 4. Functional cluster characteristics are similar in the old and young SCN. A. Cell cluster location projected on bright-field image of the SCN. The different shades represent the different clusters. Examples are given for the short photoperiod (SP) of young and old mice of both the anterior and posterior slice. Scale bar marks 200 μm . B. Average peak time of PER2::LUC rhythms for the ventromedial (VM) and medial (M), as well as the dorsolateral (DL) and lateral (L) cluster of the SCN of young and old mice entrained to either the long photoperiod (LP) or SP, plotted as external time (Ext). C. Phase distribution of peak times for the VM/M and DL/L cluster in the anterior and posterior SCN of young and old mice adapted to the LP and SP. D. Single-cell period variability for the VM/M and DL/L cluster in the anterior and posterior SCN of young and old mice adapted to the LP and SP. LP: anterior: young: $n = 5$, old: $n = 7$, posterior: young: $n = 4$, old: $n = 10$; SP: anterior: young: $n = 5$, old: $n = 12$, posterior: young: $n = 5$, old: $n = 12$. Filled circles represent SP, young; open circles represent SP, old; filled squares represent LP, young; open squares represent LP, old. Bars indicate mean \pm SD. * $P < 0.05$, ** $P < 0.01$, *** $P < 0.001$, 1-way analysis of variance, corrected for multiple comparison with Sidak's test.

table S4). Interestingly, like in our previous study there is a significant difference between de VM and DL cluster in young mice exposed to LP. However, this difference is absent in old mice (Figure 4D; Sidak's test, anterior SCN LP: in young, DL vs VM cluster, $P < 0.01$; in old, DL vs VM cluster, *n.s.*; table S4). Taken together it seems that there are small changes in PER2 rhythm characteristics of clusters of neurons in the old compared to the young SCN.

4. DISCUSSION

It is well known that with aging sleep patterns and circadian rhythms get increasingly disturbed (Dijk and Duffy, 1999; Dijk et al., 1999). Moreover, elderly humans seem less capable to adjust to shift work and changing of the seasons (Harma et al., 1994; Cepeda et al., 2018). However, it remains unclear which processes regulating circadian rhythms underlie this decreased flexibility. Therefore, we investigated the plasticity of both behavior and PER2::LUC expression rhythms in the young and old SCN under different lighting conditions. We show that aging does not affect PER2::LUC expression rhythms in an equinoctial light regime, while – in line with previous findings – behavioral rhythm strength is affected, (Asai et al., 2001; Yamazaki et al., 2002; Kolker et al., 2003; Nakamura et al., 2011; Sellix et al., 2012; Leise et al., 2013). Considering that the old SCN neuronal network might be more rigid, we wanted to assess its adaptability by exposure to changes in day-length, since this requires plasticity of the SCN network (VanderLeest et al., 2007; Porcu et al., 2018). We show that aged mice are less capable of adapting their locomotor behavioral pattern to changes in photoperiod, compared to young mice. Surprisingly, the PER2::LUC expression rhythms in the SCN of old mice show similar levels of phase distribution and single-cell period variability as in young mice, with a wider phase distribution and higher period variability under long photoperiod, compared to short photoperiod. We do see more variability in these parameters in aging mice, and a general relationship between behavioral adaptation to photoperiod and PER2::LUC period variability. These results indicate that most of the plasticity of the molecular clock remains intact in the old SCN, and deficits in photoperiod adaptation arise downstream from the molecular clock.

4.1. Aging affects behavioral adaptation to photoperiod

To our knowledge, this is the first study that investigates the effect of exposure to long and short photoperiods on the behavior and PER2 expression in old mice. Our results on locomotor behavior in different photoperiods corroborate previous studies reporting impairment of circadian entrainment in aged rodents. Scarbrough and colleagues showed that in Syrian hamsters aging attenuates the effect of short photoperiod, as it did for the mice in our study (Scarbrough et al., 1997). Aging is shown to reduce the sensitivity to light, which might explain the impairment in circadian entrainment (Zhang et al., 1996; Benloucif et al., 1997; Biello et al., 2018), and in re-entrainment to changes in the light-dark cycle that we and others report (Valentinuzzi et al., 1997; Farajnia et al., 2012; Sellix et al., 2012).

4.2. Aging has little effect on PER2::LUC rhythms in the SCN in different photoperiods

In line with our results, previous studies have found no effect of aging on the peak time of PER2 rhythm in the SCN (Asai et al., 2001; Yamazaki et al., 2002; Kolker et al., 2003; Nakamura et al., 2011; Sellix et al., 2012; Leise et al., 2013), and no effect on peak time distribution (Sellix et al., 2012). Studies that examined PER2 expression in both the SCN and peripheral clocks have found that, while the SCN retains its phase, organs like the spleen and thymus peak significantly earlier in old, compared to young mice (Sellix et al., 2012; Leise et al., 2013). In addition, the SCN of old mice still responds relatively similar to a phase shift in the light-dark cycle as young mice, while their behavioral response, as well as PER2 expression in peripheral tissue is markedly delayed (Sellix et al., 2012; Leise et al., 2013). The molecular clock of the SCN only started to show signs of decay when exposed to constant darkness or constant light (Nakamura et al., 2015; Polidarova et al., 2017). Therefore, in this study we wanted to provoke the SCN of old mice by exposure to a naturally recurring challenge of the SCN network, namely the seasonal changes in photoperiod (Buijink et al., 2016). We found no effect of this challenge in overall rhythm characteristics of PER2::LUC. In young and old mice, and in both LP and SP, the PER2::LUC expression in the anterior SCN peaks later than in the posterior SCN, and peak time SD and period variability show a similar increase in the anterior SCN for both young and old mice (Figure 3).

Studies on aging clock have previously revealed a reorganization of the neuronal (Farajnia et al., 2012) and molecular networks (Chen et al., 2016). We therefore performed a detailed analysis of clusters of neurons in the SCN, using an unbiased method we used previously to show differences in neuronal networks in the SCN (Buijink et al., 2016; Almog et al., 2019). This analysis reconfirms the results from our previous study, and also reveals some small differences in peak time and period variability between the young and old SCN. These data suggest that there are some small changes on the network level of the SCN. Taken together, both our and previous studies on PER2 expression in the SCN have not found rigorous effects of aging, which remains surprising, given that there are strong effects of aging on other SCN neuronal components, as well as on PER2 expression in peripheral clocks.

4.3. Diverse effects of aging on the molecular clock of the SCN

Previous studies investigating other core clock genes in the SCN have failed to decisively show deficits in the molecular clock due to aging. Studies consistently show no age-related changes in the expression of the clock gene *Per1* and a decay in expression of the clock gene *Bmal1* (Asai et al., 2001; Weinert et al., 2001; Yamazaki et al., 2002; Kolker et al., 2003; Wyse and Coogan, 2010; Chang and Guarente, 2013; Bonaconsa et al., 2014). On the other hand, these studies have reported contradicting results on the effect of aging on the expression level of other clock genes, like *Per2*, *Cry1*, *Cry2*, and *Clock* (see Banks et al., 2016 for a detailed account). For PER2::LUC, there are two recent studies that did find an effect of aging on PER2::LUC expression. Nakamura and colleagues found that constant darkness results in a faster decay of the amplitude, and a spread of single-cell phases of PER2 expression rhythms in the SCN of old compared to young mice, although only

after more than 24 hours *in vitro* (Nakamura et al., 2015). Polidarova and colleagues (2017) found that after exposure to constant light, there was a higher incidence in arrhythmicity in PER2::LUC expression. However, only 7 out of 15 old animals showed arrhythmic patterns (up from 3/15 in young animals) and only in one of the two slices extracted per animal (Polidarova et al., 2017). Interestingly, these two studies found no aging-induced deficits in PER2 rhythms in the regular LD 12:12, only after challenging the system with constant light or constant darkness. These data suggest that the molecular clock in the old SCN is robust enough to adapt to the substantial changes in photoperiod we used, nonetheless, the unaffected molecular clock does not alleviate the deficits seen in behavior.

4.4. Aging affects cellular and network properties of the SCN

Despite the apparent lack of effects of aging on the molecular clock we have reported here, there is mounting evidence that the SCN plays an important role in aged-related disruptions of circadian behavior on multiple levels. (1) The observation that age-related alterations in behavioral rhythmicity can be reversed by transplanting fetal SCN tissue in aged animals, suggests that the SCN plays an important role in inducing aging associated behavioral changes (Van Reeth et al., 1994; Cai et al., 1997; Hurd and Ralph, 1998). (2) The amplitude of the SCN multiunit electrical activity signal, both *in vivo* and *ex vivo*, decreases in aged mice (Watanabe et al., 1995; Nakamura et al., 2011; Farajnia et al., 2012). This decrease in amplitude can be the result of a change in phase synchrony, since a subpopulation of SCN neurons peaks in anti-phase to the main activity peak in SCN slices of old mice (Farajnia et al., 2012). (3) Other electrical properties in SCN neurons also change with age, with alterations in the circadian regulation of ionic currents and cellular membrane deficits, which likely add to the decrease in the SCN's electrical rhythm amplitude (Farajnia et al., 2012; Farajnia et al., 2015). (4) The number of SCN neurons in aged rats remains the same (Rooyendaal et al., 1987; Miller et al., 1989; Madeira et al., 1995), which is in line with our results (Figure S3). However, several morphological changes have been reported, like reduced dendritic thickness and a loss of synapses (Machado-Salas et al., 1977; Palomba et al., 2008). (5) Despite the overall number of neurons being unaffected in the old SCN, the number of arginine vasopressin (AVP) and vasoactive intestinal polypeptide (VIP) expressing neurons is decreased (Rooyendaal et al., 1987; Chee et al., 1988) and the functionality of the main neurotransmitter in the SCN, GABA, is reduced with aging (Palomba et al., 2008; Farajnia et al., 2012). If we assume that the molecular clock is the least affected by aging as the data here and in previous studies suggest, the age-related deficits in clock function leading to the circadian phenotype seem to comprise an impairment of communication between the molecular clockwork and other intracellular clock-components of SCN neurons. This may subsequently lead to neuronal network alterations, resulting in the observed deficits in the circadian behavior.

4.5. Weakened link between the molecular clock and the SCN network in aging

The available data suggest that with aging the molecular clock continues to function normally in SCN neurons, while the SCN network is weakened at the level of electrical activity and neurotransmitters. The lower amplitude output-signal of the SCN reduces its ability to drive peripheral circadian

rhythms. However, this raises the question how the molecular clock can become dissociated from the other clock-components of the SCN and at what level communication between the SCN network and the molecular clock is altered in aging. Interestingly, a recent study showed a functional dissociation between the molecular clock in the SCN, and its downstream targets: in lactating mice, rhythms in electrical activity within the SCN as well as in the periphery were dampened, while molecular oscillations were unchanged, retaining the ability for circadian timekeeping (Abitbol et al., 2017). In addition, a modeling study of the SCN neuronal network predicts that differential GABAergic signaling can dissociate the electrical activity of SCN neurons and their molecular clock (DeWoskin et al., 2015). Other recent studies show that with the loss of the SCN network, circadian rhythms in electrical activity, calcium, and the molecular clock can become dissociated from each other (Enoki et al., 2017a; Enoki et al., 2017b; Noguchi et al., 2017). When the network strength is reduced between SCN neurons by either blocking action potentials or a lack of connections in low-density neuronal cultures, electrical activity has less influence on calcium and PER2 expression rhythms (Noguchi et al., 2017).

In SCN neurons, calcium is an important mediator of signals from the membrane to the molecular clock and vice versa (Lundkvist et al., 2005; Enoki et al., 2017b). We have previously shown that aging reverses the rhythm in intracellular calcium levels in SCN neurons with higher values in the night instead of the day (Farajnia et al., 2015). Therefore, we suggest that calcium homeostasis is disturbed in the aged SCN, leading to a weakening of the link between the molecular clock and the SCN network in both directions. However, the question remains how the SCN neurons are still able to adjust their phase distribution when their main modes of communication are disrupted. Further studies will be needed to elucidate the effect of aging on communication between network and the molecular clock, and its effect on calcium homeostasis to determine if this could be a target for strengthening circadian rhythmicity.

ACKNOWLEDGEMENTS

We would like to thank Gabriella Lundkvist for providing PER2::LUC knock-in mice, and Mayke Tersteeg for technical support and animal care. This study was supported by funding from the Netherlands Foundation of Technology (STW; ONTIME 12191) and the Velux Foundation (project grant 1029 to S.M).

REFERENCES

1. Abitbol K, Debiec S, Molino F, Mesirca P, Bidaud I, Minami Y, Mangoni ME, Yagita K, Mollard P, and Bonnefont X (2017) Clock-dependent and system-driven oscillators interact in the suprachiasmatic nuclei to pace mammalian circadian rhythms. *PLoS One*, 12, e0187001.
2. Almog A, Buijink MR, Roethler O, Michel S, Meijer JH, Rohling JHT, and Garlaschelli D (2019) Uncovering functional signature in neural systems via random matrix theory. *PLoS Comput. Biol.*, 15, e1006934.
3. Asai M, Yoshinobu Y, Kaneko S, Mori A, Nikaido T, Moriya T, Akiyama M, and Shibata S (2001) Circadian profile of Per gene mRNA expression in the suprachiasmatic nucleus, paraventricular nucleus, and pineal body of aged rats. *J. Neurosci. Res.*, 66, 1133-1139.
4. Azzi A, Dallmann R, Casserly A, Rehrauer H, Patrignani A, Maier B, Kramer A, and Brown SA (2014) Circadian behavior is light-reprogrammed by plastic DNA methylation. *Nat. Neurosci.*, 17, 377-382.
5. Banks G, Nolan PM, and Peirson SN (2016) Reciprocal interactions between circadian clocks and aging. *Mamm. Genome*, 27, 332-340.
6. Benloucif S, Masana MI, and Dubocovich ML (1997) Light-induced phase shifts of circadian activity rhythms and immediate early gene expression in the suprachiasmatic nucleus are attenuated in old C3H/HeN mice. *Brain Res.*, 747, 34-42.
7. Biello SM, Bonsall DR, Atkinson LA, Molyneux PC, Harrington ME, and Lall GS (2018) Alterations in glutamatergic signaling contribute to the decline of circadian photoentrainment in aged mice. *Neurobiol. Aging*, 66, 75-84.
8. Bonaconsa M, Malpeli G, Montaruli A, Carandente F, Grassi-Zucconi G, and Bentivoglio M (2014) Differential modulation of clock gene expression in the suprachiasmatic nucleus, liver and heart of aged mice. *Exp. Gerontol.*, 55, 70-79.
9. Buijink MR, Almog A, Wit CB, Roethler O, Olde Engberink AH, Meijer JH, Garlaschelli D, Rohling JH, and Michel S (2016) Evidence for Weakened Intercellular Coupling in the Mammalian Circadian Clock under Long Photoperiod. *PLoS one*, 11, e0168954.
10. Cai A, Lehman MN, Lloyd JM, and Wise PM (1997) Transplantation of fetal suprachiasmatic nuclei into middle-aged rats restores diurnal Fos expression in host. *Am. J. Physiol.*, 272, R422-428.
11. Carvalho-Bos SS, Riemersma-van der Lek RF, Waterhouse J, Reilly T, and Van Someren EJ (2007) Strong association of the rest-activity rhythm with well-being in demented elderly women. *Am. J. Geriatr. Psychiatry*, 15, 92-100.
12. Cepeda M, Koolhaas CM, van Rooij FJA, Tiemeier H, Guxens M, Franco OH, and Schoufour JD (2018) Seasonality of physical activity, sedentary behavior, and sleep in a middle-aged and elderly population: The Rotterdam study. *Maturitas*, 110, 41-50.
13. Chang HC, and Guarente L (2013) SIRT1 mediates central circadian control in the SCN by a mechanism that decays with aging. *Cell*, 153, 1448-1460.
14. Chee CA, Roozendaal B, Swaab DF, Goudsmit E, and Mirmiran M (1988) Vasoactive intestinal polypeptide neuron changes in the senile rat suprachiasmatic nucleus. *Neurobiol. Aging*, 9, 307-312.
15. Chen CY, Logan RW, Ma T, Lewis DA, Tseng GC, Sibille E, and McClung CA (2016) Effects of aging on circadian patterns of gene expression in the human prefrontal cortex. *Proc. Natl. Acad. Sci. USA*, 113, 206-211.
16. Chen Z, Yoo SH, and Takahashi JS (2018) Development and Therapeutic Potential of Small-Molecule Modulators of Circadian Systems. *Annu. Rev. Pharmacol. Toxicol.*, 58, 231-252.
17. Davidson AJ, Sellix MT, Daniel J, Yamazaki S, Menaker M, and Block GD (2006) Chronic jet-lag increases mortality in aged mice. *Curr. Biol.*, 16, R914-916.
18. DeWoskin D, Myung J, Belle MD, Piggins HD, Takumi T, and Forger DB (2015) Distinct roles for GABA across multiple timescales in mammalian circadian timekeeping. *Proc. Natl. Acad. Sci. USA*, 112, E3911-3919.
19. Dijk DJ, and Duffy JF (1999) Circadian regulation of human sleep and age-related changes in its timing, consolidation and EEG characteristics. *Ann. Med.*, 31, 130-140.
20. Dijk DJ, Duffy JF, Riel E, Shanahan TL, and Czeisler CA (1999) Ageing and the circadian and homeostatic regulation of human sleep during

- forced desynchrony of rest, melatonin and temperature rhythms. *J. Physiol.*, 516, 611-627.
21. Dubrovsky YV, Samsa WE, and Kondratov RV (2010) Deficiency of circadian protein CLOCK reduces lifespan and increases age-related cataract development in mice. *Aging*, 2, 936-944.
 22. Enoki R, Oda Y, Mieda M, Ono D, Honma S, and Honma KI (2017a) Synchronous circadian voltage rhythms with asynchronous calcium rhythms in the suprachiasmatic nucleus. *Proc. Natl. Acad. Sci. USA*, 114, E2476-E2485.
 23. Enoki R, Ono D, Kuroda S, Honma S, and Honma KI (2017b) Dual origins of the intracellular circadian calcium rhythm in the suprachiasmatic nucleus. *Sci. Rep.*, 7, 41733.
 24. Farajnia S, Meijer JH, and Michel S (2015) Age-related changes in large-conductance calcium-activated potassium channels in mammalian circadian clock neurons. *Neurobiol. Aging*, 36, 2176-2183.
 25. Farajnia S, Michel S, Deboer T, vanderLeest HT, Houben T, Rohling JH, Ramkisoensing A, Yassenkov R, and Meijer JH (2012) Evidence for neuronal desynchrony in the aged suprachiasmatic nucleus clock. *J. Neurosci.*, 32, 5891-5899.
 26. Froy O (2011) Circadian rhythms, aging, and life span in mammals. *Physiol.*, 26, 225-235.
 27. Gaikwad S (2018) The biological clock: Future of neurological disorders therapy. *Neural. Regen. Res.*, 13, 567-568.
 28. Harma MI, Hakola T, Akerstedt T, and Laitinen JT (1994) Age and adjustment to night work. *Occup. Environ. Med.*, 51, 568-573.
 29. Herzog ED, Kiss IZ, and Mazuski C (2015) Measuring synchrony in the mammalian central circadian circuit. *Methods Enzymol.*, 552, 3-22.
 30. Hurd MW, and Ralph MR (1998) The significance of circadian organization for longevity in the golden hamster. *J. Biol. Rhythms*, 13, 430-436.
 31. Kawakami F, Okamura H, Tamada Y, Maebayashi Y, Fukui K, and Ibata Y (1997) Loss of day-night differences in VIP mRNA levels in the suprachiasmatic nucleus of aged rats. *Neurosci. Lett.*, 222, 99-102.
 32. Kolker DE, Fukuyama H, Huang DS, Takahashi JS, Horton TH, and Turek FW (2003) Aging alters circadian and light-induced expression of clock genes in golden hamsters. *J. Biol. Rhythms*, 18, 159-169.
 33. Kondratov RV, Kondratova AA, Gorbacheva VY, Vykhovanets OV, and Antoch MP (2006) Early aging and age-related pathologies in mice deficient in BMAL1, the core component of the circadian clock. *Genes Dev.*, 20, 1868-1873.
 34. Leise TL, Harrington ME, Molyneux PC, Song I, Queenan H, Zimmerman E, Lall GS, and Biello SM (2013) Voluntary exercise can strengthen the circadian system in aged mice. *Age (Dordr)*, 35, 2137-2152.
 35. Leng Y, Musiek ES, Hu K, Cappuccio FP, and Yaffe K (2019) Association between circadian rhythms and neurodegenerative diseases. *Lancet Neurol.*, 18, 307-318.
 36. Lundkvist GB, Kwak Y, Davis EK, Tei H, and Block GD (2005) A calcium flux is required for circadian rhythm generation in mammalian pacemaker neurons. *J. Neurosci.*, 25, 7682-7686.
 37. Machado-Salas J, Scheibel ME, and Scheibel AB (1977) Morphologic changes in the hypothalamus of the old mouse. *Exp. Neurol.*, 57, 102-111.
 38. Madeira MD, Sousa N, Santer RM, Paula-Barbosa MM, and Gundersen HJ (1995) Age and sex do not affect the volume, cell numbers, or cell size of the suprachiasmatic nucleus of the rat: an unbiased stereological study. *J. Comp. Neurol.*, 361, 585-601.
 39. Miller MM, Gould BE, and Nelson JF (1989) Aging and long-term ovariectomy alter the cytoarchitecture of the hypothalamic-preoptic area of the C57BL/6J mouse. *Neurobiol. Aging*, 10, 683-690.
 40. Most El, Scheltens P, and Van Someren EJ (2010) Prevention of depression and sleep disturbances in elderly with memory-problems by activation of the biological clock with light--a randomized clinical trial. *Trials*, 11, 19.
 41. Nakamura TJ, Nakamura W, Tokuda IT, Ishikawa T, Kudo T, Colwell CS, and Block GD (2015) Age-Related Changes in the Circadian System Unmasked by Constant Conditions. *eNeuro*, 2, 1-10.
 42. Nakamura TJ, Nakamura W, Yamazaki S, Kudo T, Cutler T, Colwell CS, and Block GD (2011) Age-related decline in circadian output. *J. Neurosci.*, 31, 10201-10205.
 43. Noguchi T, Leise TL, Kingsbury NJ, Diemer T, Wang LL, Henson MA, and Welsh DK (2017) Calcium Circadian Rhythmicity in

- the Suprachiasmatic Nucleus: Cell Autonomy and Network Modulation. *eNeuro*, 4, 1-12.
44. Nygard M, and Palomba M (2006) The GABAergic network in the suprachiasmatic nucleus as a key regulator of the biological clock: does it change during senescence? *Chronobiol. intern.*, 23, 427-435.
 45. Palomba M, Nygard M, Florenzano F, Bertini G, Kristensson K, and Bentivoglio M (2008) Decline of the presynaptic network, including GABAergic terminals, in the aging suprachiasmatic nucleus of the mouse. *J. Biol. Rhythms*, 23, 220-231.
 46. Pittendrigh CS, and Daan S (1976) Functional-Analysis of Circadian Pacemakers in Nocturnal Rodents. 1. Stability and Lability of Spontaneous Frequency. *J. Comp. Physiol.*, 106, 223-252.
 47. Polidarova L, Sladek M, Novosadova Z, and Sumova A (2017) Aging does not compromise in vitro oscillation of the suprachiasmatic nuclei but makes it more vulnerable to constant light. *Chronobiol. Int.*, 34, 105-117.
 48. Porcu A, Riddle M, Dulcis D, and Welsh DK (2018) Photoperiod-Induced Neuroplasticity in the Circadian System. *Neural. Plast.*, 2018, 5147585.
 49. Rolden HJ, Rohling JH, van Bodegom D, and Westendorp RG (2015) Seasonal Variation in Mortality, Medical Care Expenditure and Institutionalization in Older People: Evidence from a Dutch Cohort of Older Health Insurance Clients. *PLoS One*, 10, e0143154.
 50. Roozendaal B, van Gool WA, Swaab DF, Hoogendijk JE, and Mirmiran M (1987) Changes in vasopressin cells of the rat suprachiasmatic nucleus with aging. *Brain res.*, 409, 259-264.
 51. Scarbrough K, Losee-Olson S, Wallen EP, and Turek FW (1997) Aging and photoperiod affect entrainment and quantitative aspects of locomotor behavior in Syrian hamsters. *Am. J. Physiol.*, 272, R1219-1225.
 52. Sellix MT, Evans JA, Leise TL, Castanon-Cervantes O, Hill DD, DeLisser P, Block GD, Menaker M, and Davidson AJ (2012) Aging differentially affects the re-entrainment response of central and peripheral circadian oscillators. *J. Neurosci.*, 32, 16193-16202.
 53. Valentinuzzi VS, Scarbrough K, Takahashi JS, and Turek FW (1997) Effects of aging on the circadian rhythm of wheel-running activity in C57BL/6 mice. *Am. J. Physiol.*, 273, R1957-1964.
 54. Van Reeth O, Zhang Y, Zee PC, and Turek FW (1994) Grafting fetal suprachiasmatic nuclei in the hypothalamus of old hamsters restores responsiveness of the circadian clock to a phase shifting stimulus. *Brain Res.*, 643, 338-342.
 55. VanderLeest HT, Houben T, Michel S, Deboer T, Albus H, Vansteensel MJ, Block GD, and Meijer JH (2007) Seasonal encoding by the circadian pacemaker of the SCN. *Curr. Biol.*, 17, 468-473.
 56. Watanabe A, Shibata S, and Watanabe S (1995) Circadian rhythm of spontaneous neuronal activity in the suprachiasmatic nucleus of old hamster in vitro. *Brain Res.*, 695, 237-239.
 57. Weinert H, Weinert D, Schurov I, Maywood ES, and Hastings MH (2001) Impaired expression of the mPer2 circadian clock gene in the suprachiasmatic nuclei of aging mice. *Chronobiol. Int.*, 18, 559-565.
 58. Wyse CA, and Coogan AN (2010) Impact of aging on diurnal expression patterns of CLOCK and BMAL1 in the mouse brain. *Brain Res.*, 1337, 21-31.
 59. Yamazaki S, Straume M, Tei H, Sakaki Y, Menaker M, and Block GD (2002) Effects of aging on central and peripheral mammalian clocks. *Proc. Natl. Acad. Sci. USA* 99, 10801-10806.
 60. Zhang Y, Kornhauser JM, Zee PC, Mayo KE, Takahashi JS, and Turek FW (1996) Effects of aging on light-induced phase-shifting of circadian behavioral rhythms, fos expression and CREB phosphorylation in the hamster suprachiasmatic nucleus. *Neurosci.* 70, 951-961.

SUPPLEMENTARY MATERIALS

3

Table S1. Summary results PER2 expression in SCN slices from young and old mice in LD 12:12

Fig.	Location	Young			Old		
		<i>n</i>	ANOVA ant-post	ANOVA ant-post	<i>n</i>	ANOVA ant-post	ANOVA ant-post
1B	Anterior	6	18.90 ± 1.33	n.s.	6	18.83 ± 1.28	n.s.
	Posterior	6	17.81 ± 1.37	n.s.	6	17.95 ± 1.04	n.s.
1C	Anterior	6	24.57 ± 0.28	n.s.	6	24.40 ± 0.21	n.s.
	Posterior	6	24.58 ± 0.41	n.s.	6	24.27 ± 0.38	n.s.
1D	Anterior	6	1.45 ± 0.45	n.s.	6	1.03 ± 0.12	n.s.
	Posterior	6	1.26 ± 0.23	n.s.	6	0.95 ± 0.21	n.s.
1E	Anterior	6	1.05 ± 0.14	<i>p</i> < 0.02	6	0.90 ± 0.20	<i>p</i> < 0.05
	Posterior	6	0.74 ± 0.16		6	0.63 ± 0.16	

Data represent mean ± SD. n.s. = not significant.

Table S2. Summary results behavioral adaptation to different photoperiod in young and old mice

Fig.	rhythm strengt	alpha (h)	Tau (h)	Δ alpha 12:12 - DD (h)	Young				Old												
					12:12	LP	n	ANOVA	SP	12:12	LP	n	ANOVA	SP							
2B	rhythm strengt	12:12	0.2 ± 0.04	12																	
2C	alpha (h)	PP1	11.81 ± 0.61	6	p < 0.0001				12.72 ± 0.49	6	p < 0.0001										
		DD	8.69 ± 0.51	6	p < 0.0001	p < 0.0001			14.80 ± 0.76	6	n.s.	p < 0.0001									
		PP2	10.17 ± 0.63	6	p < 0.01	n.s.			15.06 ± 0.81	6	n.s.	n.s.									
		DD	9.08 ± 0.31	6					15.31 ± 0.46	6											
2D	Tau (h)		23.63 ± 0.15	6				23.97 ± 0.04	6										p < 0.001		
2E	Δ alpha 12:12 - DD (h)		-1.64 ± 0.42	6				2.34 ± 0.84	6										p < 0.001		
Old																					
2B	rhythm strengt	12:12	0.17 ± 0.04	18																	
2C	alpha (h)	PP1	12.48 ± 0.46	7	p < 0.0001				12.56 ± 0.50	8	n.s.										
		DD	9.31 ± 0.75	7	p < 0.0001	p < 0.001			13.17 ± 0.82	8	n.s.	n.s.								n.s.	
		PP2	11.26 ± 0.57	7	p < 0.0001	n.s.			12.90 ± 1.00	8	n.s.	n.s.									n.s.
		DD	9.48 ± 0.85	7					13.08 ± 1.11	8											
2D	Tau (h)		23.79 ± 0.17	7				23.95 ± 0.11	8											n.s.	
2E	Δ alpha 12:12 - DD (h)		-1.22 ± 0.87	7				0.34 ± 0.86	8											p < 0.01	
young-old																					
																		12:12	LP	SP	
																		p < 0.05			

Data represent mean ± SD. n.s. = not significant.

Table S3. Summary results PER2 expression in SCN slices from young and old mice under different photoperiod

Fig.	Location	Young				Old			
		LP	ANOVA ant-post	SP	n	LP	ANOVA ant-post	SP	n
3B	anterior	18.58 ± 0.46	p < 0.001	19.54 ± 0.57	5	18.79 ± 1.48	p < 0.001	19.88 ± 0.95	9
	posterior	16.05 ± 0.88		17.18 ± 0.41	5	16.38 ± 0.56		18.29 ± 1.16	11
3C	anterior	24.61 ± 0.32	n.s.	24.60 ± 0.22	5	24.37 ± 0.29	n.s.	24.51 ± 0.33	9
	posterior	24.38 ± 0.21		23.94 ± 0.12	5	24.46 ± 0.17		24.27 ± 0.31	11
3D	anterior	2.72 ± 0.25	p < 0.001	0.92 ± 0.15	5	2.60 ± 0.70	p < 0.001	1.18 ± 0.29	9
	posterior	1.28 ± 0.28		0.94 ± 0.17	4	1.59 ± 0.45		1.14 ± 0.25	11
3E	anterior	1.31 ± 0.17	p < 0.001	0.71 ± 0.02	5	1.26 ± 0.29	p < 0.001	0.87 ± 0.23	9
	posterior	0.75 ± 0.21		0.59 ± 0.08	5	0.83 ± 0.25		0.66 ± 0.17	11
3B	anterior								
	posterior								
3C	anterior								
	posterior								
3D	anterior								
	posterior								
3E	anterior								
	posterior								

Data represent mean ± SD. n.s. = not significant.

Table S4. Summary results PER2 expression in SCN slices from young and old mice under different photoperiod

Fig.	Location	Young						Old					
		LP		ANOVA		SP		LP		ANOVA		SP	
		VM-DL / M-L	n	VM-DL / M-L	n	VM-DL / M-L	n	VM-DL / M-L	n	VM-DL / M-L	n	VM-DL / M-L	n
4B	anterior - VM	16.93 ± 0.36	5	p < 0.001	5	18.89 ± 0.21	5	n.s.	n.s.	n.s.	n.s.	n.s.	n.s.
	anterior - DL	20.69 ± 0.28	5		5	20.09 ± 0.29	5	n.s.	n.s.	n.s.	n.s.	n.s.	n.s.
	posterior - M	15.06 ± 0.45	4	p < 0.05	4	16.66 ± 0.20	5	n.s.	n.s.	n.s.	n.s.	n.s.	n.s.
	posterior - L	16.65 ± 0.50	4		4	17.70 ± 0.22	5	n.s.	n.s.	n.s.	n.s.	n.s.	n.s.
	anterior - VM	2.12 ± 0.20	5	n.s.	5	0.81 ± 0.04	5	n.s.	p < 0.001	p < 0.001	p < 0.001	p < 0.001	
	anterior - DL	1.90 ± 0.13	5		5	0.60 ± 0.04	5	n.s.	p < 0.001	p < 0.001	p < 0.001	p < 0.001	
4C	posterior - M	0.88 ± 0.05	4	n.s.	4	0.62 ± 0.04	5	n.s.	n.s.	n.s.	n.s.	n.s.	n.s.
	posterior - L	1.02 ± 0.12	4		4	0.92 ± 0.09	5	n.s.	n.s.	n.s.	n.s.	n.s.	n.s.
	anterior - VM	1.12 ± 0.11	5	p < 0.001	5	0.65 ± 0.02	5	n.s.	n.s.	p < 0.01	p < 0.01	p < 0.01	
	anterior - DL	1.45 ± 0.06	5		5	0.76 ± 0.01	5	n.s.	n.s.	p < 0.001	p < 0.001	p < 0.001	
	posterior - M	0.61 ± 0.09	4	n.s.	4	0.50 ± 0.03	5	n.s.	n.s.	n.s.	n.s.	n.s.	n.s.
	posterior - L	0.74 ± 0.08	4		4	0.66 ± 0.07	5	n.s.	n.s.	n.s.	n.s.	n.s.	n.s.
4D	anterior - VM	17.03 ± 0.78	7	p < 0.001	7	19.23 ± 0.39	12	p < 0.001	p < 0.001	p < 0.001	p < 0.001	n.s.	n.s.
	anterior - DL	19.08 ± 0.47	7		7	20.37 ± 0.26	12	p < 0.001	p < 0.001	p < 0.001	p < 0.001	n.s.	n.s.
	posterior - M	15.61 ± 0.17	10	p < 0.001	10	17.63 ± 0.31	12	p < 0.001	p < 0.001	n.s.	n.s.	n.s.	n.s.
	posterior - L	17.21 ± 0.22	10		10	18.96 ± 0.36	12	p < 0.01	p < 0.01	p < 0.01	p < 0.01	n.s.	n.s.
	anterior - VM	1.67 ± 0.20	7	p < 0.01	7	0.89 ± 0.09	12	n.s.	p < 0.001	p < 0.001	p < 0.001	n.s.	n.s.
	anterior - DL	2.19 ± 0.26	7		7	0.81 ± 0.06	12	n.s.	p < 0.001	p < 0.001	p < 0.001	n.s.	n.s.
	posterior - M	1.17 ± 0.13	10	p < 0.001	10	0.81 ± 0.08	12	n.s.	n.s.	n.s.	p < 0.05	p < 0.05	n.s.
	posterior - L	1.69 ± 0.18	10		10	1.00 ± 0.09	12	p < 0.05	p < 0.05	p < 0.001	p < 0.001	n.s.	n.s.
	anterior - VM	1.07 ± 0.07	7	n.s.	7	0.83 ± 0.07	12	p < 0.05	n.s.	n.s.	n.s.	n.s.	n.s.
	anterior - DL	1.19 ± 0.05	7		7	0.93 ± 0.07	12	n.s.	n.s.	n.s.	n.s.	n.s.	n.s.
	posterior - M	0.77 ± 0.07	10	p < 0.001	10	0.62 ± 0.05	12	p < 0.01	p < 0.01	n.s.	n.s.	n.s.	n.s.
	posterior - L	0.97 ± 0.07	10		10	0.75 ± 0.05	12	p < 0.01	n.s.	n.s.	n.s.	n.s.	n.s.

Data represent mean ± SD. n.s. = not significant.

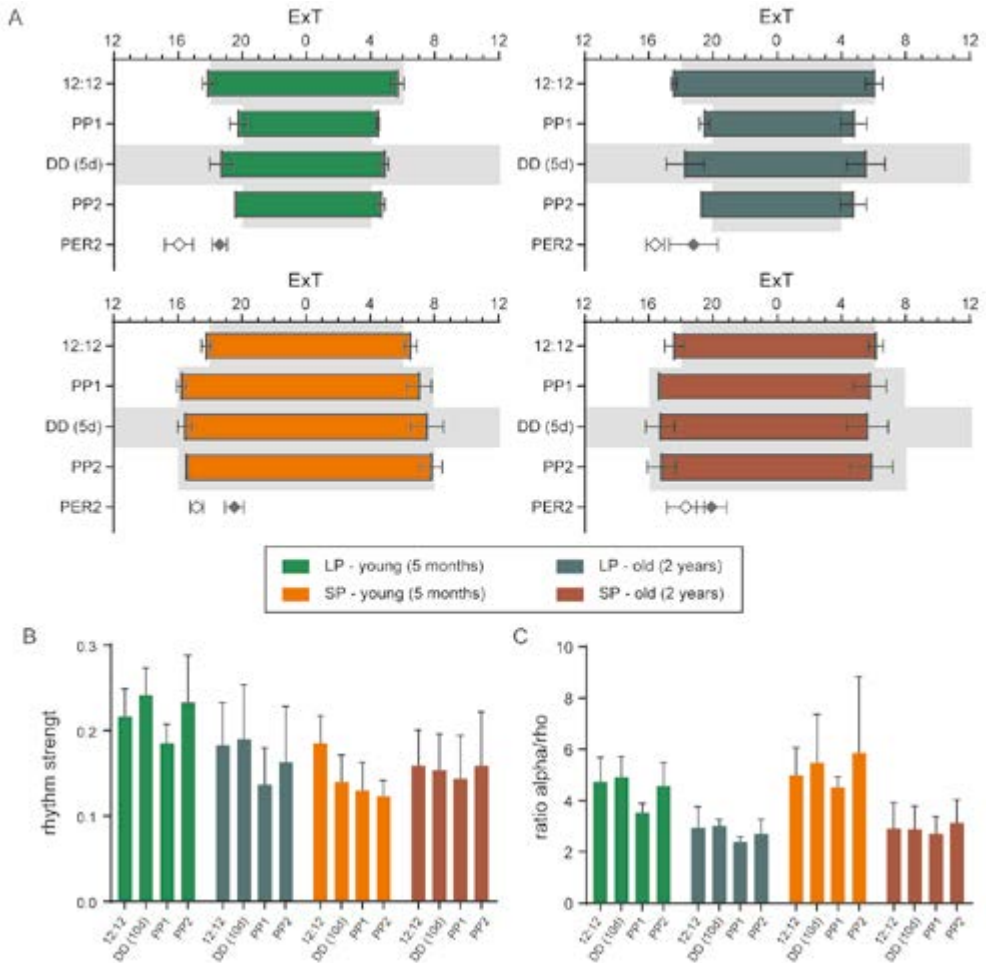


Figure S1. Behavioral changes in aging under different photoperiods. A. Average timing of activity onset and offset \pm SD given for LP (upper panels) and SP (lower panels) and for young (left panels) and old (right panels) during the different photoperiods, plotted with average PER2::LUC peak time for the anterior (filled diamond) and posterior (open diamond) SCN. B. Rhythm strength for the consecutive photoperiods, per experimental condition. C. Ratio of activity to rest (α/ρ) for all light regimes. Black bars indicate mean \pm SD.

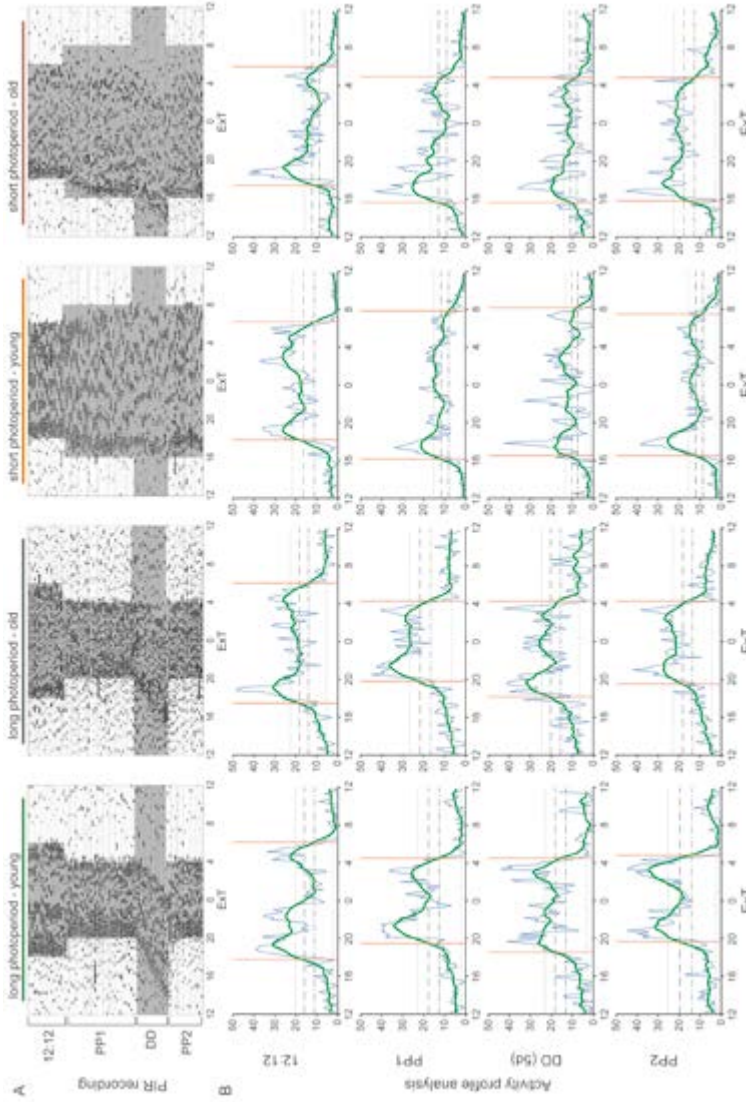


Figure S2. Analysis of activity profiles from PIR recordings for the consecutive photoperiods. A. Single-plotted actograms showing representative PIR recordings of activity from young and old mice adapted to either LP or SP. Shaded areas represent the dark period. Time on the x-axis is given in external time (EXT). B. Activity profiles of 10 consecutive days in LD 12:12 (top row), LP/SP (PP1; second row), 5 days of constant darkness (DD; corrected for Tau; third row), and 10 days on LP/SP (PP2; bottom row). Dark blue lines represent activity profiles (10 min bins), green lines represent smoothed activity profiles (2 hours), lower dotted lines represent L5; (lowest average activity in a 5 h interval), top dotted lines represent M10 (highest average activity in a 10 h interval), dash-dot lines denote $\frac{1}{2}$ value from L5 to M10 (used to determine offset of activity), dashed lines denote $\frac{1}{4}$ value from L5 to M10 (used to determine onset and offset (see Methods)). Red vertical lines show determined onset and offset (see Methods). Time on x-axis given in external time (EXT).

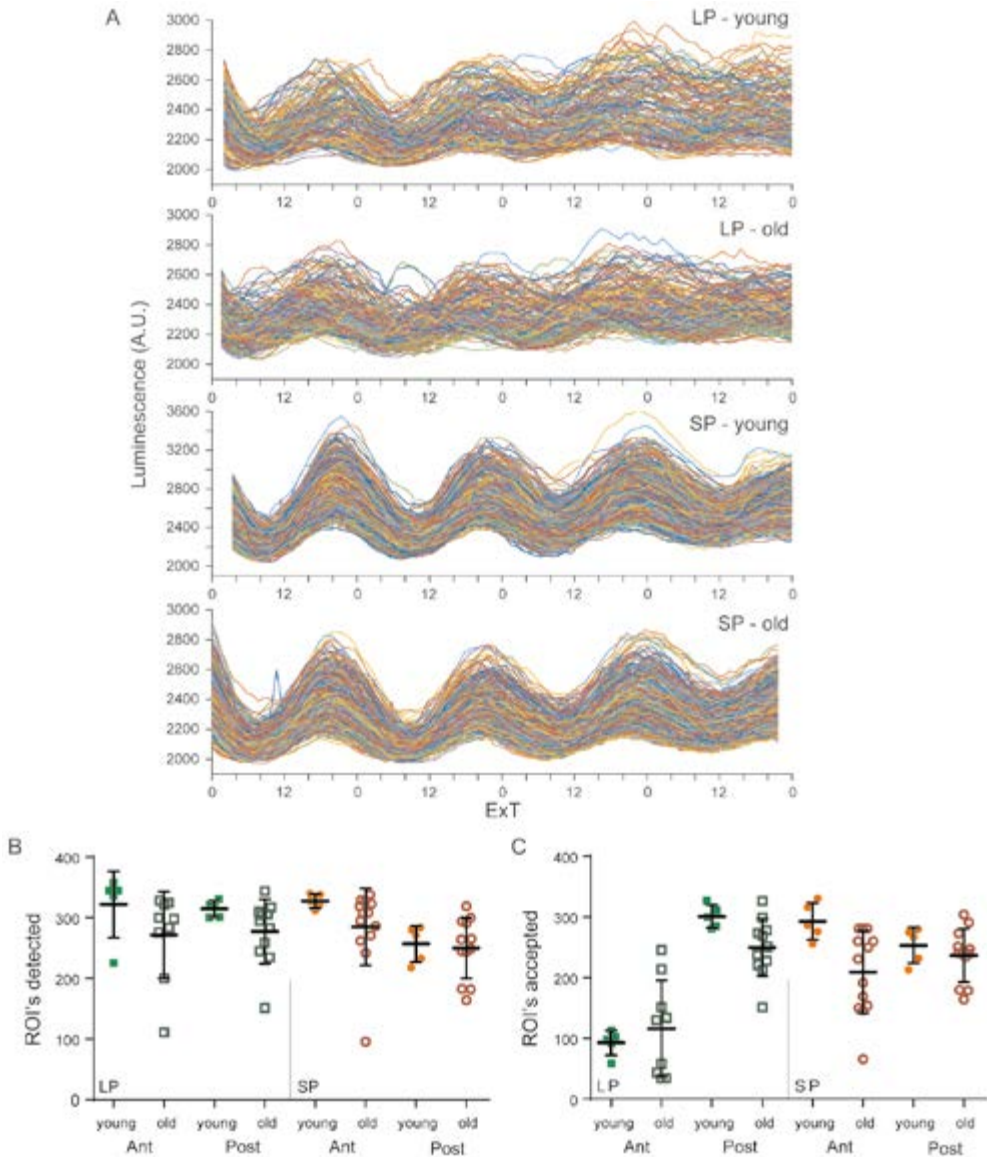


Figure S3. Number of PER2::LUC expressing cells is not altered with aging. A. Examples of raw traces of bioluminescence intensity representing PER2::LUC expression from single cells from the anterior SCN of young and old mice in LP (upper two panels; $n = 113$ cells and $n = 130$ cells) and SP (lower two panels; $n = 316$ cells and $n = 281$ cells). B. Number of ROI's detected in bioluminescence recording per slice of the anterior and posterior SCN from young and old mice, adapted to LP and SP. C. Number of ROI's that were accepted for further analysis per slice of the anterior and posterior SCN from young and old mice, adapted to LP and SP. Black bars indicate mean \pm SD.

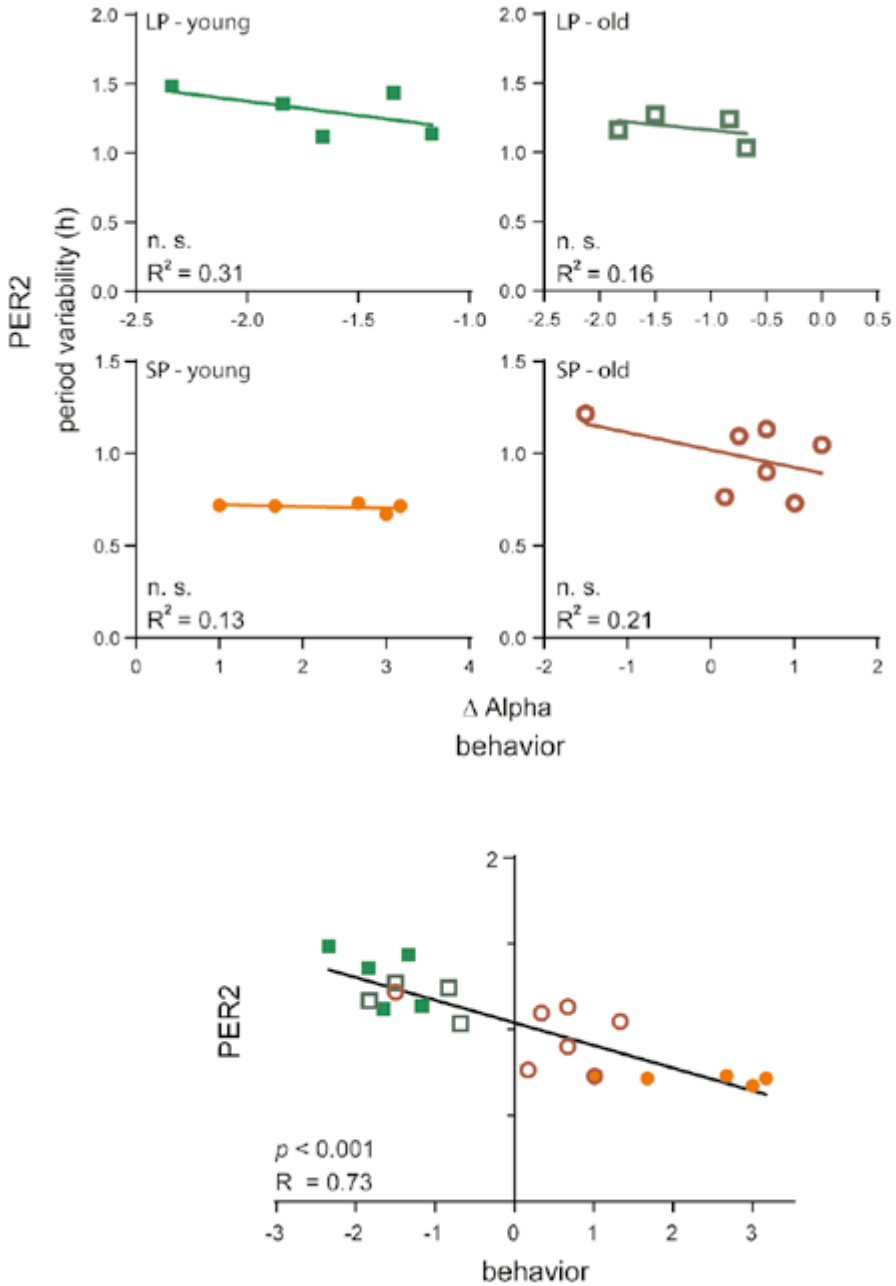


Figure S4. Association between behavior and molecular clock. A. When groups are considered separately, there is no significant correlation between behavior and PER2::LUC expression B. Taking the groups together, there is a clear correlation between the adaptation to photoperiod (alpha) and period variability in PER2::LUC expression in the SCN. Correlations are shown between PER2::LUC phase distribution (peak time SD; see Figure 3D) in the anterior SCN and behavioral adaptation to photoperiod (Δ alpha: LD 12:12 – DD; see Figure 2E) for young LP (upper right panel), old LP (upper left panel), young SP (lower right panel), and old SP (lower left panel). n. s. = slope of correlation not significantly different from zero.



four

AGING AFFECTS GABAERGIC FUNCTION AND CALCIUM LEVELS IN MAMMALIAN CENTRAL CLOCK

Anneke H.O. Olde Engberink¹, Anna Chiosso¹, Johanna H. Meijer¹, Stephan Michel¹

¹Department of Cellular and Chemical Biology, Laboratory for Neurophysiology, Leiden University Medical Center,
Einthovenweg 20, 2333 ZC, Leiden, the Netherlands.

In preparation for submission

ABSTRACT

4

Aging impairs the function of the central circadian clock in mammals, the suprachiasmatic nucleus (SCN), leading to a reduction in the output signal. The weaker timing signal from the SCN results in a decline in rhythm strength in many physiological functions, including sleep-wake patterns. Accumulating evidence suggests that the reduced amplitude of the SCN signal is caused by a decreased synchrony among the SCN neurons. The present study was aimed to investigate the hypothesis that the excitation/inhibition (E/I) balance plays a role in synchronization within the network. Using calcium (Ca^{2+}) imaging, the polarity of Ca^{2+} transients in response to GABA stimulation in SCN slices of old mice (20-24 months) and young controls were studied. We found that the amount of GABAergic excitation was increased, and that concordantly the E/I balance was higher in SCN slices of old mice when compared to young controls. Moreover, we showed an effect of aging on the baseline intracellular Ca^{2+} concentration, with higher Ca^{2+} levels in SCN neurons of old mice, indicating an alteration in Ca^{2+} homeostasis in the aged SCN. We conclude that the change in GABAergic function, and possibly the Ca^{2+} homeostasis, in SCN neurons may contribute to the altered synchrony within the aged SCN network.

1. INTRODUCTION

In mammals, the suprachiasmatic nucleus (SCN) functions as a master circadian clock that drives 24 h rhythms in both physiology and behavior. Based on molecular feedback loops, individual SCN neurons generate ~24 h rhythms in gene expression and cellular processes that in turn regulate electrical activity rhythms (Buhr & Takahashi, 2013; Hastings *et al.*, 2018). This circadian rhythmicity is maintained when the SCN neurons are isolated, demonstrating that single cells function as cell autonomous oscillators (Welsh *et al.*, 1995; Reppert & Weaver, 2002; Welsh *et al.*, 2010). Through synchronization and coupling, these individual SCN neurons produce a coherent output signal in ensemble electrical activity with a peak in the subjective day and a trough in the subjective night, which is conveyed to other brain areas and the periphery (Ramkisoensing & Meijer, 2015). Misalignment of single cell oscillators leads to a disruption or loss of SCN rhythm at the tissue level and consequently to malfunction of peripheral clocks. This can have detrimental effects on human health and is associated with, for instance, cancer, cardiovascular, metabolic, and immune disorders (Roenneberg & Merrow, 2016; Patke *et al.*, 2019). Aging promotes such circadian dysfunction by impacting the clock machinery on different levels (Buijink & Michel, 2020). Vice versa, the dysfunctional circadian clock has detrimental effects on the course of aging and is a risk factor for age-related diseases (Kondratova & Kondratov, 2012; Fonseca Costa & Ripperger, 2015). Understanding age-related mechanisms of clock dysfunction can therefore help identifying targets to intervene in this vicious cycle.

In both human and animal models, age-related changes often lead to a reduction in behavioral activity levels and fragmented sleep-wake rhythms (Dijk & Duffy, 1999; Hofman & Swaab, 2006; Farajnia *et al.*, 2012), a longer latency to re-entrain to shifted light-dark schedules (Biello, 2009; Froy, 2011), and the inability to adapt to a different photoperiod (Buijink *et al.*, 2020). These behavioral deficits are likely the effect of age-related attenuation of the timing signal generated by the SCN network (Oster *et al.*, 2003; Farajnia *et al.*, 2014a).

Both *in vivo* and *ex vivo* studies showed a significant reduction in the amplitude of the ensemble electrical activity rhythm of the aged SCN (Satinoff *et al.*, 1993; Watanabe *et al.*, 1995; Nakamura *et al.*, 2011; Farajnia *et al.*, 2012), which can partly be explained by decreased synchronization within the SCN network. *Ex vivo* electrophysiological recordings of subpopulations in SCN slices of aged mice showed redistribution of phases with a second cluster in the middle of the night. In contrast, peaks in SCN electrical activity in young control slices only clustered around the middle of the day (Farajnia *et al.*, 2012).

An important neurotransmitter that plays a role in synchronization within the SCN network is γ -aminobutyric acid (GABA), which is expressed in almost all SCN neurons (Moore & Speh, 1993; Abrahamson & Moore, 2001). Although the precise role for GABA in the process of synchronization is still under debate (Ono *et al.*, 2020), the number of GABAergic synaptic terminals in the SCN are diminished by 26% due to aging (Palomba *et al.*, 2008) and GABAergic postsynaptic currents are reduced in frequency and amplitude (Nygard *et al.*, 2005; Farajnia *et al.*, 2012). Interestingly, GABA has the ability to act both as an inhibitory and excitatory neurotransmitter in SCN neurons and therefore contributes to plasticity in the excitatory/inhibitory (E/I) balance within the SCN

(Albus *et al.*, 2005; Choi *et al.*, 2008). A narrow control over the E/I balance in neuronal networks is known to be critical for proper brain function and E/I imbalance – often caused by a reduction in GABAergic activity – has been correlated with aging-related deficits and the pathogenesis of several neurodegenerative diseases (Rissman & Mobley, 2011; Legon *et al.*, 2016; Tran *et al.*, 2019; Bruining *et al.*, 2020). The possible effects of aging on the polarity of GABAergic signaling and the corresponding E/I balance in the SCN have not yet been studied.

4

Here, we investigated the aging effect on the GABAergic E/I balance by measuring intracellular calcium levels. Specifically, we determined the polarity of Ca^{2+} transients in response to GABA stimulation in SCN slices of old mice (20-24 months) and young controls during the day, and tested our hypothesis that aging leads to an increment in excitatory responses to GABA. We confirmed that the E/I balance shifted towards more excitation in SCN slices of old mice compared to young controls. Furthermore, we found an effect of aging on the baseline intracellular Ca^{2+} concentration ($[\text{Ca}^{2+}]_i$). The cells measured from the SCN slices of old mice showed a higher $[\text{Ca}^{2+}]_i$ during the day compared to the cells from the young controls.

2. MATERIALS AND METHODS

2.1. Animals and housing

Young (2 – 4 months, N = 11) and old (20 – 24 months, N = 9) male C57BL/6 mice (Janvier Labs, Saint-Berthevin, France) were housed in a climate controlled environment (21 °C, 40-50% humidity) with full-spectrum diffused lighting with an intensity between 50 and 100 lux (Osram truelight TL) and ad libitum access to food and water throughout the experiment. The mice were kept in groups of 2 to 4 mice on an equinoctial photoperiod of 12:12 h light-dark (LD 12:12) cycle. Mice older than 20 months received, in addition to the regular food, hydration and nutritional gels as supportive care. The animals were kept under these conditions for at least 4 weeks prior to the *ex vivo* experiments. *Ex vivo* experiments were performed within a 4 h interval centered around the middle of the day. All animal experiments were performed in accordance with the regulations of the Dutch law on animal welfare, and the institutional ethics committee for animal procedures of the Leiden University Medical Center (Leiden, The Netherlands) approved the protocol (AVD 1160020185524; PE. 18.113.07).

2.2. Slice preparation

After decapitation, brains were quickly removed and placed into modified ice-cold artificial cerebrospinal fluid (ACSF), containing (in mM): NaCl 116.4, KCl 5.4, NaH_2PO_4 1.0, MgSO_4 0.8, CaCl_2 1, MgCl_2 4, NaHCO_3 23.8, glucose 15.1, and 5 mg/L gentamycin (Sigma Aldrich, Munich, Germany) and saturated with 95% O_2 – 5% CO_2 . Coronal hypothalamic slices containing the SCN (250 μm) were cut using a vibratome (VT 1000S, Leica Microsystems, Wetzlar, Germany) and sequentially maintained in a holding chamber containing regular, oxygenated ACSF (CaCl_2 increased to 2 mM and without MgCl_2). The slices were incubated in a water bath (37 °C) for 30 minutes and were then maintained at room temperature until the start of the recordings.

2.3. Ca²⁺ imaging

Neurons in brain slices were bulk-loaded with the ratiometric, membrane permeable Ca²⁺ indicator dye fura-2-acetoxymethyl ester (Fura-2-AM). First, the slices were transferred from the holding chamber to a 35 mm petri dish and reviewed under the microscope. The side of the slide that contained (the larger part of) the SCN was placed up and the ACSF was removed from the petri dish. One drop of highly concentrated Fura-2-AM (998 μM) was placed on the SCN of each slice for 1 minute after which 10 mL of a mix of ACSF containing 7 μM Fura-2-AM was added to the slices. The slices stayed in this mixture for 1 hour on room temperature while maintained saturated with 95% O₂ – 5% CO₂. The slices were then rinsed four times with fresh ACSF before being transferred back into the holding chamber where they stayed another hour on room temperature. After this loading protocol, the slices were moved (one by one) to a recording chamber (RC-26G, Warner Instruments, Hamden, CT, USA) mounted on the fixed stage of an upright fluorescence microscope (Axioskop 2-FS Plus, Carl Zeiss Microimaging, Oberkochen, Germany) and constantly perfused with oxygenated ACSF (2.5 mL/min) at room temperature. The indicator dye was excited alternatively at wavelengths of 340 and 380 nm by means of a monochromator (Polychrome V, TILL Photonics; now FEI Munich GmbH, Munich, Germany). Emitted light (505 nm) was detected by a cooled CCD camera (Sensicam, TILL Photonics; now FEI Munich GmbH, Munich, Germany), and images were acquired at 2 second intervals. The slices settled in the recording chamber for at least 5 minutes before the start of the recordings. After one minute of baseline recording, GABA (200 μM, 15 s) was applied locally using an eight-channel pressurized focal application system (ALA-VM8, ALA scientific instruments, NY, USA), and Ca²⁺ transients were recorded. After two GABA pulses, 1 minute apart, and another minute of recording in which the Ca²⁺ transients returned to baseline, ACSF containing elevated levels of K⁺ (20 mM, 15 s) was applied to identify healthy, responding neurons. Cells with at least 10% increase in [Ca²⁺]_i in response to K⁺ were considered to be healthy. The experiments as well as the analysis were accomplished using imaging software (TILLvision, TILL Photonics; now FEI Munich GmbH, Munich, Germany).

2.4. Data analysis and statistics

Single-wavelength images were background subtracted and ratio images (340/380) were generated. Region of interest-defined cells and mean ratio values were determined, from which the intracellular Ca²⁺ concentration was calculated. Neuronal Ca²⁺ responses were further analyzed using IGOR Pro (WaveMetrics, Portland, OR, USA). Cells with an amplitude less than 10% of baseline values in response to elevated levels of K⁺, or cells with instable (rising or falling) baselines or baselines > 600 nM were excluded from analyses. The transient responses in Ca²⁺ concentration within the first seconds after the stimulation were evaluated, with responses smaller than ± 10% of baseline values defined as non-responding cells. GABA-evoked responses showing Ca²⁺ transients with a decrease in amplitude of more than 10% from baseline were considered inhibitory and responses with an increase of more than 10% from baseline were defined as excitatory. Cells that showed both excitatory and inhibitory responses after a single GABA stimulation were defined as biphasic. Per animal, one to three SCN slices were analyzed and the Ca²⁺ responses to GABA application were

measured in typically 60 – 160 cells. For each animal, the distribution of the different types of responses and the E/I ratio were determined. To calculate the E/I ratio, the number of cells that responded excitatory was divided by the number of cells that responded inhibitory for per animal (i.e. slices from 1 animal were pooled) and averaged per group. In total we measured 924 cells in 27 slices from 9 old mice and 1204 cells in 26 slices from 11 young mice.

Statistical analyses were performed using GraphPad Prism (San Diego, CA, USA). The effect of age on the GABAergic response types was tested per category using the Mann-Whitney U test. The effect on the E/I ratios was tested with two-sided, unpaired t-tests. Lastly, the effect of age on baseline $[Ca^{2+}]_i$ and amplitudes of the GABAergic responses were tested with two-sided, unpaired t-tests with Welch's correction. Differences with $P \leq 0.05$ were considered significant.

3. RESULTS

3.1. GABAergic excitation increased in old SCN

We investigated the effect of aging on the GABAergic activity in SCN neurons by recording GABA-induced single cell Ca^{2+} transients in SCN slices from old (20-24 months) and young (2-4 months) mice (Figure 1A). In each SCN slice, we recorded a combination of transient increases, decreases, or no changes in $[Ca^{2+}]_i$ in response to GABA application. In another subset of SCN neurons we recorded a biphasic response to GABA. The amplitude of the GABAergic responses did not differ between the old and the young SCN neurons (Figure S1, inhibition; old: -66.53 ± 5.39 , $n = 433$, young: -59.87 ± 1.82 , $n = 691$, $P = 0.242$, excitation; old: 58.90 ± 4.32 , $n = 313$, young: 62.73 ± 5.03 , $n = 322$, $P = 0.869$). The percentages of the different GABAergic response types differed between old and young animals. Old SCN slices exhibited significantly more excitatory responses to GABA as compared to SCN slices of young controls (Figure 1B, old: $32.99 \pm 3.17\%$, $n = 9$, young: $23.41 \pm 2.29\%$, $n = 11$, $P = 0.038$). This increase in GABAergic excitation leads to an increase in the E/I balance in old SCN slices, as compared to young SCN slices (Figure 1C, old: 0.80 ± 0.12 , $n = 9$, young: 0.48 ± 0.07 , $n = 11$, $P = 0.034$). These results show that aging affects the polarity of responses to GABA.

3.2. Age-related increase in GABAergic excitation mainly in posterior part of the SCN

Several studies have shown that the amount of GABAergic excitation varies between the different SCN areas in rats (Albus *et al.*, 2005; Choi *et al.*, 2008; Irwin & Allen, 2009). Therefore, we tested whether there were regional differences in the distribution of the GABAergic response types along the anteroposterior and the dorsoventral axis. There were no significant differences in GABAergic responses between the dorsal and ventral SCN, both for the old and young mice (Figure S2). GABAergic response type only showed significant spatial differences in old SCN, but not young, along the anteroposterior axes with more excitatory responses in the posterior slices, as compared to the anterior slices (Figure 2A, 2C and 2D, old; excitation; anterior: $19.66 \pm 1.83\%$, $n = 8$, posterior: $45.05 \pm 6.24\%$, $n = 9$, $P = 0.003$, young; excitation; anterior: $16.37 \pm 2.33\%$, $n = 11$, posterior: $19.98 \pm 4.14\%$, $n = 5$, $P = 0.473$).

When comparing young and old, the posterior part of the SCN was the only region showing significant differences with more GABAergic excitation and less inhibition (Figure 2C and 2D,

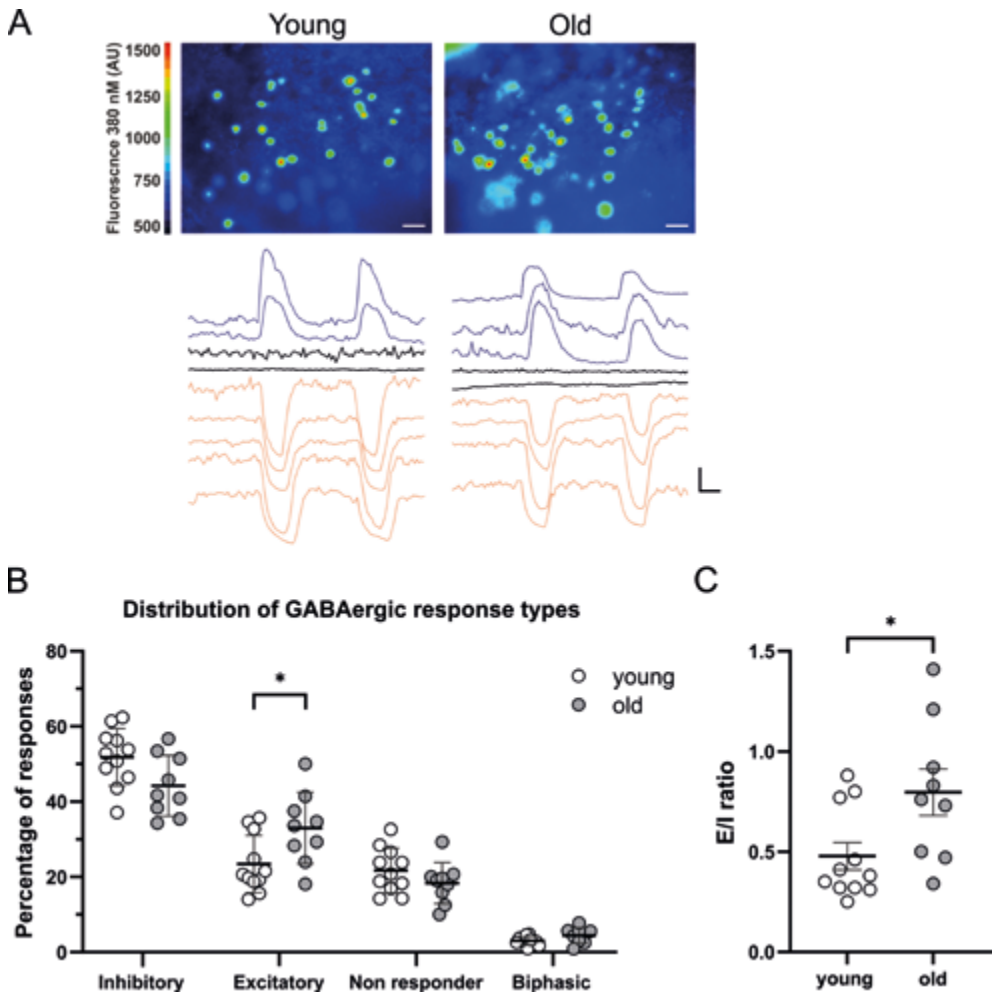


Figure 1. More GABAergic excitation in SCN slices from old mice. A. Upper panels: examples of fura-2-AM loaded SCN neurons in slices from young (left) and old (right) mice. Color scale indicates fluorescence at 380 nm excitation in arbitrary units (Scale bar, 20 μ m). Lower panels: example traces of Ca^{2+} transients in response to two GABA administrations recorded from one SCN slice from a young (left) and old (right) mouse. Excitatory responses are shown in blue, inhibitory responses in orange and non-responding cells in black (Scale bars, 50 nM, 20 s). B. The percentages of inhibitory, excitatory, non-responding, and biphasic cells. Each dot represents the mean percentage of responses per response type per SCN. Every single dot in one response type category adds up to 100% together with the corresponding dots in the other categories. C. E/I ratios in young and old mice, determined by dividing the number of excitatory responses by the number of inhibitory responses measured from each SCN. Filled dots represent values from young mice ($n = 11$) and open dots represent values from old ($n = 9$) mice. Bars indicate mean \pm SEM. * $P < 0.05$, distribution of GABAergic response types: Mann-Whitney U test for each category, E/I ratio: unpaired t-test with Welch's correction.

excitation; old: 45.05 ± 6.24 %, $n = 9$, young: 19.98 ± 4.14 %, $n = 5$, $P = 0.007$, inhibition; old: 36.81 ± 5.53 %, $n = 9$, young: 60.62 ± 4.89 %, $n = 5$, $P = 0.007$). In the anterior slices the differences between old and young were smaller, but the calculated E/I balance was significantly different between young

and old in both posterior as well as anterior SCN slices (Figure 2E, anterior; old: 0.52 ± 0.09 , $n = 8$, young: 0.29 ± 0.04 , $n = 11$, $P = 0.041$, posterior; old: 1.08 ± 0.20 , $n = 8$, young: 0.36 ± 0.10 , $n = 5$, $P = 0.070$). No differences in GABAergic responses or E/I balance were observed in the central part of the SCN slices of young and old mice (Figure 2B and 2E, E/I ratio; old: 0.79 ± 0.19 , $n = 10$, young: 0.73 ± 0.12 , $n = 10$, $P = 0.767$).

4

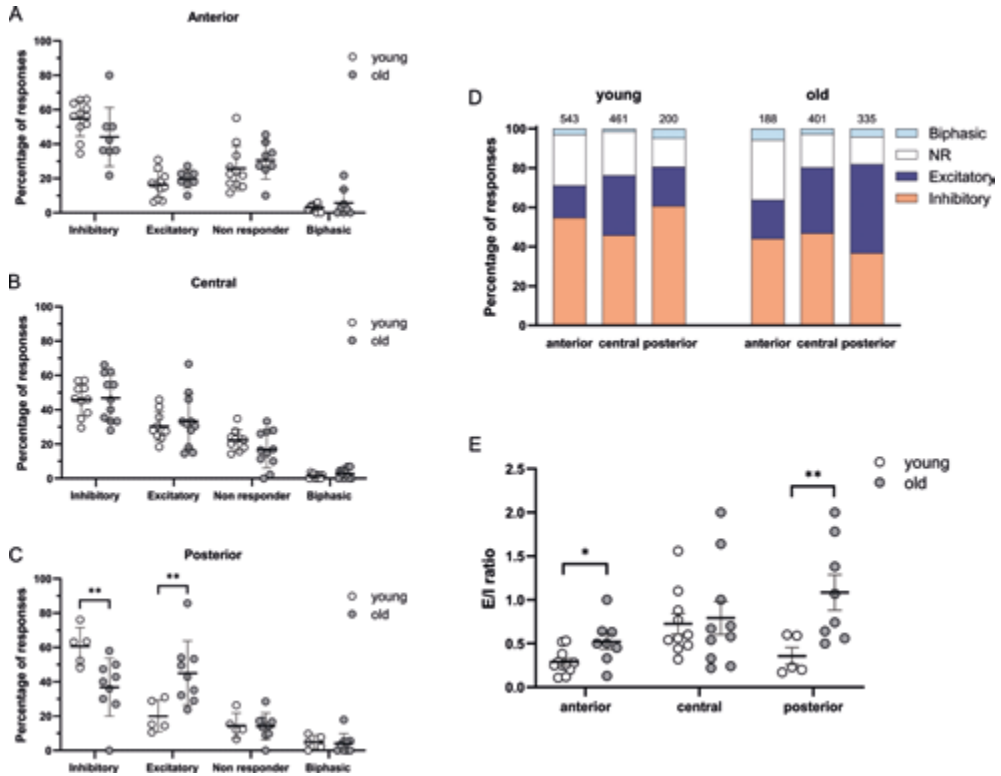


Figure 2. Spatial differences in GABAergic responses along the anteroposterior axis. A, B + C. The percentages of inhibitory, excitatory, non-responding, and biphasic cells in the anterior (A), central (B), and posterior (C) part of the young and old SCN. Each dot represents the mean percentage of responses per response type per SCN. Every single dot in one response type category adds up to 100% together with the corresponding dots in the other categories. D. Distribution of GABAergic response types for the anterior, central, and posterior part of the young (left) and the old (right) SCN. Orange represents the percentage of inhibitory responses, dark blue represents excitatory responses, white represents non-responding cells, and light blue represents biphasic responses. The value on top of the bar shows the total number of cells measured. E. E/I ratios per SCN region in young and old mice, determined by dividing the number of excitatory responses by the number of inhibitory responses measured from different parts of the SCN along the anteroposterior axis. Filled dots represent values from young mice and open dots represent values from old mice. Bars indicate mean \pm SEM. * $P < 0.05$, ** $P < 0.01$. distribution of GABAergic response types: Mann-Whitney U test for each category, E/I ratio: unpaired t-test with Welch's correction.

3.3. Intracellular Ca^{2+} concentration is higher in old SCN

To examine whether the baseline $[\text{Ca}^{2+}]_i$ changes with aging, we compared $[\text{Ca}^{2+}]_i$ (determined by the average $[\text{Ca}^{2+}]_i$ in a 20 s interval before GABA application) in SCN neurons from old and young mice during the day. We found higher baseline $[\text{Ca}^{2+}]_i$ levels in cells of the old SCN, when compared to the young SCN neurons (Figure 3A, old: 150.17 ± 3.78 nM, $n = 924$, young: 132.09 ± 2.28 nM, $n = 1204$, $P < 0.0001$). We also wondered whether this increase was specific for cells with a certain GABAergic response. In comparison with young SCN neurons, baseline $[\text{Ca}^{2+}]_i$ was higher in old SCN cells that exhibited GABAergic inhibitory and excitatory responses, but not in the non-responding or the biphasic cells. Baseline $[\text{Ca}^{2+}]_i$ was also higher in both old and young SCN neurons that exhibited GABAergic inhibitory responses, when compared to excitatory responses (Figure 3B, inhibition; old: 160.80 ± 6.80 nM, $n = 419$, young: 134.10 ± 2.78 nM, $n = 632$, $P = 0.0003$, excitation; old: 135.10 ± 4.75 nM, $n = 296$, young: 116.10 ± 3.88 nM, $n = 270$, $P = 0.002$, inh vs exc old: $P = 0.002$, young: $P = 0.0002$). These results suggest that Ca^{2+} homeostasis in the SCN neurons is affected by age and the GABAergic response type is correlated to the baseline $[\text{Ca}^{2+}]_i$ in young and old SCN.

4. DISCUSSION

In this study we examined the effect of aging on the GABAergic E/I balance and on intracellular Ca^{2+} levels in the mammalian pacemaker. Our results demonstrate that aging affects the response polarity, and thus the function, of GABA, which is the most abundant neurotransmitter in the SCN.

We measured significantly more GABAergic excitatory responses in SCN slices from old mice when compared to slices from young controls. Particularly, in the posterior part of the old SCN we found significantly more excitation and significantly less inhibition compared to the young SCN. Accordingly, we recorded increased E/I ratios in SCN slices from old mice. We also demonstrate that

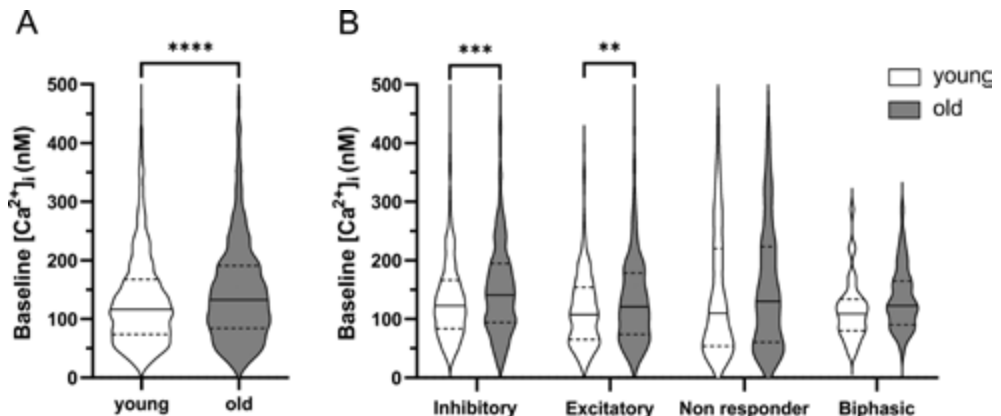


Figure 3. Baseline $[\text{Ca}^{2+}]_i$ is higher in old SCN neurons. A. Violin plots show baseline $[\text{Ca}^{2+}]_i$ levels (nM) from all SCN neurons measured in slices from young ($n = 1204$) and old ($n = 924$) mice. B. Violin plots show baseline $[\text{Ca}^{2+}]_i$ levels (nM) from all SCN neurons measured categorized per GABAergic response type. White violins represent data from young mice and grey violins represent data from old mice. Violin plots show median and quartiles, ** $P < 0.01$, *** $P < 0.001$, **** $P < 0.0001$, unpaired t-test with Welch's correction.

the baseline $[Ca^{2+}]_i$ is higher in SCN cells from old mice, compared to young mice. This is interesting considering that Ca^{2+} is an important intracellular signaling molecule and critical for molecular rhythm generation (Lundkvist *et al.*, 2005).

GABA is known to elicit both inhibitory and excitatory responses in the central clock (Choi *et al.*, 2008; Irwin & Allen, 2009; Farajnia *et al.*, 2014b) and the polarity of GABAergic activity can switch depending on the subregion of the SCN (Albus *et al.*, 2005; Choi *et al.*, 2008; Irwin & Allen, 2009; DeWoskin *et al.*, 2015; Myung *et al.*, 2015). We found spatial differences in the distribution of the different GABAergic response types, with a significant increase in excitatory responses along the anteroposterior axis in the old, but not the young SCN (Figure 2A-D). In slices from both young and old mice, we did not find a difference in the polarity of the GABAergic responses between the ventral and dorsal SCN (Figure S2). The lack of regional differences in GABAergic responses between anterior, central, and posterior SCN slices of young controls, or between dorsal and ventral SCN slices is comparable to a previous study examining the effect of photoperiod on the GABAergic responses in the mouse SCN (Farajnia *et al.*, 2014b). The spatial organization that we observed in C57BL/6 mice differed from the spatial pattern previously observed in rat, in which there are regional differences found along the dorsoventral axis (Albus *et al.*, 2005; Choi *et al.*, 2008; Irwin & Allen, 2009). We have no interpretation for this difference, but it adheres to functional and anatomical differences that are also observed between mice and rats (Morin *et al.*, 2006).

The reported increase in GABAergic excitation in the old SCN suggests an increase in $[Cl^-]_i$, since the polarity of the GABAergic signal depends in part on the $[Cl^-]_i$ and the relationship between the chloride equilibrium potential (E_{Cl^-}) and the membrane potential (V_m) (Kaila, 1994; Ben-Ari, 2002). Protein expression of the cation-chloride co-transporter responsible for the influx of chloride, the NKCC1, displays circadian rhythmicity in hamsters under constant conditions and is regulated by environmental lighting conditions, as NKCC1 protein levels in the SCN of hamsters housed in constant light are higher than of hamsters entrained to 14:10 LD cycles or under constant darkness (McNeill *et al.*, 2020). There is no clear consensus on the distribution of co-transporter expression in the SCN. NKCC1 protein expression is shown to be higher in the dorsal part of the rat SCN at night, with no differences in subregion during the day (Choi *et al.*, 2008), however, in hamsters exposed to constant darkness or 14:10 LD cycles, NKCC1 expression is higher in the ventral SCN compared to the dorsal part (McNeill *et al.*, 2020). Another study shows higher $[Cl^-]_i$ during the day than during the night in both the ventral and dorsal mouse SCN neurons. Additionally, the KCCs – the extruders of chloride – plays a major role in $[Cl^-]_i$ regulation, while NKCC1 has a relatively minor role (Klett & Allen, 2017). Our results suggest that the expression of NKCC1 and/or KCC2 is also affected by aging, since we demonstrated an alteration in the polarity of the GABAergic response in the old SCN.

4.1. E/I balance and synchronization within the SCN network

The increase in excitatory responses in the old SCN may be part of mechanisms that contribute to the degree of synchronization within the SCN network. Both *in vivo* and *ex vivo* studies showed a significant reduction in the amplitude of the ensemble electrical activity rhythms of the aged SCN that is likely the consequence of decreased synchronization within the SCN network (Satinoff *et al.*,

1993; Watanabe *et al.*, 1995; Nakamura *et al.*, 2011; Farajnia *et al.*, 2012). Ex vivo electrophysiological recordings showed changes in neuronal phase distribution in SCN slices of aged mice (Farajnia *et al.*, 2012) and these alterations at the network level underlie the diminished SCN output signal. Although the mechanisms that regulate neuronal phase distribution in the SCN are still unknown, there are studies suggesting that an increase in E/I balance might be responsible for modulating the phase distribution (Farajnia *et al.*, 2014b; Rohr *et al.*, 2019). GABA is expressed in almost all SCN neurons and is, because of its dual action as inhibitor and activator, an important contributor to the E/I balance in the SCN (Albus *et al.*, 2005; Choi *et al.*, 2008). Even though evidence suggest that GABA is involved in phase adjustment and synchronization of the SCN network, no consensus exists on the precise role of GABA in network synchronization (Ono *et al.*, 2020). Our results contribute to this debate by showing increased levels of GABAergic excitation in an SCN network that is in a more desynchronized state (Farajnia *et al.*, 2012), suggesting GABA regulation is involved in phase distribution. Other studies also suggest that GABA does not promote synchrony, or works as a destabilizer or phase desynchronizer within the SCN, but these studies do not distinguish between GABAergic inhibition or excitation (Aton *et al.*, 2006; Freeman *et al.*, 2013). Whether there is an actual causal link between either the E/I balance and synchronization, or whether this reflects aging-related compensatory mechanisms for the alterations at the network level, still needs further investigation.

Alterations in the SCN network are involved in aging, as well as in the adaptation to photoperiods. As with aging, exposure to a long day photoperiod causes more phase dispersal in the SCN (VanderLeest *et al.*, 2007; Brown & Piggins, 2009; Buijink *et al.*, 2016) and a switch in the polarity of GABAergic activity from inhibition to excitation in many SCN neurons (Farajnia *et al.*, 2014b). Farajnia *et al.* proposes that the relation between GABAergic inhibition and excitation may contribute to the photoperiod-induced phase adjustments within the network. Our results show an increase in the number of excitatory GABAergic responses and an increase in the E/I balance in the old SCN (Figure 1), similar to the changes in the SCN of mice entrained to a long photoperiod, and thus our data support this hypothesis.

4.2. Plasticity in E/I balance in the SCN

The polarity of the GABAergic response in the SCN, and thus the E/I balance, can vary depending on time of day or the photoperiod to which the animals are exposed (Albus *et al.*, 2005; Choi *et al.*, 2008; Farajnia *et al.*, 2014b). In addition, a recent study showed that lighting conditions affect the circadian regulation and levels of NKCC1 protein expression, and thus the action of GABA (McNeill *et al.*, 2020). The plasticity in GABAergic function is thought to support adaptation to environmental conditions. It is not clear whether the excitatory action of GABA in aging is also functional by contributing to a compensatory mechanism to reorganize the neuronal network of the SCN, or else, is a consequence of a loss of function in the aging SCN. Moreover, it remains to be investigated whether there is still plasticity in the E/I balance in the SCN of old mice, or if the increase that we show here is static and irreversibly changed in the SCN network. In an recent study we were able to show that the aging SCN is still able to adapt its molecular clock to different

photoperiods as well as the young, suggesting that the SCN network is still flexible in aging (Buijink *et al.*, 2020).

4.3. Aging and intracellular Ca^{2+} levels in the SCN

One important intracellular component involved in phase adjustment is Ca^{2+} , which we determined in our baseline measurements before GABA application. Therefore, we were able to compare baseline $[\text{Ca}^{2+}]_i$ of SCN neurons from slices of old and young mice. Our results show that the baseline $[\text{Ca}^{2+}]_i$ is higher in SCN cells from old mice, compared to young controls (Figure 3) which is in accordance with previous studies in other brain areas (Galla *et al.*, 2020; Uryash *et al.*, 2020; Mozolewski *et al.*, 2021). In both young and old SCN slices, the neurons that showed GABAergic inhibition exhibited the highest baseline calcium levels. GABA induced Ca^{2+} transients can depend on baseline $[\text{Ca}^{2+}]_i$ (Irwin & Allen, 2009). A possible cause for the relationship between baseline $[\text{Ca}^{2+}]_i$ and GABAergic response type could be the different levels of electrical activity of the neuron. At a higher firing rate, the $[\text{Ca}^{2+}]_i$ baseline would be increased due to influx of Ca^{2+} through voltage-activated Ca^{2+} channels and an inhibitory input would have a larger effect compared to a silent neuron. Also, it is plausible that a neuron with a low or high $[\text{Ca}^{2+}]_i$ may not be able to further lower or raise $[\text{Ca}^{2+}]_i$ after a GABAergic stimulus, respectively. Our evidence implies that both baseline calcium levels and calcium homeostasis are altered in the old SCN which could further impair cellular phase adjustments. Even though Ca^{2+} is one of the most essential and well-studied signaling molecules, surprisingly little is known about the influence of aging on the Ca^{2+} signaling or Ca^{2+} homeostasis in the SCN. Studies in other brain areas have focused on the contribution of plasma membrane Ca^{2+} pumps, intracellular stores like the endoplasmic reticulum, and the mitochondria in aged neurons or neurodegenerative disorders (Supnet & Bezprozvanny, 2010; Zaidi *et al.*, 2018; Calvo-Rodriguez *et al.*, 2020; Trombetta-Lima *et al.*, 2021). It should be noted though, that the SCN neurons can already tolerate higher levels of $[\text{Ca}^{2+}]_i$ when compared to other brain areas (Diekman *et al.*, 2013). Given the essential role of calcium in both intracellular signaling pathways and rhythm generation and its association with multiple neurodegenerative disorders (Foster, 2007; Berridge, 2013), restoring calcium signaling in old SCN neurons could be an interesting target for therapy.

Additionally, maintenance of an adequate balance of excitation and inhibition could benefit healthy aging. Several studies have shown a shift in E/I balance, with heightened neuronal activity in the hippocampus or prefrontal cortex due to decreased inhibitory networks (Legon *et al.*, 2016; Tran *et al.*, 2019). This loss of inhibition, and thus an increased E/I ratio, was correlated to aging and the pathogenesis of neurodegenerative disorders (Rissman & Mobley, 2011; Bruining *et al.*, 2020). Moreover, the E/I ratio increased in aged rats with impaired memory function, however aged rats with unimpaired memory function had similar hippocampal E/I ratios as young controls, showing that a proper balance between inhibition and excitation is crucial for maintaining memory performance during aging (Tran *et al.*, 2019) and stresses the importance of an adequate balance in the aged brain. Our study demonstrates that the E/I balance of the neuronal network of the central clock is also challenged by aging with potential consequences for clock function. The stabilization of SCN E/I ratio to a healthy range in aging will not only benefit SCN network properties, but may

also counteract the detrimental effects of the clock on neurodegenerative diseases (Leng *et al.*, 2019; Fifel & De Boer, 2021).

REFERENCES

1. Abrahamson, E.E. & Moore, R.Y. (2001) Suprachiasmatic nucleus in the mouse: retinal innervation, intrinsic organization and efferent projections. *Brain Res.*, 916, 172-191.
2. Albus, H., Vansteensel, M.J., Michel, S., Block, G.D. & Meijer, J.H. (2005) A GABAergic mechanism is necessary for coupling dissociable ventral and dorsal regional oscillators within the circadian clock. *Curr. Biol.*, 15, 886-893.
3. Aton, S.J., Huettner, J.E., Straume, M. & Herzog, E.D. (2006) GABA and *Gi/o* differentially control circadian rhythms and synchrony in clock neurons. *Proc. Natl. Acad. Sci. U. S. A.*, 103, 19188-19193.
4. Ben-Ari, Y. (2002) Excitatory actions of gaba during development: the nature of the nurture. *Nature reviews. Neuroscience*, 3, 728-739.
5. Berridge, M.J. (2013) Dysregulation of neural calcium signaling in Alzheimer disease, bipolar disorder and schizophrenia. *Prion*, 7, 2-13.
6. Biello, S.M. (2009) Circadian clock resetting in the mouse changes with age. *Age (Dordrecht, Netherlands)*, 31, 293-303.
7. Brown, T.M. & Piggins, H.D. (2009) Spatiotemporal heterogeneity in the electrical activity of suprachiasmatic nuclei neurons and their response to photoperiod. *J. Biol. Rhythms*, 24, 44-54.
8. Bruining, H., Hardstone, R., Juarez-Martinez, E.L., Sprengers, J., Avramiea, A.E., Simpraga, S., Houtman, S.J., Poil, S.S., Dallares, E., Palva, S., Oranje, B., Matias Palva, J., Mansvelde, H.D. & Linkenkaer-Hansen, K. (2020) Measurement of excitation-inhibition ratio in autism spectrum disorder using critical brain dynamics. *Sci. Rep.*, 10, 9195.
9. Buhr, E.D. & Takahashi, J.S. (2013) Molecular Components of the Mammalian Circadian Clock. In Kramer, A., Mewes, M. (eds) *Circadian Clocks*. Springer Berlin Heidelberg, Berlin, Heidelberg, pp. 3-27.
10. Buijink, M.R., Almog, A., Wit, C.B., Roethler, O., Olde Engberink, A.H., Meijer, J.H., Garlaschelli, D., Rohling, J.H. & Michel, S. (2016) Evidence for Weakened Intercellular Coupling in the Mammalian Circadian Clock under Long Photoperiod. *PLoS One*, 11, e0168954.
11. Buijink, M.R. & Michel, S. (2020) A multi-level assessment of the bidirectional relationship between aging and the circadian clock. *J. Neurochem.*
12. Buijink, M.R., Olde Engberink, A.H.O., Wit, C.B., Almog, A., Meijer, J.H., Rohling, J.H.T. & Michel, S. (2020) Aging Affects the Capacity of Photoperiodic Adaptation Downstream from the Central Molecular Clock. *J. Biol. Rhythms*, 35, 167-179.
13. Calvo-Rodríguez, M., Hernando-Pérez, E., López-Vázquez, S., Núñez, J., Villalobos, C. & Núñez, L. (2020) Remodeling of Intracellular Ca(2+) Homeostasis in Rat Hippocampal Neurons Aged In Vitro. *Int. J. Mol. Sci.*, 21.
14. Choi, H.J., Lee, C.J., Schroeder, A., Kim, Y.S., Jung, S.H., Kim, J.S., Kim, D.Y., Son, E.J., Han, H.C., Hong, S.K., Colwell, C.S. & Kim, Y.I. (2008) Excitatory actions of GABA in the suprachiasmatic nucleus. *J. Neurosci.*, 28, 5450-5459.
15. DeWoskin, D., Myung, J., Belle, M.D., Piggins, H.D., Takumi, T. & Forger, D.B. (2015) Distinct roles for GABA across multiple timescales in mammalian circadian timekeeping. *Proc. Natl. Acad. Sci. USA*, 112, E3911-3919.
16. Diekmann, C.O., Belle, M.D., Irwin, R.P., Allen, C.N., Piggins, H.D. & Forger, D.B. (2013) Causes and consequences of hyperexcitation in central clock neurons. *PLoS Comput. Biol.*, 9, e1003196.
17. Dijk, D.J. & Duffy, J.F. (1999) Circadian regulation of human sleep and age-related changes in its timing, consolidation and EEG characteristics. *Ann. Med.*, 31, 130-140.
18. Farajnia, S., Deboer, T., Rohling, J.H., Meijer, J.H. & Michel, S. (2014a) Aging of the suprachiasmatic clock. *Neuroscientist*, 20, 44-55.
19. Farajnia, S., Michel, S., Deboer, T., vanderLeest, H.T., Houben, T., Rohling, J.H., Ramkisoensing, A., Yassenkov, R. & Meijer, J.H. (2012) Evidence for neuronal desynchrony in the aged suprachiasmatic nucleus clock. *J. Neurosci.*, 32, 5891-5899.
20. Farajnia, S., van Westering, T.L.E., Meijer, J.H. & Michel, S. (2014b) Seasonal induction of GABAergic excitation in the central mammalian clock. *Proc. Natl. Acad. Sci. USA*, 111, 9627-9632.
21. Fifel, K. & De Boer, T. (2021) The circadian system in Parkinson's disease, multiple system atrophy, and progressive supranuclear palsy. *Handb. Clin. Neurol.*, 179, 301-313.

22. Fonseca Costa, S.S. & Ripperger, J.A. (2015) Impact of the circadian clock on the aging process. *Front. Neurol.*, 6, 43.
23. Foster, T.C. (2007) Calcium homeostasis and modulation of synaptic plasticity in the aged brain. *Aging cell*, 6, 319-325.
24. Freeman, G.M., Krock, R.M., Aton, S.J., Thaben, P. & Herzog, E.D. (2013) GABA networks destabilize genetic oscillations in the circadian pacemaker. *Neuron*, 78, 799-806.
25. Froy, O. (2011) Circadian rhythms, aging, and life span in mammals. *Physiology (Bethesda)*, 26, 225-235.
26. Galla, L., Redolfi, N., Pozzan, T., Pizzo, P. & Greotti, E. (2020) Intracellular Calcium Dysregulation by the Alzheimer's Disease-Linked Protein Presenilin 2. *Int. J. Mol. Sci.*, 21.
27. Hastings, M.H., Maywood, E.S. & Brancaccio, M. (2018) Generation of circadian rhythms in the suprachiasmatic nucleus. *Nat. Rev. Neurosci.*, 19, 453-469.
28. Hofman, M.A. & Swaab, D.F. (2006) Living by the clock: The circadian pacemaker in older people. *Ageing Research Reviews*, 5, 33-51.
29. Irwin, R.P. & Allen, C.N. (2009) GABAergic signaling induces divergent neuronal Ca²⁺ responses in the suprachiasmatic nucleus network. *Eur. J. Neurosci.*, 30, 1462-1475.
30. Kaila, K. (1994) Ionic basis of GABA_A receptor channel function in the nervous system. *Prog. Neurobiol.*, 42, 489-537.
31. Klett, N.J. & Allen, C.N. (2017) Intracellular Chloride Regulation in AVP+ and VIP+ Neurons of the Suprachiasmatic Nucleus. *Sci. Rep.*, 7, 10226.
32. Kondratova, A.A. & Kondratov, R.V. (2012) The circadian clock and pathology of the ageing brain. *Nat. Rev. Neurosci.*, 13, 325-335.
33. Legon, W., Punzell, S., Dowlati, E., Adams, S.E., Stiles, A.B. & Moran, R.J. (2016) Altered Prefrontal Excitation/Inhibition Balance and Prefrontal Output: Markers of Aging in Human Memory Networks. *Cereb. Cortex*, 26, 4315-4326.
34. Leng, Y., Musiek, E.S., Hu, K., Cappuccio, F.P. & Yaffe, K. (2019) Association between circadian rhythms and neurodegenerative diseases. *Lancet Neurol.*, 18, 307-318.
35. Lundkvist, G.B., Kwak, Y., Davis, E.K., Tei, H. & Block, G.D. (2005) A calcium flux is required for circadian rhythm generation in mammalian pacemaker neurons. *J. Neurosci.*, 25, 7682-7686.
36. McNeill, J.K., Walton, J.C., Ryu, V. & Albers, H.E. (2020) The Excitatory Effects of GABA within the Suprachiasmatic Nucleus: Regulation of Na-K-2Cl Cotransporters (NKCCs) by Environmental Lighting Conditions. *J. Biol. Rhythms*, 35, 275-286.
37. Moore, R.Y. & Speh, J.C. (1993) GABA is the principal neurotransmitter of the circadian system. *Neurosci. Lett.*, 150, 112-116.
38. Morin, L.P., Shivers, K.Y., Blanchard, J.H. & Muscat, L. (2006) Complex organization of mouse and rat suprachiasmatic nucleus. *Neuroscience*, 137, 1285-1297.
39. Mozolewski, P., Jeziorek, M., Schuster, C.M., Bading, H., Frost, B. & Dobrowolski, R. (2021) The role of nuclear Ca²⁺ in maintaining neuronal homeostasis and brain health. *J. Cell Sci.*, 134.
40. Myung, J., Hong, S., DeWoskin, D., De Schutter, E., Forger, D.B. & Takumi, T. (2015) GABA-mediated repulsive coupling between circadian clock neurons in the SCN encodes seasonal time. *Proc. Natl. Acad. Sci. USA*, 112, E3920-3929.
41. Nakamura, T.J., Nakamura, W., Yamazaki, S., Kudo, T., Cutler, T., Colwell, C.S. & Block, G.D. (2011) Age-related decline in circadian output. *J. Neurosci.*, 31, 10201-10205.
42. Nygard, M., Hill, R.H., Wikstrom, M.A. & Kristensson, K. (2005) Age-related changes in electrophysiological properties of the mouse suprachiasmatic nucleus in vitro. *Brain Res. Bull.*, 65, 149-154.
43. Ono, D., Honma, K.I. & Honma, S. (2020) GABAergic mechanisms in the suprachiasmatic nucleus that influence circadian rhythm. *J. Neurochem.*
44. Oster, H., Baeriswyl, S., Van Der Horst, G.T. & Albrecht, U. (2003) Loss of circadian rhythmicity in aging mPer1^{-/-}-mCry2^{-/-} mutant mice. *Genes Dev.*, 17, 1366-1379.
45. Palomba, M., Nygård, M., Florenzano, F., Bertini, G., Kristensson, K. & Bentivoglio, M. (2008) Decline of the Presynaptic Network, Including GABAergic Terminals, in the Aging Suprachiasmatic Nucleus of the Mouse. *J. Biol. Rhythms*, 23, 220-231.
46. Patke, A., Young, M.W. & Axelrod, S. (2019) Molecular mechanisms and physiological importance of circadian rhythms. *Nature Reviews Molecular Cell Biology*.

47. Ramkisoensing, A. & Meijer, J.H. (2015) Synchronization of Biological Clock Neurons by Light and Peripheral Feedback Systems Promotes Circadian Rhythms and Health. *Front. Neurol.*, 6, 128.
48. Reppert, S.M. & Weaver, D.R. (2002) Coordination of circadian timing in mammals. *Nature*, 418, 935-941.
49. Rissman, R.A. & Mobley, W.C. (2011) Implications for treatment: GABAA receptors in aging, Down syndrome and Alzheimer's disease. *J. Neurochem.*, 117, 613-622.
50. Roenneberg, T. & Mrosovsky, M. (2016) The Circadian Clock and Human Health. *Curr. Biol.*, 26, R432-443.
51. Rohr, K.E., Pancholi, H., Haider, S., Karow, C., Modert, D., Raddatz, N.J. & Evans, J. (2019) Seasonal plasticity in GABAA signaling is necessary for restoring phase synchrony in the master circadian clock network. *eLife*, 8.
52. Satinoff, E., Li, H., Tchong, T.K., Liu, C., McArthur, A.J., Medanic, M. & Gillette, M.U. (1993) Do the suprachiasmatic nuclei oscillate in old rats as they do in young ones? *Am. J. Physiol.*, 265, R1216-1222.
53. Supnet, C. & Bezprozvany, I. (2010) Neuronal calcium signaling, mitochondrial dysfunction, and Alzheimer's disease. *J. Alzheimers Dis.*, 20 Suppl 2, S487-498.
54. Tran, T., Bridi, M., Koh, M.T., Gallagher, M. & Kirkwood, A. (2019) Reduced cognitive performance in aged rats correlates with increased excitation/inhibition ratio in the dentate gyrus in response to lateral entorhinal input. *Neurobiol. Aging*, 82, 120-127.
55. Trombetta-Lima, M., Sabogal-Guáqueta, A.M. & Dolga, A.M. (2021) Mitochondrial dysfunction in neurodegenerative diseases: A focus on iPSC-derived neuronal models. *Cell Calcium*, 94, 102362.
56. Uryash, A., Flores, V., Adams, J.A., Allen, P.D. & Lopez, J.R. (2020) Memory and Learning Deficits Are Associated With Ca(2+) Dyshomeostasis in Normal Aging. *Front. Aging Neurosci.*, 12, 224.
57. VanderLeest, H.T., Houben, T., Michel, S., Deboer, T., Albus, H., Vansteensel, M.J., Block, G.D. & Meijer, J.H. (2007) Seasonal encoding by the circadian pacemaker of the SCN. *Curr. Biol.*, 17, 468-473.
58. Watanabe, A., Shibata, S. & Watanabe, S. (1995) Circadian rhythm of spontaneous neuronal activity in the suprachiasmatic nucleus of old hamster in vitro. *Brain Res.*, 695, 237-239.
59. Welsh, D.K., Logothetis, D.E., Meister, M. & Reppert, S.M. (1995) Individual neurons dissociated from rat suprachiasmatic nucleus express independently phased circadian firing rhythms. *Neuron*, 14, 697-706.
60. Welsh, D.K., Takahashi, J.S. & Kay, S.A. (2010) Suprachiasmatic nucleus: cell autonomy and network properties. *Annu. Rev. Physiol.*, 72, 551-577.
61. Zaidi, A., Adewale, M., McLean, L. & Ramlow, P. (2018) The plasma membrane calcium pumps-The old and the new. *Neurosci. Lett.*, 663, 12-17.

SUPPLEMENTARY MATERIALS

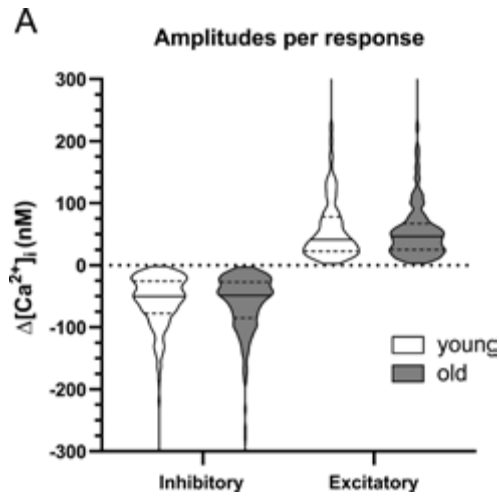


Figure S1. Amplitudes of GABAergic responses. A. Violin plots show amplitudes ($\Delta[Ca^{2+}]_i$) of all SCN neurons that responded in an inhibitory and excitatory manner. White violins represent data from SCN slices from young mice and grey violins represent data from SCN slices from old mice. Unpaired t-test with Welch's correction, n.s.

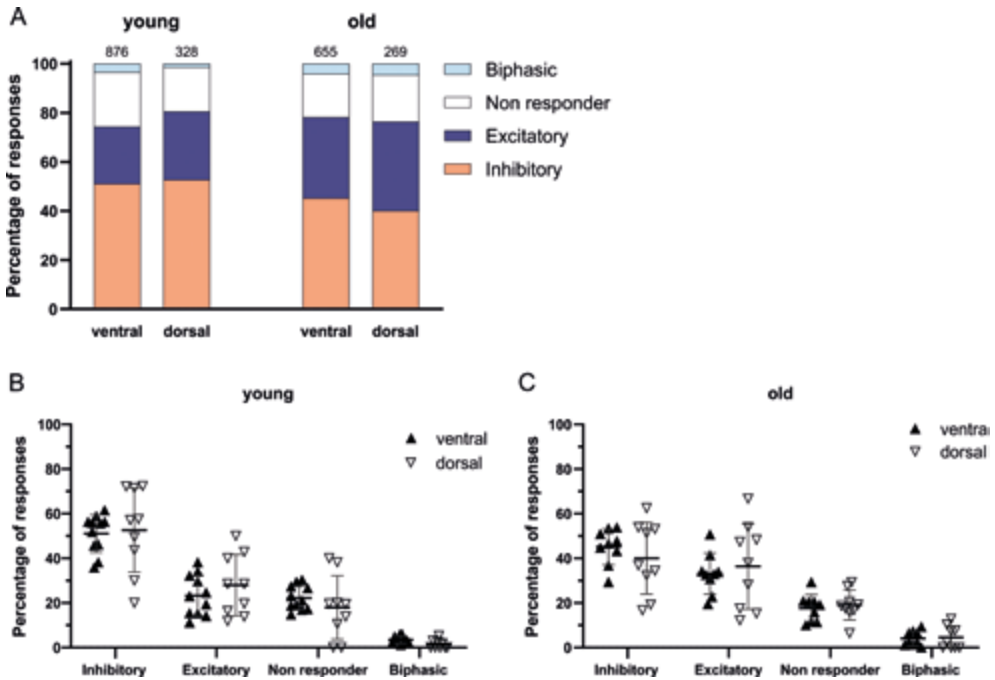


Figure S2. GABAergic responses along the dorsoventral axis. A. Distribution of GABAergic response types for the ventral and dorsal part of the young (left) and the old (right) SCN. Orange represents the percentage of inhibitory responses, dark blue represents excitatory responses, white represents non-responding cells, and light blue represents biphasic responses. The value on top of the bar represents the total number of cells measured. B + C. The percentages of inhibitory, excitatory, non-responding, and biphasic cells in the dorsal and ventral part of the young (B) and old (C) SCN. Each dot represents the mean percentage of responses per response type per SCN position. Every single dot in one response type category adds up to 100% together with the corresponding dots in the other categories. Filled triangles represent values from the ventral part and open triangles represent values from the dorsal part of the SCN. Bars indicate mean \pm SEM. Mann-Whitney U test, n.s.



five

CHLORIDE COTRANSPORTER KCC2 IS ESSENTIAL FOR GABAERGIC INHIBITION IN THE SCN

Anneke H.O. Olde Engberink¹, Johanna H. Meijer¹, Stephan Michel¹

¹Department of Cellular and Chemical Biology, Laboratory for Neurophysiology, Leiden University Medical Center,
Einthovenweg 20, 2333 ZC, Leiden, the Netherlands.

Published in Neuropharmacology, 2018, 138, 80-86

ABSTRACT

One of the principal neurotransmitters of the central nervous system is GABA. In the adult brain, GABA is predominantly inhibitory, but there is growing evidence indicating that GABA can shift to excitatory action depending on environmental conditions. In the mammalian central circadian clock of the suprachiasmatic nucleus (SCN) GABAergic activity shifts from inhibition to excitation when animals are exposed to long day photoperiod. The polarity of the GABAergic response (inhibitory versus excitatory) depends on the GABA equilibrium potential determined by the intracellular Cl^- concentration ($[\text{Cl}^-]_i$). Chloride homeostasis can be regulated by Cl^- cotransporters like NKCC1 and KCC2 in the membrane, but the mechanisms for maintaining $[\text{Cl}^-]_i$ are still under debate. This study investigates the role of KCC2 on GABA-induced Ca^{2+} transients in SCN neurons from mice exposed to different photoperiods. We show for the first time that blocking KCC2 with the newly developed blocker ML077 can cause a shift in the polarity of the GABAergic response. This will increase the amount of excitatory responses in SCN neurons and thus cause a shift in excitatory/inhibitory ratio. These results indicate that KCC2 is an essential component in regulating $[\text{Cl}^-]_i$ and the equilibrium potential of Cl^- and thereby determining the sign of the GABAergic response. Moreover, our data suggest a role for the Cl^- cotransporters in the switch from inhibition to excitation observed under long day photoperiod.

1. INTRODUCTION

The balance between neuronal inhibition and excitation is critical for proper brain functioning (Buzsaki et al., 2007; Haider et al., 2006). Accordingly, an imbalance is implicated in several neurological disorders, like epilepsy and autism (Marín, 2012; Nelson and Valakh, 2015; Sgadò et al., 2011). One of the important factors for keeping this balance is γ -Aminobutyric acid (GABA), known as the major inhibitory neurotransmitter in the central nervous system (Costa, 1998; Sivilotti and Nistri, 1991). In the developing brain, however, GABA can act as an excitatory neurotransmitter (Ben-Ari, 2002), and even in the mature brain, the phenomenon of GABAergic depolarization has recently been recognized and characterized in multiple areas (Chung, 2012). One of these brain areas is the mammalian central circadian clock, located in the suprachiasmatic nucleus (SCN) of the anterior hypothalamus (Choi et al., 2008; De Jeu and Pennartz, 2002; Wagner et al., 1997). GABA is the prevalent neurotransmitter in the SCN and involved in synchronization within the neuronal network and in processing photic as well as non-photoc entrainment (Albers et al., 2017). While exogenous applied GABA causes an inhibitory effect on the firing rate in many SCN neurons, it has a distinct excitatory effect on a subset of neurons in the SCN. The excitation is typically found in the neurons of the dorsal part of the SCN and is especially present during the night (Choi et al., 2008). Interestingly, exposure to long day photoperiod changes the GABAergic excitation/inhibition ratio (E/I ratio) in SCN neurons towards more excitation compared to short day photoperiod (Farajnia et al., 2014). This demonstrates that GABAergic excitation can have a physiological function in the SCN of the mature brain, and that its effect is plastic, i.e. under the control of environmental conditions.

The major ion that passes through the GABA_A receptor is chloride (Cl⁻) (Macdonald and Olsen, 1994). The concentration gradient of Cl⁻ (the difference between internal and external concentrations) determines the equilibrium potential of chloride (E_{Cl}). Depending on the relationship between the E_{Cl} and the membrane potential (V_m), GABA acts either excitatory or inhibitory when binding to its receptor (Ben-Ari, 2002; Kaila, 1994).

It has generally been assumed that cation-chloride-cotransporters (CCCs) play a crucial role in maintaining the intracellular chloride concentration ([Cl⁻]_i). In neurons, mainly two types of CCCs regulate [Cl⁻]_i; the Na⁺-K⁺-2Cl⁻ cotransporter 1 (NKCC1) and the K⁺-Cl⁻ cotransporter 2 (KCC2), which carry Cl⁻ in and out of the cell, respectively (Blaesse et al., 2009; Deeb et al., 2011; Gamba, 2005). Glykys et al. recently challenged this view by showing that immobile negative charges near the extracellular surface of the cell membrane and cytoplasmic impermeant anions may also play a prominent role in determining [Cl⁻]_i (Glykys et al., 2014a).

Investigating the mechanism of [Cl⁻]_i regulation requires specific blockers for CCCs and a recent study using an improved KCC2 antagonist suggests a primary role of KCC2 in [Cl⁻]_i of SCN neurons (Klett and Allen, 2017). We used a recently developed and highly selective KCC2 antagonist; VU0255011; also known as ML077, which has over a hundredfold higher specificity for KCC2 over NKCC1 (Delpire et al., 2009; Lindsley et al., 2010). With this pharmacological tool, we were able to investigate the role of KCC2 in the GABAergic response. Here, we show that blocking KCC2 with ML077 can cause a shift in the polarity of the GABAergic response by inducing excitatory responses

in previously inhibitory responding neurons. These results indicate that KCC2 is an essential component in regulating $[Cl^-]_i$ and the E_{Cl} , thereby determining the sign of the GABAergic response.

2. MATERIALS AND METHODS

2.1. Animals and housing

Male C57BL/6J mice (Envigo, Horst, the Netherlands; 8 – 10 weeks old; $n = 35$) were housed in a climate-controlled environment (21°C, 40-50% humidity) on an equinoctial photoperiod of 12h light-dark (12:12; LD 12:12), a long photoperiod (LP; LD 16:8), or a short photoperiod (SP; LD 8:16). Food and water were available *ad libitum*. Before recordings, the mice were exposed to their respective photoperiod for a minimum of 30 days to ensure entrainment to the given light schedule. Experiments were performed within a 4 hours interval centered around the middle of the light-phase of the photoperiod. All animal experiments were performed in accordance with the regulations of the Dutch law on animal welfare, and the institutional ethics committee for animal procedures of the Leiden University Medical Center (Leiden, the Netherlands) approved the protocol.

2.2. Slice preparation

After decapitation, brains were quickly removed and placed into modified ice-cold artificial cerebrospinal fluid (ACSF), containing (in mM): NaCl 116.4, KCl 5.4, NaH_2PO_4 1.0, $MgSO_4$ 0.8, $CaCl_2$ 1, $MgCl_2$ 4, $NaHCO_3$ 23.8, glucose 15.1, and 5 mg/L of gentamycin (Sigma Aldrich, Munich, Germany) and saturated with 95% O_2 – 5% CO_2 . Coronal hypothalamic slices containing the SCN (250 μm) were cut using a vibrating microtome (VT 1000S, Leica Microsystems, Wetzlar, Germany) and sequentially maintained in regular, oxygenated ACSF ($CaCl_2$ increased to 2 mM and without $MgCl_2$, compared to modified ACSF). The slices were incubated in a water bath (37°C) for 30 minutes and were then maintained at room temperature until the start of the recordings.

2.3. Ca^{2+} imaging

Neurons in brain slices were bulk-loaded with the ratiometric, membrane permeable Ca^{2+} indicator dye fura-2-acetoxymethyl ester (Fura-2-AM) as described previously (Michel et al., 2013). Briefly, the slices were submerged into a mix of ACSF containing 7 μM Fura-2-AM for 10 minutes at 37°C. The slices were then rinsed four times with fresh ACSF before being transferred to a recording chamber (RC-26G, Warner Instruments, Hamden, CT, USA) mounted on the fixed stage of an upright fluorescence microscope (Axioskop 2-FS Plus, Carl Zeiss Microimaging, Oberkochen, Germany) and constantly perfused with oxygenated ACSF (2.5 mL/min) at room temperature. The indicator dye was excited alternatively at wavelengths of 340 and 380 nm by means of a monochromator (Polychrome V, TILL Photonics; now FEI Munich GmbH, Munich, Germany). Emitted light (505 nm) was detected by a cooled CCD camera (Sensicam, TILL Photonics; now FEI Munich GmbH, Munich, Germany), and images were acquired at 2 second intervals (Figure 1). Using an eight-channel pressurized focal application system (ALA-VM8, ALA scientific instruments, NY, USA) GABA (200 μM , 15 s) was applied locally and neuronal responses were recorded as Ca^{2+} transients. After two GABA pulses, which were

separated by 1 minute baseline recording, ACSF containing elevated levels of K^+ (20 mM, 15 s) was applied to identify healthy, responding neurons. Cells with at least 10% increase in $[Ca^{2+}]_i$ in response to high levels of K^+ were considered as healthy cells. This protocol was repeated after 10 minutes incubation with either the drug ML077 (diluted in ACSF, 10 μ M from 28 mM DMSO stock) or DMSO (diluted in ACSF, 4 ppm) via bath application (ML077: LP: n = 557 cells from eight animals; SP: n = 387 cells from eight animals; 12:12: n = 499 cells from eight animals. DMSO: LP: n = 319 cells from four animals; SP: n = 149 cells from three animals; 12:12: n = 248 cells from four animals). Both experiments and analysis were accomplished using imaging software (TILLvision, TILL Photonics; now FEI Munich GmbH, Munich, Germany). Single-wavelength images were background subtracted, and ratio images (340/380) were generated. Region of interest-defined cells and mean ratio values were determined, from which the intracellular Ca^{2+} concentration was calculated.

2.4. Chemicals

GABA, DMSO and all salts were purchased from Sigma-Aldrich. The first badge of ML077 was generously provided by Dr. Craig Lindsley (Vanderbilt University, Nashville, TN, USA) and thereafter purchased from AOBIIOUS (Gloucester, MA, USA). Fura-2-AM was purchased from TEFlabs (Austin, TX, USA).

2.5. Data analysis and statistics

Neuronal Ca^{2+} responses were analyzed using IGOR Pro (WaveMetrics, Portland, OR, USA). The transient responses in Ca^{2+} concentration within the first seconds after the stimulation were

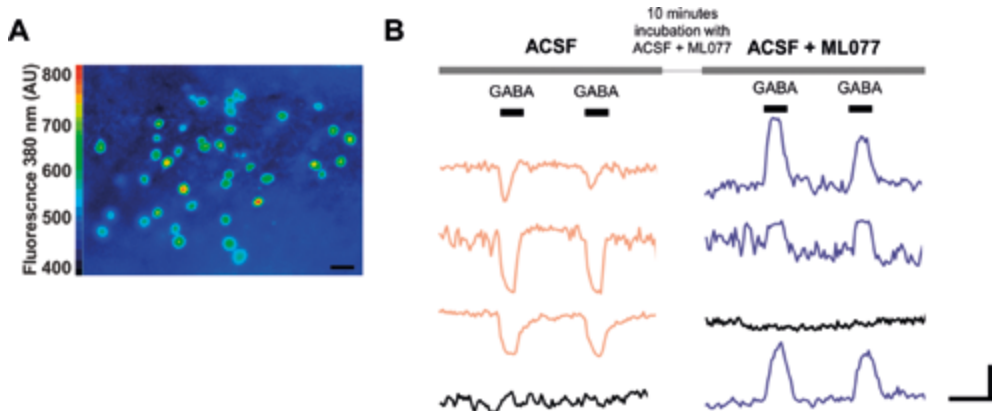


Figure 1. SCN neurons can change GABAergic response after blocking KCC2 with ML077. A. Examples of Fura-2-AM loaded SCN neurons from mice entrained to LD12:12. Color scale indicates fluorescence intensity at 380 nm excitation in arbitrary units. (Scale bar, 10 μ m) B. On top, a sketch of the experimental protocol is depicted. SCN slices were continuously superfused with ACSF and Ca^{2+} transients were recorded in response to focal applications of GABA (200 μ M) given before and after a 10 minutes incubation with ML077. Below, example traces of Ca^{2+} transients of 4 neurons are shown demonstrating the changes in GABAergic response after blocking KCC2 with ML077. (Scale bars, 50 nM, 30 s)

evaluated, with responses smaller than $\pm 5\%$ of baseline values defined as non-responding cells. GABA-evoked responses showing Ca^{2+} transients with a decrease in amplitude lower than 5% from baseline were considered inhibitory and responses with an increase higher than 5% from baseline were defined as excitatory. Cells that showed both excitatory and inhibitory responses after one GABA stimulation were defined as biphasic. Per animal, two to three SCN slices were analyzed and the Ca^{2+} responses to GABA application were measured in 50 – 80 cells. For each animal we calculated the distribution of the different types of responses and the E/I ratio. To calculate the E/I ratio, we divided the number of cells that responded excitatory by the number of cells that responded inhibitory, per animal. Subsequently, we took the average of all the E/I ratios of all animals per group.

Statistical analysis was performed using SPSS (IBM, Armonk, NY, USA). We have used generalized estimating equations (GEE) to test if the average distribution of the GABA-induced responses (percentages of the 4 different types of responses) differs before and after treatment (ML077 or DMSO). We have used a multinomial regression model for the GEE and robust standard errors were calculated. We have used the number of cells per animal as a scale weight variable in the GEE to (extra) take into account the variability of the number of cells measured per SCN. Additional Wald tests shows whether the outcome of the GEE is significant. The effect of the treatment on the E/I ratio was tested with two-sided, paired t-tests, and the effect on baseline $[\text{Ca}^{2+}]_i$ was tested with the Mann-Whitney test, because these data did not pass the Shapiro-Wilk normality tests. Differences with $P \leq 0.05$ were considered significant.

3. RESULTS/DISCUSSION

Using Ca^{2+} imaging, we tested the effect of the recently developed KCC2 blocker ML077 on GABAergic responses in SCN cells. Previous studies have shown that Ca^{2+} transients are a reliable estimate of the neuronal activity, with elevations and reductions in $[\text{Ca}^{2+}]_i$ reflecting depolarization and hyperpolarization, respectively (Choi et al., 2008; Irwin and Allen, 2007; Irwin and Allen, 2009). GABAergic responses have been shown to be more excitatory during the night compared to the day (Choi et al., 2008; De Jeu and Pennartz, 2002), so we selected the mid-day for recordings to maximize the effect of ML077. Blocking KCC2 with ML077 caused an increase in excitatory responses after exogenous application of GABA (Figure 1 and 2A; Wald $\chi^2(1) = 23.61$, $P = 1 \times 10^{-6}$, $n = 8$), leading to a change in E/I ratio from 0.95 to 3.41 (Figure 2B and C; $t(7) = 3.45$, $P = 0.011$, $n = 8$).

To investigate which cells switched to the excitatory response type, we compared neurons before and after incubation with ML077. In 37% of all the cells, the type of the GABAergic response changed as a result of KCC2 blockage. Of the cells that initially responded to GABA in an inhibitory manner, 26% ($n=55$) became excitatory after incubation with ML077. About half of the inhibitory cells stayed inhibitory ($n = 107$; 51%) and the remaining inhibitory neurons became either biphasic ($n = 14$; 7%) or did not respond to GABA anymore ($n = 35$; 17%). Moreover, half of the neurons that initially did not respond to GABA ($n = 48$; 56%) and the majority of the biphasic responding neurons ($n = 20$; 69%) became excitatory as a result of ML077 application (Figure S1 and 3A; Wald $\chi^2(1) = 23.61$, $P = 1 \times 10^{-6}$, $n = 8$). Since ML077 was dissolved in DMSO, we have used DMSO as control

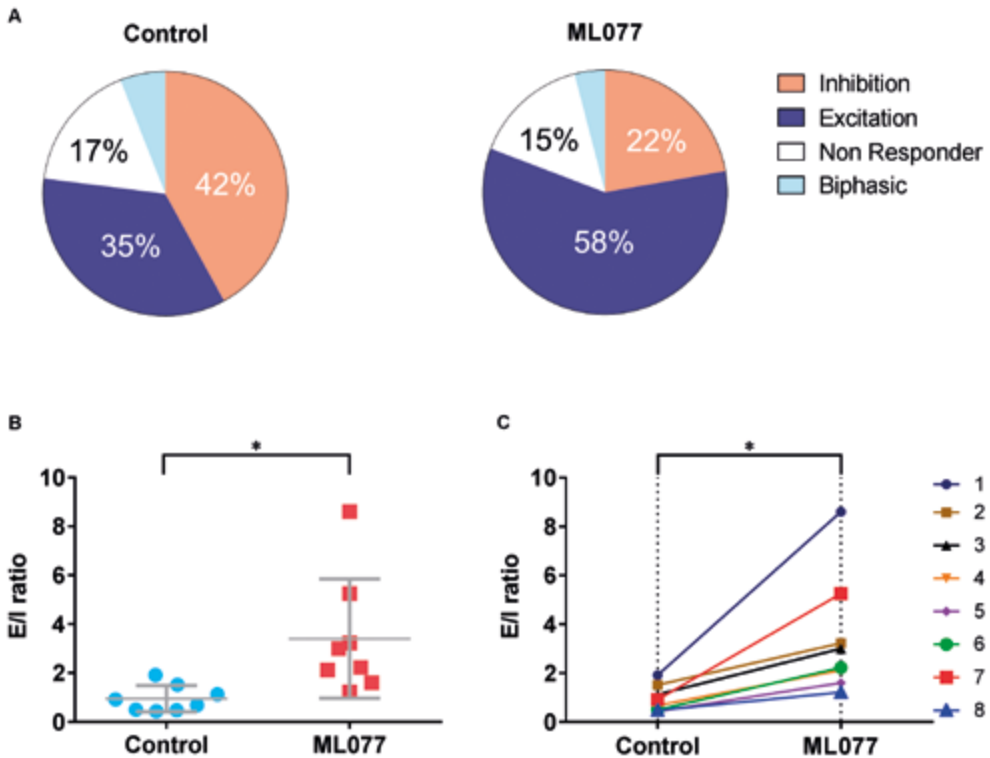


Figure 2. Blocking KCC2 with ML077 caused an increase in GABA-mediated excitation in SCN neurons of mice entrained to LD 12:12. A. Pie charts depicting the distributions of response types of the same SCN neurons on GABAergic stimulation before and after incubation with ML077 (number of cells: n = 499; measured in 23 slices of 8 animals). B. Ratios of excitatory to inhibitory GABAergic signaling before and after incubation with ML077. Each value indicates the ratio of all the cells measured from one animal. C. Increase in E/I ratio for each experiment after incubation with ML077 (B + C: (paired t-test; $P = 0.011$)).

experiments. The control slices, incubated in ACSF containing the solvent DMSO (4 ppm), did not show alteration in the GABAergic response types (Figure S2 and 3B; Wald $\chi^2(1) = 1.40$, $P = 0.24$, $n = 4$) nor did it show a shift in the E/I ratio (0.68 to 1.07, paired t-test; $t(3) = 2.60$, $P = 0.08$). Thus, the data demonstrate that the shift in E/I ratio is caused by inhibition of KCC2 by ML077.

We next performed Ca^{2+} imaging experiments with slices from animals entrained to long and short days to determine whether KCC2 may play a role in photoperiod-induced changes in E/I ratio as reported previously (Farajnia et al., 2014). ML077 increased the percentage of cells showing excitatory responses in short photoperiod from 24% to 43%, which is equivalent to the fraction found after adaptation to long photoperiod conditions (Figure 4A1 and B1 and (Farajnia et al., 2014)). Note that even in the presence of the KCC2 blocker, a difference in the E/I ratio between photoperiods still remains. This is in line with the observation that the percentage of excitatory cells increased to a similar degree in slices from mice adapted to long photoperiod and 12:12 condition, suggesting that KCC2 activity is important for maintaining E/I balance under all photoperiods.

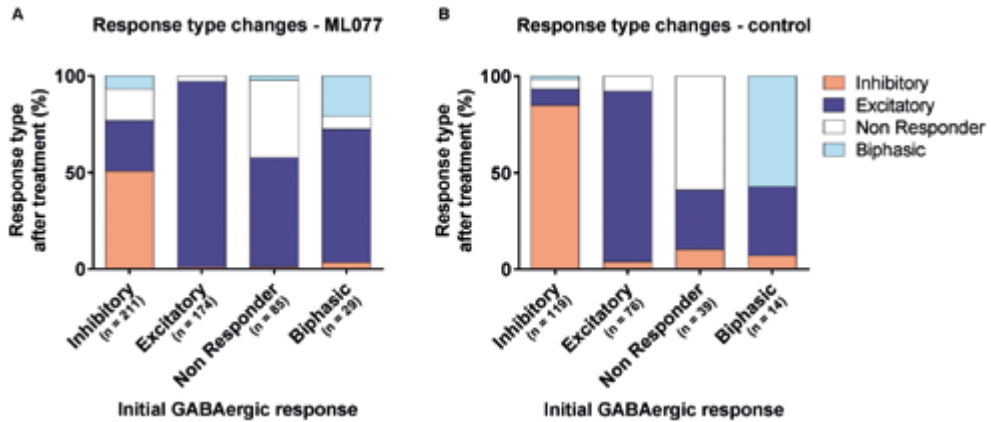
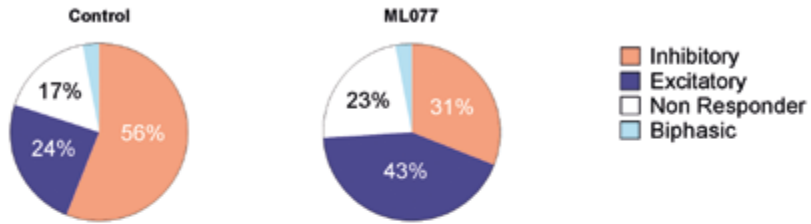


Figure 3. GABAergic response type changes in SCN neurons (LD 12:12) after blocking KCC2 with ML077. A. Distribution of GABAergic response types after incubation with ML077 grouped per initial GABAergic response type (number of cells per initial response type shown on the x-axis). The fraction of cells for each response type resulting from the ML077 treatment is depicted on the y-axis and shows a significant effect of the drug on response type distribution (total number of cells: $n = 499$; measured in 23 slices of 8 animals, Wald Chi square test; $P = 1 \times 10^{-6}$). B. Distribution of GABAergic response types after incubation with control solution (4 ppm DMSO in ACSF) grouped per initial GABAergic response type (number of cells per initial response type shown on the x-axis). The fraction of cells for each response type resulting from the DMSO treatment is depicted on the y-axis and shows no significant effect of the solvent (total number of cells: $n = 248$, measured in 11 slices of 4 animals, Wald Chi square test; $P = 0.24$).

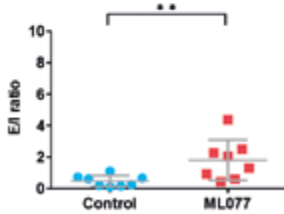
Figure 4. Changes in response type in SCN neurons after blocking KCC2 with ML077 is similar for all photoperiods. A. Pie charts depicting the distributions of response types on GABAergic stimulation before and after incubation with ML077 (number of cells: $n = 387$; measured in 19 slices of 8 SCN) for SP entrained neurons. B. Ratios of excitatory to inhibitory GABAergic signaling before and after incubation with ML077 for SP entrained neurons. Each value indicates the ratio of all the cells measured from one animal. C. Increase in E/I ratio for each experiment after incubation with ML077 (B + C: (paired t-test; $P = 0.006$)). D. Distribution of GABAergic response types after incubation with ML077 grouped per initial GABAergic response in SCN cells of mice entrained to SP (number of cells per initial response type shown on the x-axis). The fraction of cells for each response type resulting from the ML077 treatment is depicted on the y-axis and shows a significant effect of the drug on response type distribution (Wald Chi square test; $P = 1.44 \times 10^{-9}$). E. Pie charts depicting the distributions of response types on GABAergic stimulation before and after incubation with ML077 (number of cells: $n = 557$; measured from 24 slices of 8 SCN) for LP entrained neurons. F. Ratios of excitatory to inhibitory GABAergic signaling before and after incubation with ML077 for LP entrained neurons. Each value indicates the ratio of all the cells measured from one animal. G. Increase in E/I ratio for each experiment after incubation with ML077 (F + G: (paired t-test; $P = 0.003$)). H. Distribution of GABAergic response types after incubation with ML077 grouped per initial GABAergic response in SCN cells of mice entrained to LP (number of cells per initial response type shown on the x-axis). The fraction of cells for each response type resulting from the ML077 treatment is depicted on the y-axis and shows a significant effect of the drug on response type distribution (Wald Chi square test; $P = 0.019$).

Short photoperiod

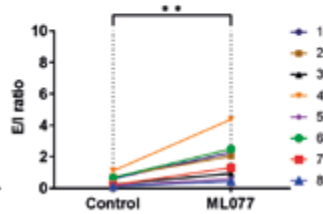
A



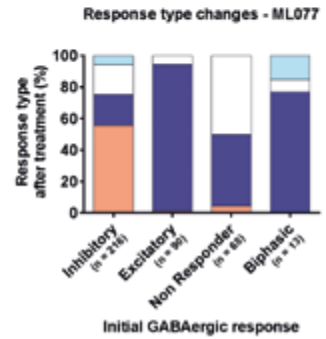
B



C

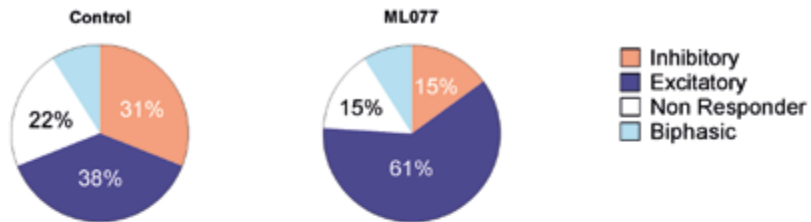


D

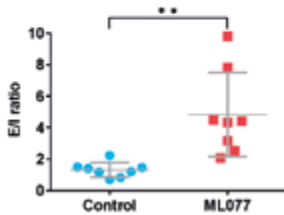


Long photoperiod

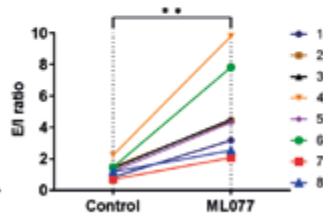
E



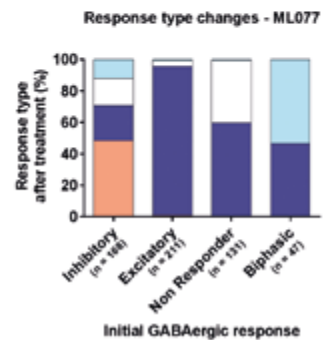
F



G



H



From all neurons that were initially inhibitory, about 50% stayed inhibitory, approximately 20-25% turned excitatory, and the remaining 25-30% became either non-responsive or responded in a biphasic manner.

Moreover, about half of the non-responders and a significant part of the biphasic cells turned excitatory (Figure 3A and 4A4; Wald $\chi^2(1) = 36.62$, $P = 1.44 \times 10^{-9}$ + 4B4; Wald $\chi^2(1) = 5.52$, $P = 0.019$). From all the slices measured, regardless of the photoperiod of the animal, the E/I ratio increased after blocking KCC2 (SP: Figure 4A2 and A3; $t(7) = 3.92$, $P = 0.006$, $n = 8$, and, LP: Figure 4B2 and B3; $t(7) = 4.40$, $P = 0.003$, $n = 8$). Together, these data show that, irrespective of their photoperiod, blocking KCC2 increases the amount of GABAergic excitation.

5

To determine if the drug influences the baseline $[Ca^{2+}]_i$, we analyzed the baseline $[Ca^{2+}]_i$ before and after application of either ML077 or DMSO. For all three photoperiods, we found an increase in baseline $[Ca^{2+}]_i$ after administration of ML077, which was not different to treatment with DMSO (Figure S3). Consequently, we can conclude that the rise in baseline $[Ca^{2+}]_i$ is not an effect of blocking KCC2 with ML077.

Furosemide and bumetanide are two pharmacological blockers that have been widely used to block the cotransporters KCC2 and NKCC1. Bumetanide has a higher affinity for NKCC1 than for KCC2 (Gillen et al., 1996; Payne et al., 2003), but furosemide is known to block both NKCC1 and KCC2 with equal potency (Blaesse et al., 2009; Delpire et al., 2009). Moreover, furosemide inhibits N-methyl D-aspartate (NMDA) and GABA_A receptors (Staley, 2002). Blocking NKCC1 with bumetanide, and thus the intrusion of Cl^- , does have an effect on the GABAergic response, but not on the polarity of the response. Bumetanide lowered the amplitude of GABA-evoked elevations in $[Ca^{2+}]_i$, but could not substantially convert GABAergic excitation into inhibition (Choi et al., 2008; Farajnia et al., 2014). A recent study by Klett and Allen (2017) demonstrated a larger effect on $[Cl^-]_i$ in SCN neurons due to application of the KCC2 blocker VU0240551 compared to bumetanide, suggesting a significant role of KCCs in the regulation of $[Cl^-]_i$. Our results show, for the first time, that a specific blocker for KCC2, ML077 (VU0255011), not only attenuates the GABAergic response in the SCN, but can even cause a reversal of the polarity of the GABAergic response from inhibition to excitation.

GABA is a dominant neurotransmitter in the SCN and has important roles in synchronization and entrainment (Albus et al., 2005). Modeling approaches and experimental evidence show that GABA signaling has significant impact on network function determining basic properties and plasticity of the SCN clock (Azzi et al., 2017; DeWoskin et al., 2015). Modulation of SCN network underlies encoding seasonal day length changes with clustering of neuronal activity in short days and wider phase distribution of the pacemaker cells in the SCN during long days (VanderLeest et al., 2007). While there is still some controversy on the potential excitatory action of GABA in the adult SCN (see (Albers et al., 2017)), there is mounting evidence for excitatory GABA responses and the role of KCCs to regulate Cl^- concentration (Choi et al., 2008; Farajnia et al., 2014; Irwin and Allen, 2009; Myung et al., 2015). Functionally, the modulation of GABA response types and subsequent changes in E/I balance may affect SCN network plasticity. Our data show that just blocking KCC2 can already change the E/I balance in the SCN from a short-day to a long-day phenotype. Whether the changes in GABAergic E/I balance are sufficient or necessary for photoperiodic encoding by the SCN still needs to be established.

An imbalance between GABAergic excitation and inhibition is implicated in several neurological disorders (Marín, 2012; Sgadò et al., 2011) and because of its ability to reduce the level of GABAergic excitation, bumetanide is already used in several clinical trials for epilepsy and autism (Bruining et al., 2015; Du et al., 2015; Eftekhari et al., 2013; Lemonnier et al., 2012; Pressler et al., 2015). Still, there is a demand for improved pharmacological blockers for the cotransporters, since the kinetics of bumetanide and furosemide are not optimal due to short half-life time and bad passage of the blood-brain barrier (Brandt et al., 2010). Our results already show the high effectiveness of ML077 for manipulating E/I balance in neuronal networks and this drug has been further optimized as VU0463271 (Delpire et al., 2012). Studies have shown that this new inhibitor leads to hippocampal hyper-excitability and seizure activity both in slices and in vivo (Kelley et al., 2016; Sivakumaran et al., 2015). These new and optimized KCC2 blockers are important tools for fundamental research on the role of chloride homeostasis in regulating E/I balance in neuronal networks.

While the mechanisms regulating and maintaining $[Cl^-]_i$ are still under debate, previous studies have shown a prominent role for CCCs (for review: (Ben-Ari, 2002; Payne et al., 2003)). Reduction or absence of KCC2 or its functionality leads to decreased inhibitory GABAergic actions (Deeb et al., 2011; Doyon et al., 2015; Hubner et al., 2001; Rivera et al., 1999; Zhu et al., 2005). Moreover, chloride dysregulation caused by reduced KCC2 expression or function is associated with numerous neurological disorders including epilepsy, chronic pain, and schizophrenia (Ben-Ari et al., 2012; Kelley et al., 2016; Miles et al., 2012; Price et al., 2005). Recently, Glykys et al. questioned the prominent role of KCC2 and NKCC1 by showing that blocking these cotransporters with VU0240551 and bumetanide did not change $[Cl^-]_i$, but that local intracellular and extracellular concentrations of anions determined $[Cl^-]_i$ (Glykys et al., 2014a). Since the argument on the role of immobile anions in $[Cl^-]_i$ regulation is not fully resolved yet (Glykys et al., 2014b; Luhmann et al., 2014; Voipio et al., 2014), this alternative or additional mechanism deserves further study. With our data, we show a significant increase in GABAergic excitation after blocking KCC2 with the new antagonist ML077. This GABA-mediated neuronal excitation presumably results from an increased $[Cl^-]_i$ and a correlated shift in GABA reversal potential. While impermeable anions may still contribute to the maintenance of $[Cl^-]_i$, our results support the hypothesis that cation-chloride-cotransporters play an important role in regulating the chloride homeostasis.

The question remains how photoperiod can affect chloride cotransporters to induce a change in E/I balance. Myung et al. recently demonstrated an increase in $[Cl^-]_i$ in the SCN cells after entrainment to long photoperiod. Moreover, application of furosemide to long photoperiod entrained SCN slices increased synchronization and lengthened the period of the circadian rhythms in *Bmal1*-Eluc in 12:12 entrained SCN explants to levels shown for the short photoperiod entrained SCN (Myung et al., 2015). Combined, these results suggest that modulation of the chloride levels in the cells can play a role in day length encoding in the SCN. At the transcript level, the expression of both KCC2 and NKCC1 were upregulated in long photoperiod, when compared to short photoperiod, and the relative expression ratio between NKCC1 and KCC2 was significantly higher under long photoperiod in the dorsal SCN (Myung et al., 2015). Because these results only show the increase at mRNA level, one cannot conclude that NKCC1 causes the higher $[Cl^-]_i$ under long photoperiod. More important than mRNA, or even protein expression, is the functional expression

and/or regulation of KCC2 vs NKCC1. The functionality of KCC2 is modulated by both transcriptional and post-transcriptional routes. (De)phosphorylation, recycling, and intracellular trafficking are, amongst others, examples of how KCC2 can be modulated and its function can be influenced (Kahle et al., 2013; Kahle and Delpire, 2016; Kaila et al., 2014; Lee et al., 2011; Mahadevan and Woodin, 2016). Therefore, the decrease in functional KCC2 and/or increase in functional NKCC1 in long photoperiod may contribute to elevated $[Cl^-]_i$ and consequently to the rise in GABAergic excitation. From our data we conclude that KCC2 plays an important role in the hyperpolarizing effect of GABA and thus in maintaining a low $[Cl^-]_i$. These data have potential societal impact as use of artificial light in modern society leads to “longer day length”. Moreover, GABAergic function is essential for sleep, anxiety, and depression. Whether day length also affects GABAergic function in other brain areas through this mechanism remains to be investigated.

5

ACKNOWLEDGEMENTS

We thank Dr. Craig Lindsley from the Vanderbilt University (Nashville, TN, USA) for providing us the first batch of ML077. We also thank Mayke Tersteeg for her technical assistance. This work was supported by The Netherlands Organisation for Scientific Research/Netherlands Organisation for Health Research and Development (Grant TOPGo 91210064 to J.H.M.), and the Velux Foundation (project grant 1029 to S.M).

REFERENCES

1. Albers, H. E., Walton, J. C., Gamble, K. L., McNeill, J. K. t., Hummer, D. L., 2017. The dynamics of GABA signaling: Revelations from the circadian pacemaker in the suprachiasmatic nucleus. *Front. Neuroendocrin.*, 44, 35-82.
2. Albus, H., Vansteensel, M. J., Michel, S., Block, G. D., Meijer, J. H., 2005. A GABAergic mechanism is necessary for coupling dissociable ventral and dorsal regional oscillators within the circadian clock. *Curr. Biol.*, 15, 886-893.
3. Azzi, A., Evans, J. A., Leise, T., Myung, J., Takumi, T., Davidson, A. J., Brown, S. A., 2017. Network Dynamics Mediate Circadian Clock Plasticity. *Neuron*, 93, 441-450.
4. Ben-Ari, Y., 2002. Excitatory actions of gaba during development: the nature of the nurture. *Nat. Rev. Neurosci.*, 3, 728-739.
5. Ben-Ari, Y., Khalilov, I., Kahle, K. T., Cherubini, E., 2012. The GABA excitatory/inhibitory shift in brain maturation and neurological disorders. *Neuroscientist*, 18, 467-486.
6. Blaesse, P., Airaksinen, M. S., Rivera, C., Kaila, K., 2009. Cation-chloride cotransporters and neuronal function. *Neuron*, 61, 820-838.
7. Brandt, C., Nozadze, M., Heuchert, N., Rattka, M., Loscher, W., 2010. Disease-modifying effects of phenobarbital and the NKCC1 inhibitor bumetanide in the pilocarpine model of temporal lobe epilepsy. *J. Neurosci.*, 30, 8602-8612.
8. Bruining, H., Passtoors, L., Goriounova, N., Jansen, F., Hakvoort, B., de Jonge, M., Poil, S. S., 2015. Paradoxical Benzodiazepine Response: A Rationale for Bumetanide in Neurodevelopmental Disorders? *Pediatrics*, 136, e539-543.
9. Buzsáki, G., Kaila, K., Raichle, M., 2007. Inhibition and brain work. *Neuron*, 56, 771-783.
10. Choi, H. J., Lee, C. J., Schroeder, A., Kim, Y. S., Jung, S. H., Kim, J. S., Kim, D. Y., Son, E. J., Han, H. C., Hong, S. K., Colwell, C. S., Kim, Y. I., 2008. Excitatory actions of GABA in the suprachiasmatic nucleus. *J. Neurosci.*, 28, 5450-5459.
11. Chung, L., 2012. Recent progress in GABAergic excitation from mature brain. *Arch. Pharm. Res.*, 35, 2035-2044.
12. Costa, E., 1998. From GABAA receptor diversity emerges a unified vision of GABAergic inhibition. *Annu. Rev. Pharmacol.*, 38, 321-350.
13. De Jeu, M., Pennartz, C., 2002. Circadian modulation of GABA function in the rat suprachiasmatic nucleus: excitatory effects during the night phase. *J. Neurophys.*, 87, 834-844.
14. Deeb, T. Z., Lee, H. H. C., Walker, J. A., Davies, P. A., Moss, S. J., 2011. Hyperpolarizing GABAergic transmission depends on KCC2 function and membrane potential. *Channels*, 5, 475-481.
15. Delpire, E., Baranczak, A., Waterson, A. G., Kim, K., Kett, N., Morrison, R. D., Daniels, J. S., Weaver, C. D., Lindsley, C. W., 2012. Further optimization of the K-Cl cotransporter KCC2 antagonist ML077: development of a highly selective and more potent in vitro probe. *Bioorg. Med. Chem. Lett.*, 22, 4532-4535.
16. Delpire, E., Days, E., Lewis, L. M., Mi, D., Kim, K., Lindsley, C. W., Weaver, C. D., 2009. Small-molecule screen identifies inhibitors of the neuronal K-Cl cotransporter KCC2. *Proc. Natl. Acad. Sci. USA*, 106, 5383-5388.
17. DeWoskin, D., Myung, J., Belle, M. D., Piggins, H. D., Takumi, T., Forger, D. B., 2015. Distinct roles for GABA across multiple timescales in mammalian circadian timekeeping. *Proc. Natl. Acad. Sci. USA*, 112, E3911-3919.
18. Doyon, N., Prescott, S. A., De Koninck, Y., 2015. Mild KCC2 Hypofunction Causes Inconspicuous Chloride Dysregulation that Degrades Neural Coding. *Front. Cell. Neurosci.*, 9, 516.
19. Du, L., Shan, L., Wang, B., Li, H., Xu, Z., Staal, W. G., Jia, F., 2015. A Pilot Study on the Combination of Applied Behavior Analysis and Bumetanide Treatment for Children with Autism. *J. Child Adol. Psychop.*, 25, 585-588.
20. Eftekhari, S., Mehvari Habibabadi, J., Najafi Ziarani, M., Hashemi Fesharaki, S. S., Charakhani, M., Mostafavi, H., Joghataei, M. T., Beladimoghadam, N., Rahimian, E., Hadjighassem, M. R., 2013. Bumetanide reduces seizure frequency in patients with temporal lobe epilepsy. *Epilepsia*, 54, e9-12.
21. Farajnia, S., van Westering, T. L. E., Meijer, J. H., Michel, S., 2014. Seasonal induction of

- GABAergic excitation in the central mammalian clock. *Proc. Natl. Acad. Sci. USA*, 111, 9627-9632.
22. Gamba, G., 2005. Molecular physiology and pathophysiology of electroneutral cation-chloride cotransporters. *Physiol. Rev.*, 85, 423-493.
 23. Gillen, C. M., Brill, S., Payne, J. A., Forbush, B., 3rd, 1996. Molecular cloning and functional expression of the K-Cl cotransporter from rabbit, rat, and human. A new member of the cation-chloride cotransporter family. *J. Biol. Chem.*, 271, 16237-16244.
 24. Glykys, J., Dzhalala, V., Egawa, K., Balena, T., Saponjian, Y., Kuchibhotla, K. V., Bacskai, B. J., Kahle, K. T., Zeuthen, T., Staley, K. J., 2014a. Local impermeant anions establish the neuronal chloride concentration. *Science*, 343, 670-675.
 25. Glykys, J., Dzhalala, V., Egawa, K., Balena, T., Saponjian, Y., Kuchibhotla, K. V., Bacskai, B. J., Kahle, K. T., Zeuthen, T., Staley, K. J., 2014b. Response to comments on "Local impermeant anions establish the neuronal chloride concentration". *Science*, 345, 1130.
 26. Haider, B., Duque, A., Hasenstaub, A. R., McCormick, D. A., 2006. Neocortical network activity in vivo is generated through a dynamic balance of excitation and inhibition. *J. Neurosci.*, 26, 4535-4545.
 27. Hubner, C. A., Stein, V., Hermans-Borgmeyer, I., Meyer, T., Ballanyi, K., Jentsch, T. J., 2001. Disruption of KCC2 reveals an essential role of K-Cl cotransport already in early synaptic inhibition. *Neuron*, 30, 515-524.
 28. Irwin, R. P., Allen, C. N., 2007. Calcium response to retinohypothalamic tract synaptic transmission in suprachiasmatic nucleus neurons. *J. Neurosci.*, 27, 11748-11757.
 29. Irwin, R. P., Allen, C. N., 2009. GABAergic signaling induces divergent neuronal Ca²⁺ responses in the suprachiasmatic nucleus network. *Eur. J. Neurosci.*, 30, 1462-1475.
 30. Kahle, K. T., Deeb, T. Z., Puskarjov, M., Silayeva, L., Liang, B., Kaila, K., Moss, S. J., 2013. Modulation of neuronal activity by phosphorylation of the K-Cl cotransporter KCC2. *Trends Neurosci.*, 36, 726-737.
 31. Kahle, K. T., Delpire, E., 2016. Kinase-KCC2 coupling: Cl⁻ rheostasis, disease susceptibility, therapeutic target. *J. Neurophysiol.*, 115, 8-18.
 32. Kaila, K., 1994. Ionic basis of GABAA receptor channel function in the nervous system. *Prog. Neurobiol.*, 42, 489-537.
 33. Kaila, K., Price, T. J., Payne, J. A., Puskarjov, M., Voipio, J., 2014. Cation-chloride cotransporters in neuronal development, plasticity and disease. *Nat. Rev. Neurosci.*, 15, 637-654.
 34. Kelley, M. R., Deeb, T. Z., Brandon, N. J., Dunlop, J., Davies, P. A., Moss, S. J., 2016. Compromising KCC2 transporter activity enhances the development of continuous seizure activity. *Neuropharmacol.*, 108, 103-110.
 35. Klett, N. J., Allen, C. N., 2017. Intracellular Chloride Regulation in AVP+ and VIP+ Neurons of the Suprachiasmatic Nucleus. *Sci., Rep.* 7, 10226.
 36. Lee, H. H. C., Deeb, T. Z., Walker, J. A., Davies, P. A., Moss, S. J., 2011. NMDA receptor activity downregulates KCC2 resulting in depolarizing GABAA receptor-mediated currents. *Nat. Neurosci.*, 14, 736-743.
 37. Lemonnier, E., Degrez, C., Phelep, M., Tyzio, R., Josse, F., Grandgeorge, M., Hadjikhani, N., Ben-Ari, Y., 2012. A randomised controlled trial of bumetanide in the treatment of autism in children. *Transl. Psychiat.*, 2, e202.
 38. Lindsley, C., Lewis, M., Weaver, D., Delpire, E., 2010. Discovery of a Highly Selective KCC2 Antagonist. In: Probe Reports from the NIH Molecular Libraries Program. National Center for Biotechnology Information (US), Bethesda (MD). <https://www.ncbi.nlm.nih.gov/books/NBK47347/>
 39. Luhmann, H. J., Kirischuk, S., Kilb, W., 2014. Comment on "Local impermeant anions establish the neuronal chloride concentration". *Science*, 345, 1130.
 40. Macdonald, R. L., Olsen, R. W., 1994. GABAA receptor channels. *Annu. Rev. Neurosci.*, 17, 569-602.
 41. Mahadevan, V., Woodin, M. A., 2016. Regulation of neuronal chloride homeostasis by neuromodulators. *J. Physiol.*, 594, 2593-2605.
 42. Marín, O., 2012. Interneuron dysfunction in psychiatric disorders. *Nat. Rev. Neurosci.*, 13, 107-120.
 43. Michel, S., Marek, R., Vanderleest, H. T., Vansteensel, M. J., Schwartz, W. J., Colwell, C. S., Meijer, J. H., 2013. Mechanism of bilateral communication in the suprachiasmatic nucleus. *Eur. J. Neurosci.*, 37, 964-971.
 44. Miles, R., Blaesse, P., Huberfeld, G., Wittner, L., Kaila, K., 2012. Chloride homeostasis and GABA

- signaling in temporal lobe epilepsy. In: Noebels JL, Avoli M, Rogawski MA, et al., (Eds.), Jasper's Basic Mechanisms of the Epilepsies. National Center for Biotechnology Information (US), Bethesda (MD).
45. Myung, J., Hong, S., DeWoskin, D., De Schutter, E., Forger, D. B., Takumi, T., 2015. GABA-mediated repulsive coupling between circadian clock neurons in the SCN encodes seasonal time. *Proc. Natl. Acad. Sci. USA*, 112, E3920-3929.
 46. Nelson, S. B., Valakh, V., 2015. Excitatory/Inhibitory Balance and Circuit Homeostasis in Autism Spectrum Disorders. *Neuron*, 87, 684-698.
 47. Payne, J. A., Rivera, C., Voipio, J., Kaila, K., 2003. Cation-chloride co-transporters in neuronal communication, development and trauma. *Trends Neurosci.*, 26, 199-206.
 48. Pressler, R. M., Boylan, G. B., Marlow, N., Blennow, M., Chiron, C., Cross, J. H., de Vries, L. S., Hallberg, B., Hellstrom-Westas, L., Jullien, V., Livingstone, V., Mangum, B., Murphy, B., Murray, D., Pons, G., Rennie, J., Swarte, R., Toet, M. C., Vanhatalo, S., Zohar, S., 2015. Bumetanide for the treatment of seizures in newborn babies with hypoxic ischaemic encephalopathy (NEMO): an open-label, dose finding, and feasibility phase 1/2 trial. *Lancet Neurol.*, 14, 469-477.
 49. Price, T. J., Cervero, F., de Koninck, Y., 2005. Role of cation-chloride-cotransporters (CCC) in pain and hyperalgesia. *Curr. Top. Med. Chem.*, 5, 547-555.
 50. Rivera, C., Voipio, J., Payne, J. A., Ruusuvuori, E., Lahtinen, H., Lamsa, K., Pirvola, U., Saarma, M., Kaila, K., 1999. The K⁺/Cl⁻ co-transporter KCC2 renders GABA hyperpolarizing during neuronal maturation. *Nature*, 397, 251-255.
 51. Sgadò, P., Dunleavy, M., Genovesi, S., Provenzano, G., Bozzi, Y., 2011. The role of GABAergic system in neurodevelopmental disorders: a focus on autism and epilepsy. *Int. J. Physiol. Pathophysiol. Pharmacol.*, 3, 223-235.
 52. Sivakumaran, S., Cardarelli, R. A., Maguire, J., Kelley, M. R., Silayeva, L., Morrow, D. H., Mukherjee, J., Moore, Y. E., Mather, R. J., Duggan, M. E., Brandon, N. J., Dunlop, J., Zicha, S., Moss, S. J., Deeb, T. Z., 2015. Selective inhibition of KCC2 leads to hyperexcitability and epileptiform discharges in hippocampal slices and in vivo. *J. Neurosci.*, 35, 8291-8296.
 53. Sivilotti, L., Nistri, A., 1991. GABA receptor mechanisms in the central nervous system. *Prog. Neurobiol.*, 36, 35-92.
 54. Staley, K. J., 2002. Diuretics as Antiepileptic Drugs: Should We Go with the Flow? *Epilepsy Curr.*, 2, 35-38.
 55. VanderLeest, H. T., Houben, T., Michel, S., Deboer, T., Albus, H., Vansteensel, M. J., Block, G. D., Meijer, J. H., 2007. Seasonal encoding by the circadian pacemaker of the SCN. *Curr. Biol.*, 17, 468-473.
 56. Voipio, J., Boron, W. F., Jones, S. W., Hopfer, U., Payne, J. A., Kaila, K., 2014. Comment on "Local impermeant anions establish the neuronal chloride concentration". *Science*, 345, 1130.
 57. Wagner, S., Castel, M., Gainer, H., Yarom, Y., 1997. GABA in the mammalian suprachiasmatic nucleus and its role in diurnal rhythmicity. *Nature*, 387, 598-603.
 58. Zhu, L., Lovinger, D., Delpire, E., 2005. Cortical neurons lacking KCC2 expression show impaired regulation of intracellular chloride. *J. Neurophysiol.*, 93, 1557-1568.

SUPPLEMENTARY MATERIALS

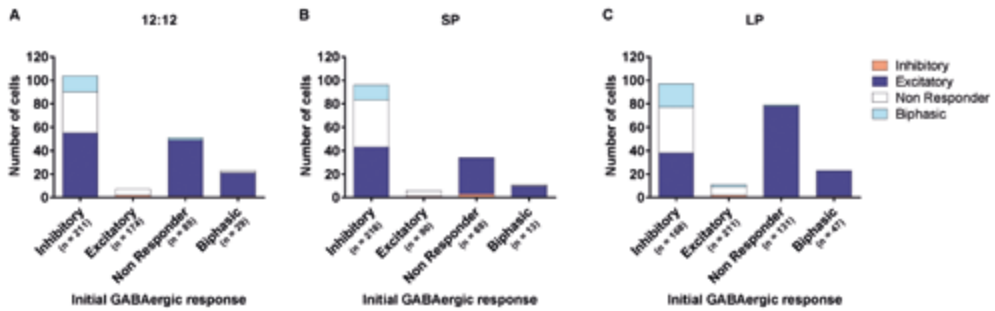


Figure S1. Changes in response type in SCN neurons after blocking KCC2 with ML077. Number of cells that change response type after incubation with ML077 grouped per initial GABAergic response in SCN cells of mice entrained to (A) LD12:12, (B) SP, and (C) LP. The number of cells for each response type resulting from the ML077 treatment is depicted on the y-axis and shows a significant effect of the drug on response type distribution (number of cells per initial response type shown on the x-axis) (LD12:12: Wald Chi square test; $p = 1 \times 10^{-6}$ SP: Wald Chi square test; $p = 1.44 \times 10^{-9}$ LP: Wald Chi square test; $p = 0.019$).

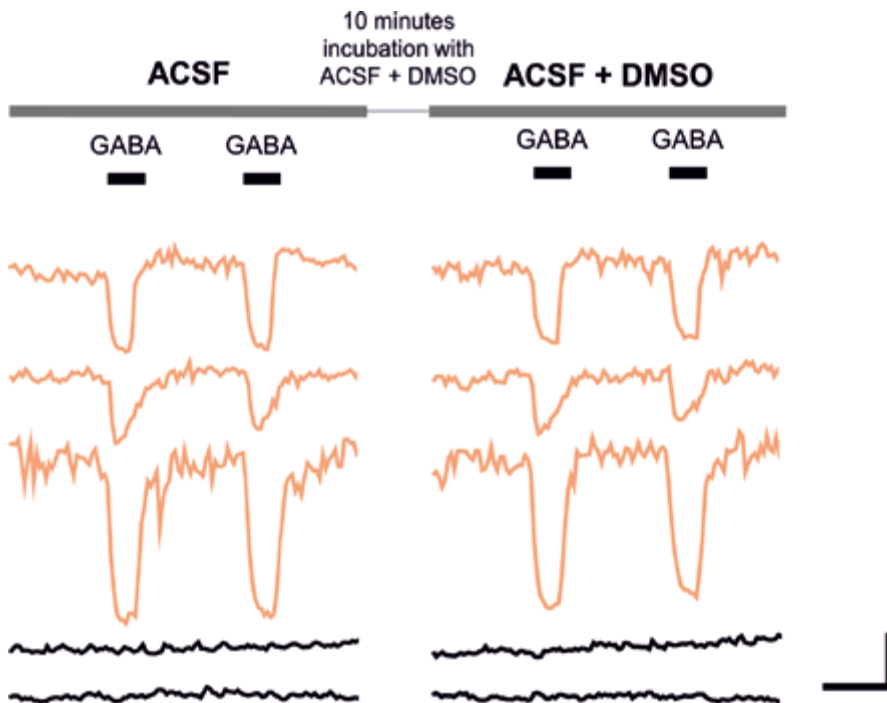


Figure S2. DMSO treatment does not affect GABAergic responses. On top, a sketch of the experimental protocol is depicted. SCN slices were continuously superfused with ACSF and Ca^{2+} transients were recorded in response to focal applications of GABA ($200 \mu\text{M}$) given before and after a 10-minute incubation with DMSO in ACSF (4 ppm). Below example traces of Ca^{2+} transients of 5 neurons are shown demonstrating the GABAergic responses before and after incubation with control solution (4 ppm DMSO in ACSF). (Scale bars, 50 nM , 30 s)

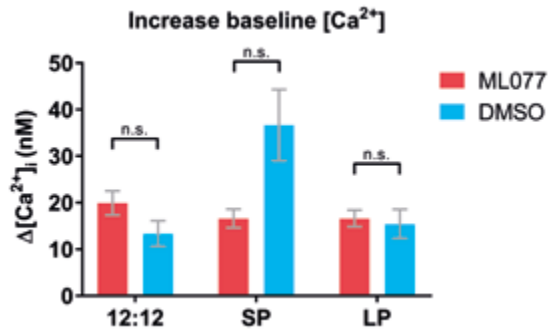


Figure S3. Rise in baseline $[Ca^{2+}]_i$ is not an effect of blocking KCC2 with ML077. Bar graphs show average increase (means \pm SEM) in baseline $[Ca^{2+}]_i$ after application of ML077 and DMSO from all cells of animals entrained to LD12:12 (Mann-Whitney test: $p = 0.069$, ML077: $n = 499$, DMSO: $n = 269$), SP (Mann-Whitney test: $p = 0.0141$, ML077: $n = 387$, DMSO: $n = 149$), and LP (Mann-Whitney test: $p = 0.153$, ML077: $n = 557$, DMSO: $n = 319$).



six

GENERAL DISCUSSION

The central circadian clock in mammals resides in the suprachiasmatic nucleus (SCN) of the anterior hypothalamus in the brain. The SCN clock is composed of multiple, single-cell oscillators which together generate an output signal, synchronized to the environmental light-dark cycle, and convey this “timing information” to the periphery. The functioning of the SCN as the major pacemaker relies on the communication and coupling between the cells in the network, and on the ability of the network to adjust to environmental cycles. Besides its role as a daily clock, the SCN also serve as a seasonal clock by adjusting the output signal to the duration of light per day (i.e. photoperiod). Seasonal encoding by the SCN is a good example of the functionality of the network – opposed to the individual SCN neurons being autonomous oscillators –, since it is a composite tissue property that relies on the network organization, and amongst others, on the synchronization of single-cell oscillators.

The work in this thesis enhances our understanding of what is needed for this type of network plasticity. Specifically, we focused on the potential role of the neurotransmitter GABA and the GABAergic Excitation/Inhibition (E/I) balance in coupling mechanisms within the SCN network under different conditions, like changing light regimes and aging. We showed for the first time that brief light exposure at the beginning and end of the day can change the function of GABA. We also provided evidence that chloride cotransporter modulation is responsible for light regime induced changes in E/I balance. Moreover, we discovered a shift in E/I balance in the aging central clock that may explain network plasticity. In this chapter I will explain and discuss the implications of these outcomes.

1. E/I BALANCE IN THE BRAIN

The right balance between excitation and inhibition is crucial for proper brain function, because synaptic E/I balance underlies efficient neuronal information processing (Zhou & Yu, 2018). Loss of a tight control over the E/I balance could result in hyperexcitability or excessive quiescence, which in turn cause deficits in information processing (Figure 1) (Kinouchi & Copelli, 2006). The implications of an E/I imbalance can be detrimental. Abnormalities in inhibition or excitation are linked to disorders that occur particularly at the beginning and the end of our life, like several neurodevelopmental as well as neurodegenerative disorders (Gatto & Broadie, 2010; Rissman & Mobley, 2011; Canitano & Pallagrosi, 2017; Bi *et al.*, 2020; Bruining *et al.*, 2020).

Moreover, dysregulation of the E/I balance is correlated to the pathophysiology of migraine and epilepsy (Sgadò *et al.*, 2011; Vecchia & Pietrobon, 2012). The mechanisms by which a balance between excitation and inhibition is established and maintained is still a subject of debate. Physiologically, there are homeostatic and developmental processes that maintain the E/I balance in a narrow range at the level of single cells and at the level of cortical networks over long timescales (Zhou *et al.*, 2014; He *et al.*, 2016). The E/I balance of single cells is determined by the relative contributions of excitatory and inhibitory synaptic currents (Shu *et al.*, 2003; Okun & Lampl, 2008). It is widely accepted that an E/I balance is kept approximately constant and that deviations from the E/I ratio beyond acceptable tolerances result in aberrant hyper- or hypo-activity. However, there is also evidence that small changes of the E/I balance are physiologically relevant. For instance, during

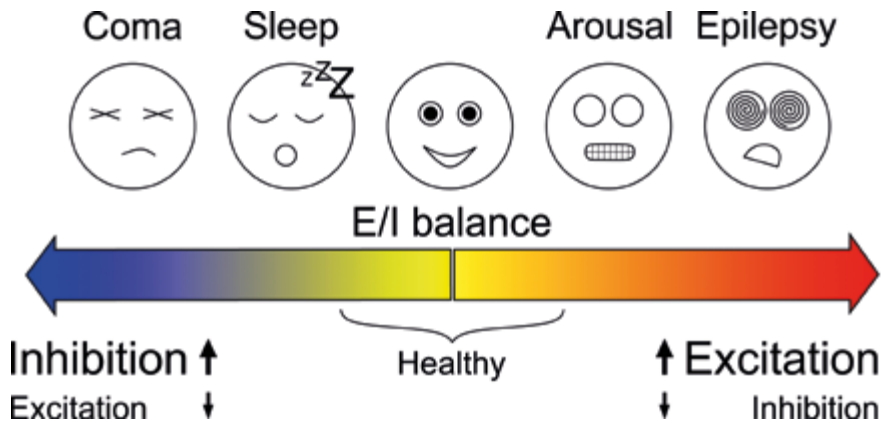


Figure 1. The excitation/inhibition balance. A schematic overview of the balance between excitation and inhibition in the brain. A proper balance between excitation and inhibition is crucial for brain functioning. When the scale turns towards more inhibition, this results in excessive hypo-activity like sleepiness or even a coma. When the scale turns towards too much excitation, this results in hyper-excitability like arousal or even seizures.

sensory stimulation in the auditory cortex, E/I balance can be transiently perturbed, but generally recovers within tens of minutes (Froemke *et al.*, 2007). On a longer timescale, there is a circadian regulation in E/I balance in cortical areas in humans (Chellappa *et al.*, 2016; Ly *et al.*, 2016) and there are indications for seasonal variability (Meyer *et al.*, 2015). Moreover, the E/I balance in the SCN has shown to be modulated within a presumably “healthy” range under normal physiological conditions (Albus *et al.*, 2005; Choi *et al.*, 2008; Farajnia *et al.*, 2014).

2. E/I BALANCE IN THE SCN

In the experiments described in this thesis, we measured the E/I balance in SCN slices of mice under different circumstances, like changing light regimes or in aging. The E/I ratio was calculated by determining the GABAergic response of individual SCN neurons using calcium imaging. By applying this imaging technique, we were able to measure about 80 – 120 neurons per SCN, divided over 2 – 3 slices. This way, the different regions of the SCN – both anterior to posterior and ventral to dorsal – were represented in the measurements to ensure a proper distribution. We showed an increase in GABAergic excitation and E/I balance in the aged SCN (**chapter 4**) and after exposure to long photoperiod (**chapter 5**). We also demonstrated a decrease in inhibitory responses after exposure to skeleton long photoperiod (**chapter 2**).

The neurotransmitter GABA is mainly inhibitory to most adult neurons and because of its abundance it plays a critical role in setting the E/I balance. There are, however, parts of the mature brain, among which the SCN, with GABAergic depolarization and excitation in physiologically healthy states (Chung, 2012). In the SCN, GABA has the ability to act both inhibitory and excitatory and because most SCN neurons contain GABA, it is believed to be a major contributor to the E/I balance in the SCN (Wagner *et al.*, 1997; Albus *et al.*, 2005; Choi *et al.*, 2008; Irwin & Allen, 2009).

Previous studies have shown plasticity in the E/I balance in the SCN. For instance, there is a daily modulation of the E/I ratio in the SCN with more GABAergic excitation during the night compared to the day (Choi *et al.*, 2008; Irwin & Allen, 2009; Farajnia *et al.*, 2014). Also, the length of the day impacts the E/I balance, as the E/I ratio increases in SCN slices of mice adapted to a long day photoperiod, when compared to a short day photoperiod (Farajnia *et al.*, 2014; Myung *et al.*, 2015). Hence, the E/I balance fluctuates over the different seasons. These E/I changes seem functional, since plasticity in GABA_A signaling was shown to be crucial for neuromodulation of the SCN network when adapting to different photoperiods (Rohr *et al.*, 2019). Several studies demonstrated that GABAergic excitation occurred mostly in the dorsal part of the SCN (Albus *et al.*, 2005; Choi *et al.*, 2008; Irwin & Allen, 2009). We therefore always tested for regional variances, but found no differences in the distribution of the different GABAergic responses along the dorsoventral axis. The lack of regional differences in GABAergic response types is comparable to a previous study examining the effect of photoperiod on the GABAergic responses in the mouse SCN (Farajnia *et al.*, 2014). The difference in spatial organization between our studies and the studies showing more excitation in the dorsal area of the SCN are difficult to explain, but it probably involves functional and anatomical differences in the brains of mice and rats (Morin *et al.*, 2006).

As the GABA_A receptor is a GABA-gated chloride channel, the polarity of the GABAergic signal depends on the intracellular chloride concentration ($[Cl^-]_i$) and the relationship between the chloride equilibrium potential (E_{Cl^-}) and the membrane potential (V_m) (Kaila, 1994; Ben-Ari, 2002). Different classes of cation-chloride-cotransporters regulate $[Cl^-]_i$, of which at least two are expressed in the SCN; the chloride importer NKCC1 and exporter KCC2 (Belenky *et al.*, 2008). KCC2 extrudes Cl^- from the cell, thus when KCC2 is expressed and GABA binds to its receptor, the channel opens and because of the low $[Cl^-]_i$ there is an inward flow of Cl^- causing an inhibitory response. When NKCC1 expression dominates in neurons, the $[Cl^-]_i$ is relatively high, which results in an outward flow of Cl^- and subsequently an excitatory GABA response, after GABA binds to its receptor.

3. HOW DOES LIGHT INFLUENCE THE E/I BALANCE IN THE SCN?

As described above and in more detail in **chapter 1**, the time of the day and the length of the day influence the E/I balance in the SCN. In **chapter 5**, we confirmed that when mice were exposed to long photoperiods (i.e. 16 h of daylight), the E/I balance in SCN slices shifts towards more excitation and when exposed to short photoperiods (i.e. 8 h of daylight) it shifts towards more inhibition. In **chapter 5** we also demonstrated that the chloride cotransporter KCC2 – and thus the $[Cl^-]_i$ – plays a major role in the establishment of the E/I balance in the SCN. When KCC2 was blocked with the highly specific antagonist ML077, resulting in an increase in $[Cl^-]_i$ of the SCN cells, the polarity of the GABAergic response in many SCN neurons changed within minutes after application and the overall E/I balance got larger. This increase in E/I balance was evident and similar in all the experiments using ML077, indicating that KCC2 plays a role in regulating $[Cl^-]_i$, regardless of the baseline $[Cl^-]_i$ set by adaptation to long or short photoperiod. Interestingly, blocking KCC2 with ML077 in the SCN of mice adapted to short photoperiod resulted in an E/I balance that is very similar to the E/I ratio under long photoperiod (**chapter 5, figure 4A and 4E**). This showed that ML077

is a suitable tool to manipulate the E/I balance and can be useful for researching the functional mechanisms of E/I balance in seasonal encoding. More recent work focused on the role of both cotransporters NKCC1 and KCC2 in regulating $[Cl^-]_i$ in different parts of the SCN (Klett & Allen, 2017). NKCC1 contributed to $[Cl^-]_i$ regulation, however, KCC2 was shown to be the primary regulator. Interestingly, it seems to be differentially regulated between VIP and AVP (i.e. core and shell) expressing neurons, because blocking KCC2 had a larger effect on VIP neurons, when compared to AVP neurons (Klett & Allen, 2017). Additionally, the switch in GABAergic signaling after adaptation to long photoperiod corresponded with KCC2 downregulation in the core region of the SCN (Rohr *et al.*, 2019). Another study showed that NKCC1 protein expression was increased in the ventral SCN of hamsters exposed to a photoperiod of LD 14:10, when compared to the dorsal part (McNeill *et al.*, 2020). Concluding, the data from these studies indicate a role for both NKCC1 and KCC2 in the polarity of the GABAergic response in SCN neurons, though to a different extent, and thereby on the SCN network plasticity when challenged with environmental changes.

There are studies proposing that the variability in GABAergic responses in the SCN could support adaptation to environmental conditions and is therefore functional (Farajnia *et al.*, 2014; Myung *et al.*, 2015; Rohr *et al.*, 2019). The exact mechanism of how changes in E/I balance will contribute to phase distribution of SCN neurons is still under debate and has to be further investigated (McNeill *et al.*, 2020). A recent study on the expression level of NKCC1 in the SCN of hamsters showed increased protein levels after exposure to constant light, suggesting that light duration may influence the expression of NKCC1. However, when the hamsters were exposed to a long day of LD 14:10, the NKCC1 protein levels were not different from those of hamsters housed under constant darkness, suggesting that specific ratios of GABAergic excitation/inhibition are not required for seasonal entrainment (McNeill *et al.*, 2020). But, as described above, KCC2 might play a more prominent role in setting $[Cl^-]_i$ in SCN neurons than NKCC1 (Klett & Allen, 2017) and exposure to long photoperiod has resulted in KCC2 downregulation (Rohr *et al.*, 2019). Since entrainment to longer photoperiods decreases the magnitude of phase shifting effects of light (Pittendrigh *et al.*, 1984; Evans *et al.*, 2004; vanderLeest *et al.*, 2009), the increased E/I ratio in SCN neurons could also influence the phase shifting response of the SCN to light. However, *in vivo* injections of an NKCC1 inhibitor into the SCN decreased light induced phase delays, indicating that the excitatory effects of GABA in the SCN contribute to the phase delaying effect of light (McNeill *et al.*, 2018). These results seem to contradict our proposed consequence of increased E/I levels, considering that the behavioral phase shifts are smaller and the amount of excitatory GABA is higher in animals entrained to long photoperiods (vanderLeest *et al.*, 2009; Farajnia *et al.*, 2014). A possible explanation is that the acute use of cotransporter blockers, and the resulting acute change in chloride levels, is mechanistically different from adaptation to long photoperiod. In line with this, as demonstrated in **chapter 5**, application of the KCC2 blocker ML077 also show that, regardless of the baseline chloride levels, there is an additive, acute effect of the blocker. After entrainment to long photoperiod, cotransporter expressions and chloride levels in the SCN cells are changed, but this is a gradual change that takes weeks and is accompanied by a change in phase distribution. Studies based on experimental data, strengthened with modeling data, indicate that the chloride homeostasis and the polarity of the GABAergic signaling influence the coupling within the SCN

network and ultimately lead to phase adjustment (DeWoskin *et al.*, 2015; Myung *et al.*, 2015). It is likely that the decreased phase-shifting capacity, as seen after entrainment to long photoperiod, is the result of the increased phase dispersal in the SCN network. This, in turn, will result in a change in phase distribution, which has been shown to be the critical factor determining the phase shifting capacity in the SCN (vanderLeest *et al.*, 2009).

3.1. Brief light exposure influences the E/I balance in the SCN

In **chapter 2** we examined whether the reception of the full photoperiod was needed for photoperiodic encoding in the SCN at the level of network reorganization. As mentioned in the beginning of this chapter, seasonal encoding is a great example of cellular organization within the SCN network and its functional role. The SCN adjusts its ensemble electrical output to the length of the day of the changing photoperiod, caused by a change in distribution of phases of the individual SCN neurons (Mrugala *et al.*, 2000; VanderLeest *et al.*, 2007). Moreover, seasonal related network changes also induce changes in the E/I balance (Farajnia *et al.*, 2014) (**chapter 5**). In **chapter 2** we aimed to investigate which of these network changes occur when the circadian system is exposed to skeleton photoperiods, i.e. exposed to brief light pulses that mark the beginning and end of the day.

We showed that at different levels – ranging from molecular and cellular to behavioral – all characteristic changes when encoding for full long photoperiod, could be mimicked by just two light pulses of 30 minutes marking the beginning and end of the day. When mice were exposed to skeleton long photoperiod, the waveform of the ensemble electrical activity in SCN slices was broader than in slices from mice exposed to skeleton short photoperiod which is equivalent after entrainment to the full photoperiod. Similar increase in phase distribution was also shown by imaging single cell *per2* clock gene expression in SCN slices of mice entrained to skeleton long photoperiod, compared to skeleton short photoperiod. Moreover, like entrainment to full long photoperiods, exposure to skeleton long photoperiod resulted in a compression of the behavioral activity pattern and a reduction in the magnitude of phase delays in response to a light stimulus, when compared to skeleton short photoperiod. Lastly, there was less GABAergic inhibition in SCN slices of mice adapted to skeleton long photoperiod compared to skeleton short photoperiod, although the overall E/I balance did not differ between the skeleton long and short photoperiod. Taken together, these results showed that brief light exposure at the beginning and end of the day are sufficient for photoperiodic encoding at the network level of the SCN.

The lack of a significant difference between the E/I ratios of skeleton long and short photoperiod, when compared to the full photoperiods, is based on a higher E/I balance in skeleton short photoperiod. Thus, the E/I ratio under skeleton short photoperiod is higher compared to a full short photoperiod. Remarkably, skeleton long photoperiod affected the SCN network to the same degree as full long photoperiod, but there are more differences between skeleton and full short photoperiod. The waveform of the ensemble electrical activity has a more compressed peak under full short photoperiod, when compared to skeleton short photoperiod. Also, the behavioral phase shift is less pronounced in animals entrained to skeleton short photoperiod compared to full

short photoperiod. The similarities between skeleton and full photoperiod when encoding long photoperiod and the differences when encoding for a short photoperiod suggest an additive effect of the full photoperiod. This is in line with recent evidence showing that specific components of light cycles have distinct effects on the circadian system (Tackenberg *et al.*, 2020). Previous work proposed that seasonal encoding depended on a subset of SCN neurons that respond to tonic photic cues, suggesting that seasonal adaptation would require exposure to the full photoperiod (Yan & Silver, 2008). This is in contrast to our work which clearly shows that characteristic cellular reorganization in the SCN, after adapting to long photoperiod, can be achieved by exposure to two brief light pulses. One explanation could be that the previous work was conducted in Syrian hamsters, whereas we worked with mice. Syrian hamsters are, in contrast to our mice, seasonal breeders that contain melatonin. Seasonal encoding by the SCN might be mechanistically different between these species.

The implications of the work from **chapter 2** are interesting, not only in terms of circadian adaptation mechanisms, but also from an ecological point of view. In the modern society, the use of electrical light at night increased immensely in the past decades causing disturbances in the activity patterns of nocturnal animals (Dominoni *et al.*, 2016; Sanders & Gaston, 2018). The skeleton photoperiods that we used actually resemble the natural lighting situation more closely compared to full photoperiods, at least for nocturnal animals. Many nocturnal animals sleep underground, thereby creating their own skeleton photoperiod. The electrical light at night, especially in wintertime, can be harmful to these animals considering the light pulses late at night can be interpreted as a sign for summer. This, in turn, can lead to maladaptive physiological behavior, like the production of offspring at the wrong time of year.

Chapter 2 underscores that even brief light exposure can have physiological effect and should be considered in light management programs aimed at protecting the clock function of nocturnal rodents in the natural environment.

4. AGING

The above mentioned fragmentation of light is also interesting in terms of optimizing light therapy to help the circadian rhythms in the elderly (Goudriaan *et al.*, 2021; Rubiño-Díaz *et al.*, 2021). In **chapter 3 and 4** several aspects of the circadian system – behavioral, molecular, and cellular – were investigated to further identify components that might be affected by aging and thus could be potential targets for such chronotherapeutic interventions. We showed that with aging, mice have a reduced ability to behaviorally adapt to short photoperiods, but there were no impairments in the PER2 rhythms after photoperiodic encoding (**chapter 3**). Additionally, the proportion of GABAergic excitatory responses and the subsequent E/I balance increased in SCN slices of aged mice (**chapter 4**).

Aging is an unavoidable and irreversible process that affects many aspects of physiology and behavior, including the central nervous system. Brain alterations due to aging are evident on various levels with, for instance, a decline in brain volume (Resnick *et al.*, 2003), loss of synaptic function (Jacobs *et al.*, 1997), and a decay in neurotransmitter function (Mora *et al.*, 2007). As detailed

reported in **chapter 1**, aging also affects the circadian system on multiple levels. On the behavioral level, there are age-related disruptions in locomotor activity that lead to more fragmented sleep-wake patterns and an overall reduction in behavioral activity (Valentinuzzi *et al.*, 1997; Dijk & Duffy, 1999; Farajnia *et al.*, 2012). Aging is also associated with reduced synchronization and diminished amplitude of electrical activity rhythms in the SCN neuronal network (Nakamura *et al.*, 2011; Farajnia *et al.*, 2012). Furthermore, at the cellular level, the physiology of the SCN neuron itself is impacted by aging (Aujard *et al.*, 2001; Farajnia *et al.*, 2012). Long term disruption of circadian rhythmicity can be detrimental and is associated to age-related diseases (Kondratova & Kondratov, 2012; Steponenaite *et al.*, 2018). Thus, understanding the mechanisms of aging-related clock disorders will allow targeting for repair of the circadian system.

4.1. Aging affects the E/I balance in the SCN

As mentioned earlier this chapter, alterations in the E/I balance occur at the cellular level, with neurons being inhibitory or excitatory, but likely also contribute to network changes. In **chapter 4** we aimed to investigate whether there is an aging-effect on the GABAergic E/I balance in the SCN, that could contribute to the aging-related network alterations. By measuring GABA stimulated changes in Ca^{2+} transients, we observed significantly more excitatory responses in SCN slices from old mice, compared to young mice. In addition, in the posterior SCN from old mice, we showed a significant decrease in inhibitory responses. Also, the baseline Ca^{2+} levels in the old SCN neurons was higher compared to SCN neurons from young mice. These results demonstrated that aging affects the polarity response, and thus the E/I balance, in the SCN and indicated that the Ca^{2+} homeostasis is altered in the aged SCN network. Whether the increased E/I balance has functional relevance to the aging clock, or is a sign of loss of function remains unclear. Cortical excitability has been associated with age-related cognitive decline. A reduction in circadian rhythms of cortical excitability was found in aged human volunteers during sleep deprivation, which was likely the consequence of a diminished impact of sleep homeostasis and might underlie the reduction in cognitive flexibility in aging (Gaggioni *et al.*, 2019). Alterations in E/I balance also occur in age-related diseases like Alzheimer's Disease (AD) and may be a primary mechanism contributing to seizure activity and cognitive decline in AD patients (Rissman & Mobley, 2011; Bi *et al.*, 2020). Recently, evidence from human post-mortem parietal cortex samples of individuals with AD demonstrated elevations in the synaptic E/I ratios that contributed to cortical hyper-excitability and cognitive impairment in AD patients (Lauterborn *et al.*, 2021). Besides the cognitive decline in AD patients, there are numerous studies that have shown an age-related shift in the E/I balance with heightened hippocampal and prefrontal cortical activity which contributes to memory-impairment (Legon *et al.*, 2016; Tran *et al.*, 2019; Koh *et al.*, 2020). Aged rats without cognitive impairment most likely have a compensational mechanism as they display increased inhibitory postsynaptic currents in recordings from dentate gyrus cells and a larger tonic inhibitory current in the pyramidal neurons, which is lacking in rats with memory impairment (Tran *et al.*, 2018; Tran *et al.*, 2019; Koh *et al.*, 2020). This emphasizes the importance of an adequate balance between inhibition and excitation, also for healthy aging.

Within the SCN, several lines of evidence suggest a possible role for the E/I balance in synchronization mechanisms (Farajnia *et al.*, 2014; Myung *et al.*, 2015; Rohr *et al.*, 2019). Others presented results that GABA plays a role in (de)synchronization, but without distinguishing between the inhibitory or excitatory action of GABA (Liu & Reppert, 2000; Albus *et al.*, 2005; Aton *et al.*, 2006; Evans *et al.*, 2013; Freeman *et al.*, 2013). We showed in **chapter 2, 4, and 5** alterations in the distribution of GABAergic responses, with more excitation and/or less inhibition, in SCN slices in which the phases of the individual neurons were more distributed. In aging (**chapter 4**), under long photoperiod (**chapter 5**), or after exposure to skeleton long photoperiod (**chapter 2**) the degree of synchronization is lower compared to the young SCN or the SCN of mice exposed to short (skeleton) photoperiod (**chapter 2**) (VanderLeest *et al.*, 2007; Farajnia *et al.*, 2012). Although the mechanisms that regulate neuronal phase distribution in the SCN are still unknown, the results from this thesis consistently indicate that changing the amount of GABAergic inhibition or excitation in the SCN contribute to the network alterations. Future research with in vivo measurements of E/I balance in the SCN during entrainment to different photoperiods would help to elucidate the role of E/I balance in seasonal encoding and network reorganization. We consider the seasonal changes in the E/I balance as a functional and physiological process, supporting clock function. The question remains whether this is also the case with aging and if there is still plasticity in the E/I ratio in the aged SCN.

4.2. Aging affects calcium levels in the SCN

Ca^{2+} is an important intracellular component involved in phase adjustment and network stability. Besides a shifted E/I balance in the aged SCN, the data from **chapter 4** suggest that aging causes an altered Ca^{2+} homeostasis as the baseline Ca^{2+} levels are higher in SCN neurons from aged mice. These increased baseline levels of Ca^{2+} could impact cellular phase adjustments, as Ca^{2+} is implicated in rhythm generation and light-induced phase shifts by activating clock gene expression (Kim *et al.*, 2005; Golombek & Rosenstein, 2010). With aging, phase shifting capacity and network stability could be reduced due to the increase in $[\text{Ca}^{2+}]_i$. Research has shown a circadian rhythmicity in $[\text{Ca}^{2+}]_i$ with higher levels during the day, compared to the night (Colwell, 2000; Ikeda *et al.*, 2003) and one study demonstrated that this rhythm is reversed in old mice (Farajnia *et al.*, 2015). The latter, however, did not find differences in Ca^{2+} levels during daytime, when compared with young controls, which is in contrast to our results on baseline Ca^{2+} levels. Since Ca^{2+} is a key cell signaling molecule and an important link between the molecular clock and electrophysiological properties of the SCN neurons, Ca^{2+} could be an interesting target for intervention aimed at strengthen the clock in aging.

4.3. Photoperiodic encoding is affected in aging

In **chapter 2 and 5**, we showed that photoperiodic entrainment requires plasticity of the SCN network and in **chapter 4** we demonstrated that aging causes changes in the E/I balance and Ca^{2+} levels in the SCN cells. **Chapter 3** aimed to study if, and how, seasonal encoding is affected by aging by investigating the plasticity of both behavior and clock gene expression rhythms. We showed that aging does not affect the expression pattern of the clock gene PER2 in an equinoctial light regime, while the behavioral rhythm strength in the aged mice declined. Exposure to long or short

photoperiods requires plasticity of the SCN network (VanderLeest *et al.*, 2007; Meijer *et al.*, 2010; Porcu *et al.*, 2018) which is displayed, for instance, by changing the phase distribution of single cell PER2 expression rhythms (Buijink *et al.*, 2016). Surprisingly, the PER2::LUC expression rhythms of the SCN of old mice showed similar levels of phase distribution as the SCN of young mice, with a wider phase distribution after adaptation to long photoperiod as compared to short photoperiods. In contrast to the intact molecular clock of old mice, behavioral rhythms were less adjusted to the changing photoperiod. This demonstrates that most of the plasticity of the molecular clock remains intact with aging, and deficits in photoperiodic adaptation, like the increased E/I balance that we showed in **chapter 4**, arise downstream from the molecular clock.

Studies on the effect of aging on other components of the core molecular clock also indicate that the molecular clock in SCN neurons remains largely functional, although more research is required to fully confirm this (Banks *et al.*, 2016; Buijink & Michel, 2020). If so, several possibilities exist that could explain the age-related deficits of the circadian clock. Specifically, aging causes a dampened amplitude of the SCN output signal that is expected to be the result of reduced synchronization within the network (Nakamura *et al.*, 2011; Farajnia *et al.*, 2012). When the SCN amplitude is diminished, electrical activity has less influence on PER2 expression rhythms (Noguchi *et al.*, 2017) and circadian rhythms in electrical activity, Ca²⁺ and the molecular clock can become dissociated (Enoki *et al.*, 2017a; Enoki *et al.*, 2017b). Aging affects the rhythm and baseline levels (**chapter 4**) of intracellular calcium in SCN neurons. This disturbed calcium homeostasis could account for a weakened link between the molecular clock and the SCN network. Moreover, the E/I balance is shifted in aging (**chapter 4**) suggesting that the E/I ratio is downstream from the molecular clock and influenced by other mechanisms.

5. CONCLUDING REMARKS AND FUTURE DIRECTIONS

In this thesis, I was able to demonstrate that the SCN network is plastic and under different conditions – like exposure to different light regimes or under the influence of aging – it can reorganize the phase relationships between the individual neurons. Even though characteristics of individual SCN neurons can also change due to environmental influences, it is the network that is of critical importance for proper adaptation. The communication and synchronization between the SCN neurons is key in entrainment and loss of intercellular communication can cause decrement of the network functionality. Therefore, a better understanding of the functioning of the SCN network, and especially the (repulsive) coupling among the SCN neurons, could provide insights in how to deal with the circadian disturbances and challenges in our modern lifestyle or aging. The work in this thesis suggests that the GABAergic E/I balance in the SCN plays a role in network changes and could be a possible target for interference when circadian rhythms are disturbed. There are several pharmacological tools that can manipulate E/I balance, but their application as therapeutics might be challenging due to difficult pharmacokinetics (Gagnon *et al.*, 2013). There are, however, novel therapies that aim to normalize E/I ratio (Ghatak *et al.*, 2021) which could also be interesting for circadian research. These are promising targets to strengthen the circadian clock in the case of disturbances due to environmental light or due to aging.

REFERENCES

1. Albus, H., Vansteensel, M.J., Michel, S., Block, G.D. & Meijer, J.H. (2005) A GABAergic mechanism is necessary for coupling dissociable ventral and dorsal regional oscillators within the circadian clock. *Curr. Biol.*, 15, 886-893.
2. Aton, S.J., Huettner, J.E., Straume, M. & Herzog, E.D. (2006) GABA and *Gi/o* differentially control circadian rhythms and synchrony in clock neurons. *Proc. Natl. Acad. Sci. U. S. A.*, 103, 19188-19193.
3. Aujard, F., Herzog, E.D. & Block, G.D. (2001) Circadian rhythms in firing rate of individual suprachiasmatic nucleus neurons from adult and middle-aged mice. *Neuroscience*, 106, 255-261.
4. Banks, G., Nolan, P.M. & Peirson, S.N. (2016) Reciprocal interactions between circadian clocks and aging. *Mamm. Genome*, 27, 332-340.
5. Belenky, M.A., Yarom, Y. & Pickard, G.E. (2008) Heterogeneous expression of gamma-aminobutyric acid and gamma-aminobutyric acid-associated receptors and transporters in the rat suprachiasmatic nucleus. *J. Comp. Neurol.*, 506, 708-732.
6. Ben-Ari, Y. (2002) Excitatory actions of gaba during development: the nature of the nurture. *Nature reviews. Neuroscience*, 3, 728-739.
7. Bi, D., Wen, L., Wu, Z. & Shen, Y. (2020) GABAergic dysfunction in excitatory and inhibitory (E/I) imbalance drives the pathogenesis of Alzheimer's disease. *Alzheimer's & dementia : the journal of the Alzheimer's Association*, 16, 1312-1329.
8. Bruining, H., Hardstone, R., Juarez-Martinez, E.L., Sprengers, J., Avramiea, A.E., Simpraga, S., Houtman, S.J., Poil, S.S., Dallares, E., Palva, S., Oranje, B., Matias Palva, J., Mansvelder, H.D. & Linkenkaer-Hansen, K. (2020) Measurement of excitation-inhibition ratio in autism spectrum disorder using critical brain dynamics. *Sci. Rep.*, 10, 9195.
9. Buijink, M.R., Almog, A., Wit, C.B., Roethler, O., Olde Engberink, A.H., Meijer, J.H., Garlaschelli, D., Rohling, J.H. & Michel, S. (2016) Evidence for Weakened Intercellular Coupling in the Mammalian Circadian Clock under Long Photoperiod. *PLoS One*, 11, e0168954.
10. Buijink, M.R. & Michel, S. (2020) A multi-level assessment of the bidirectional relationship between aging and the circadian clock. *J. Neurochem.*
11. Canitano, R. & Pallagrosi, M. (2017) Autism Spectrum Disorders and Schizophrenia Spectrum Disorders: Excitation/Inhibition Imbalance and Developmental Trajectories. *Frontiers in psychiatry*, 8, 69.
12. Chellappa, S.L., Gaggioni, G., Ly, J.Q.M., Papachilleos, S., Borsu, C., Brzozowski, A., Rosanova, M., Sarasso, S., Luxen, A., Middleton, B., Archer, S.N., Dijk, D.-J., Massimini, M., Maquet, P., Phillips, C., Moran, R.J. & Vandewalle, G. (2016) Circadian dynamics in measures of cortical excitation and inhibition balance. *Sci. Rep.*, 6, 33661.
13. Choi, H.J., Lee, C.J., Schroeder, A., Kim, Y.S., Jung, S.H., Kim, J.S., Kim, D.Y., Son, E.J., Han, H.C., Hong, S.K., Colwell, C.S. & Kim, Y.I. (2008) Excitatory actions of GABA in the suprachiasmatic nucleus. *J. Neurosci.*, 28, 5450-5459.
14. Chung, L. (2012) Recent progress in GABAergic excitation from mature brain. *Arch. Pharm. Res.*, 35, 2035-2044.
15. Colwell, C.S. (2000) Circadian modulation of calcium levels in cells in the suprachiasmatic nucleus. *Eur. J. Neurosci.*, 12, 571-576.
16. DeWoskin, D., Myung, J., Belle, M.D., Piggins, H.D., Takumi, T. & Forger, D.B. (2015) Distinct roles for GABA across multiple timescales in mammalian circadian timekeeping. *Proc. Natl. Acad. Sci. USA*, 112, E3911-3919.
17. Dijk, D.J. & Duffy, J.F. (1999) Circadian regulation of human sleep and age-related changes in its timing, consolidation and EEG characteristics. *Ann. Med.*, 31, 130-140.
18. Dominoni, D.M., Borniger, J.C. & Nelson, R.J. (2016) Light at night, clocks and health: from humans to wild organisms. *Biol. Lett.*, 12, 20160015.
19. Enoki, R., Oda, Y., Mieda, M., Ono, D., Honma, S. & Honma, K.I. (2017a) Synchronous circadian voltage rhythms with asynchronous calcium rhythms in the suprachiasmatic nucleus. *Proc. Natl. Acad. Sci. U. S. A.*, 114, E2476-e2485.
20. Enoki, R., Ono, D., Kuroda, S., Honma, S. & Honma, K.I. (2017b) Dual origins of the intracellular circadian calcium rhythm in the suprachiasmatic nucleus. *Sci. Rep.*, 7, 41733.
21. Evans, J.A., Elliott, J.A. & Gorman, M.R. (2004) Photoperiod differentially modulates photic and nonphotic phase response curves of

- hamsters. *Am. J. Physiol. Regul. Integr. Comp. Physiol.*, 286, R539-546.
22. Evans, J.A., Leise, T.L., Castanon-Cervantes, O. & Davidson, A.J. (2013) Dynamic Interactions Mediated by Nonredundant Signaling Mechanisms Couple Circadian Clock Neurons. *Neuron*, 80, 973-983.
 23. Farajnia, S., Meijer, J.H. & Michel, S. (2015) Age-related changes in large-conductance calcium-activated potassium channels in mammalian circadian clock neurons. *Neurobiol. Aging*, 36, 2176-2183.
 24. Farajnia, S., Michel, S., Deboer, T., vanderLeest, H.T., Houben, T., Rohling, J.H., Ramkisoensing, A., Yassenkov, R. & Meijer, J.H. (2012) Evidence for neuronal desynchrony in the aged suprachiasmatic nucleus clock. *J. Neurosci.*, 32, 5891-5899.
 25. Farajnia, S., van Westering, T.L.E., Meijer, J.H. & Michel, S. (2014) Seasonal induction of GABAergic excitation in the central mammalian clock. *Proc. Natl. Acad. Sci. USA*, 111, 9627-9632.
 26. Freeman, G.M., Krock, R.M., Aton, S.J., Thaben, P. & Herzog, E.D. (2013) GABA networks destabilize genetic oscillations in the circadian pacemaker. *Neuron*, 78, 799-806.
 27. Froemke, R.C., Merzenich, M.M. & Schreiner, C.E. (2007) A synaptic memory trace for cortical receptive field plasticity. *Nature*, 450, 425-429.
 28. Gaggioni, G., Ly, J.Q.M., Muto, V., Chellappa, S.L., Jaspas, M., Meyer, C., Delfosse, T., Vanvinckenroye, A., Dumont, R., Coppieters 't Wallant, D., Berthomier, C., Narbutas, J., Van Egroo, M., Luxen, A., Salmon, E., Collette, F., Phillips, C., Schmidt, C. & Vandewalle, G. (2019) Age-related decrease in cortical excitability circadian variations during sleep loss and its links with cognition. *Neurobiol. Aging*, 78, 52-63.
 29. Gagnon, M., Bergeron, M.J., Lavertu, G., Castonguay, A., Tripathy, S., Bonin, R.P., Perez-Sanchez, J., Boudreau, D., Wang, B., Dumas, L., Valade, I., Bachand, K., Jacob-Wagner, M., Tardif, C., Kianicka, I., Isenring, P., Attardo, G., Coull, J.A. & De Koninck, Y. (2013) Chloride extrusion enhancers as novel therapeutics for neurological diseases. *Nat. Med.*, 19, 1524-1528.
 30. Gatto, C.L. & Broadie, K. (2010) Genetic controls balancing excitatory and inhibitory synaptogenesis in neurodevelopmental disorder models. *Front. Synaptic Neurosci.*, 2, 4.
 31. Ghatak, S., Talantova, M., Mc Kercher, S.R. & Lipton, S.A. (2021) Novel Therapeutic Approach for Excitatory/Inhibitory Imbalance in Neurodevelopmental and Neurodegenerative Diseases. *Annu. Rev. Pharmacol. Toxicol.*, 61, 701-721.
 32. Golombek, D.A. & Rosenstein, R.E. (2010) Physiology of Circadian Entrainment. *Physiol. Rev.*, 90, 1063-1102.
 33. Goudriaan, I., van Boekel, L.C., Verbiest, M.E.A., van Hoof, J. & Luijckx, K.G. (2021) Dementia Enlightened?! A Systematic Literature Review of the Influence of Indoor Environmental Light on the Health of Older Persons with Dementia in Long-Term Care Facilities. *Clin. Interv. Aging*, 16, 909-937.
 34. He, H.Y., Shen, W., Hiramoto, M. & Cline, H.T. (2016) Experience-Dependent Bimodal Plasticity of Inhibitory Neurons in Early Development. *Neuron*, 90, 1203-1214.
 35. Ikeda, M., Sugiyama, T., Wallace, C.S., Gompf, H.S., Yoshioka, T., Miyawaki, A. & Allen, C.N. (2003) Circadian dynamics of cytosolic and nuclear Ca²⁺ in single suprachiasmatic nucleus neurons. *Neuron*, 38, 253-263.
 36. Irwin, R.P. & Allen, C.N. (2009) GABAergic signaling induces divergent neuronal Ca²⁺ responses in the suprachiasmatic nucleus network. *Eur. J. Neurosci.*, 30, 1462-1475.
 37. Jacobs, B., Driscoll, L. & Schall, M. (1997) Life-span dendritic and spine changes in areas 10 and 18 of human cortex: a quantitative Golgi study. *J. Comp. Neurol.*, 386, 661-680.
 38. Kaila, K. (1994) Ionic basis of GABAA receptor channel function in the nervous system. *Prog. Neurobiol.*, 42, 489-537.
 39. Kim, D.Y., Choi, H.J., Kim, J.S., Kim, Y.S., Jeong, D.U., Shin, H.C., Kim, M.J., Han, H.C., Hong, S.K. & Kim, Y.I. (2005) Voltage-gated calcium channels play crucial roles in the glutamate-induced phase shifts of the rat suprachiasmatic circadian clock. *Eur. J. Neurosci.*, 21, 1215-1222.
 40. Kinouchi, O. & Copelli, M. (2006) Optimal dynamical range of excitable networks at criticality. *Nature Physics*, 2, 348-351.
 41. Klett, N.J. & Allen, C.N. (2017) Intracellular Chloride Regulation in AVP+ and VIP+ Neurons of the Suprachiasmatic Nucleus. *Sci. Rep.*, 7, 10226.
 42. Koh, M.T., Branch, A., Haberman, R. & Gallagher, M. (2020) Significance of inhibitory recruitment in aging with preserved cognition:

- limiting gamma-aminobutyric acid type A $\alpha 5$ function produces memory impairment. *Neurobiol. Aging*, 91, 1-4.
43. Kondratova, A.A. & Kondratov, R.V. (2012) The circadian clock and pathology of the ageing brain. *Nat. Rev. Neurosci.*, 13, 325-335.
 44. Lauterborn, J.C., Scaduto, P., Cox, C.D., Schulmann, A., Lynch, G., Gall, C.M., Keene, C.D. & Limon, A. (2021) Increased excitatory to inhibitory synaptic ratio in parietal cortex samples from individuals with Alzheimer's disease. *Nat Commun*, 12, 2603.
 45. Legon, W., Punzell, S., Dowlati, E., Adams, S.E., Stiles, A.B. & Moran, R.J. (2016) Altered Prefrontal Excitation/Inhibition Balance and Prefrontal Output: Markers of Aging in Human Memory Networks. *Cereb. Cortex*, 26, 4315-4326.
 46. Liu, C. & Reppert, S.M. (2000) GABA synchronizes clock cells within the suprachiasmatic circadian clock. *Neuron*, 25, 123-128.
 47. Ly, J.Q.M., Gaggioni, G., Chellappa, S.L., Papachilleos, S., Brzozowski, A., Borsu, C., Rosanova, M., Sarasso, S., Middleton, B., Luxen, A., Archer, S.N., Phillips, C., Dijk, D.-J., Maquet, P., Massimini, M. & Vandewalle, G. (2016) Circadian regulation of human cortical excitability. *Nature Communications*, 7, 11828.
 48. McNeill, J.K., Walton, J.C. & Albers, H.E. (2018) Functional Significance of the Excitatory Effects of GABA in the Suprachiasmatic Nucleus. *J. Biol. Rhythms*, 33, 376-387.
 49. McNeill, J.K., Walton, J.C., Ryu, V. & Albers, H.E. (2020) The Excitatory Effects of GABA within the Suprachiasmatic Nucleus: Regulation of Na-K-2Cl Cotransporters (NKCCs) by Environmental Lighting Conditions. *J. Biol. Rhythms*, 35, 275-286.
 50. Meijer, J.H., Michel, S., Vanderleest, H.T. & Rohling, J.H.T. (2010) Daily and seasonal adaptation of the circadian clock requires plasticity of the SCN neuronal network. *The European journal of neuroscience*, 32, 2143-2151.
 51. Meyer, C., Gaggioni, G., Ly, J.Q.M., Rosanova, M., Sarasso, S., Archer, S.N., Dijk, D.J., Massimini, M., Maquet, P., Phillips, C., Moran, R.J., Vandewalle, G. & Chellappa, S.L. (2015) Neurons for all seasons: human neuronal drive across photoperiod. *Worldsleep 2015 Abstractbook*, pp. 102-103.
 52. Mora, F., Segovia, G. & del Arco, A. (2007) Aging, plasticity and environmental enrichment: structural changes and neurotransmitter dynamics in several areas of the brain. *Brain research reviews*, 55, 78-88.
 53. Morin, L.P., Shivers, K.Y., Blanchard, J.H. & Muscat, L. (2006) Complex organization of mouse and rat suprachiasmatic nucleus. *Neuroscience*, 137, 1285-1297.
 54. Mrugala, M., Zlomanczuk, P., Jagota, A. & Schwartz, W.J. (2000) Rhythmic multiunit neural activity in slices of hamster suprachiasmatic nucleus reflect prior photoperiod. *Am. J. Physiol. Regul. Integr. Comp. Physiol.*, 278, R987-994.
 55. Myung, J., Hong, S., DeWoskin, D., De Schutter, E., Forger, D.B. & Takumi, T. (2015) GABA-mediated repulsive coupling between circadian clock neurons in the SCN encodes seasonal time. *Proc. Natl. Acad. Sci. USA*, 112, E3920-3929.
 56. Nakamura, T.J., Nakamura, W., Yamazaki, S., Kudo, T., Cutler, T., Colwell, C.S. & Block, G.D. (2011) Age-related decline in circadian output. *J. Neurosci.*, 31, 10201-10205.
 57. Noguchi, T., Leise, T.L., Kingsbury, N.J., Diemer, T., Wang, L.L., Henson, M.A. & Welsh, D.K. (2017) Calcium Circadian Rhythmicity in the Suprachiasmatic Nucleus: Cell Autonomy and Network Modulation. *eNeuro*, 4.
 58. Okun, M. & Lampl, I. (2008) Instantaneous correlation of excitation and inhibition during ongoing and sensory-evoked activities. *Nat. Neurosci.*, 11, 535-537.
 59. Pittendrigh, C.S., Elliott, J.A. & Takamura, T. (1984) The Circadian Component in Photoperiodic induction. In R., P., G.M., C. (eds) *Photoperiodic Regulation of Insect and Molluscan Hormones*. Pitman, London, pp. 26-47.
 60. Porcu, A., Riddle, M., Dulcis, D. & Welsh, D.K. (2018) Photoperiod-Induced Neuroplasticity in the Circadian System. *Neural Plast.*, 2018, 5147585.
 61. Resnick, S.M., Pham, D.L., Kraut, M.A., Zonderman, A.B. & Davatzikos, C. (2003) Longitudinal magnetic resonance imaging studies of older adults: a shrinking brain. *J. Neurosci.*, 23, 3295-3301.
 62. Rissman, R.A. & Mobley, W.C. (2011) Implications for treatment: GABA receptors in aging, Down syndrome and Alzheimer's disease. *J. Neurochem.*, 117, 613-622.

63. Rohr, K.E., Pancholi, H., Haider, S., Karow, C., Modert, D., Raddatz, N.J. & Evans, J. (2019) Seasonal plasticity in GABAA signaling is necessary for restoring phase synchrony in the master circadian clock network. *eLife*, 8.
64. Rubiño-Díaz, J., Nicolau-Llobera, C., Martín-Reina, A., Rial-Planas, R. & Canellas, F. (2021) [Positive effect of bright light therapy on mood and sleep quality in institutionalized older people]. *Revista española de geriatría y gerontología*.
65. Sanders, D. & Gaston, K.J. (2018) How ecological communities respond to artificial light at night. *Journal of experimental zoology. Part A, Ecological and integrative physiology*, 329, 394-400.
66. Sgadò, P., Dunleavy, M., Genovesi, S., Provenzano, G. & Bozzi, Y. (2011) The role of GABAergic system in neurodevelopmental disorders: a focus on autism and epilepsy. *Int. J. Physiol. Pathophysiol. Pharmacol.*, 3, 223-235.
67. Shu, Y., Hasenstaub, A. & McCormick, D.A. (2003) Turning on and off recurrent balanced cortical activity. *Nature*, 423, 288-293.
68. Steponenaite, A., Biello, S.M. & Lall, G.S. (2018) Aging clocks: disrupted circadian rhythms. *Aging (Albany NY)*, 10, 3065-3066.
69. Tackenberg, M.C., Hughey, J.J. & McMahan, D.G. (2020) Distinct Components of Photoperiodic Light Are Differentially Encoded by the Mammalian Circadian Clock. *J. Biol. Rhythms*, 35, 353-367.
70. Tran, T., Bridi, M., Koh, M.T., Gallagher, M. & Kirkwood, A. (2019) Reduced cognitive performance in aged rats correlates with increased excitation/inhibition ratio in the dentate gyrus in response to lateral entorhinal input. *Neurobiol. Aging*, 82, 120-127.
71. Tran, T., Gallagher, M. & Kirkwood, A. (2018) Enhanced postsynaptic inhibitory strength in hippocampal principal cells in high-performing aged rats. *Neurobiol. Aging*, 70, 92-101.
72. Valentinuzzi, V.S., Scarbrough, K., Takahashi, J.S. & Turek, F.W. (1997) Effects of aging on the circadian rhythm of wheel-running activity in C57BL/6 mice. *Am. J. Physiol.*, 273, R1957-1964.
73. VanderLeest, H.T., Houben, T., Michel, S., Deboer, T., Albus, H., Vansteensel, M.J., Block, G.D. & Meijer, J.H. (2007) Seasonal encoding by the circadian pacemaker of the SCN. *Curr. Biol.*, 17, 468-473.
74. vanderLeest, H.T., Rohling, J.H.T., Michel, S. & Meijer, J.H. (2009) Phase shifting capacity of the circadian pacemaker determined by the SCN neuronal network organization. *PLoS One*, 4, e0004976.
75. Vecchia, D. & Pietrobon, D. (2012) Migraine: a disorder of brain excitatory-inhibitory balance? *Trends Neurosci.*, 35, 507-520.
76. Wagner, S., Castel, M., Gainer, H. & Yarom, Y. (1997) GABA in the mammalian suprachiasmatic nucleus and its role in diurnal rhythmicity. *Nature*, 387, 598-603.
77. Yan, L. & Silver, R. (2008) Day-length encoding through tonic photic effects in the retinorecipient SCN region. *Eur. J. Neurosci.*, 28, 2108-2115.
78. Zhou, M., Liang, F., Xiong, X.R., Li, L., Li, H., Xiao, Z., Tao, H.W. & Zhang, L.I. (2014) Scaling down of balanced excitation and inhibition by active behavioral states in auditory cortex. *Nat. Neurosci.*, 17, 841-850.
79. Zhou, S. & Yu, Y. (2018) Synaptic E-I Balance Underlies Efficient Neural Coding. *Front. Neurosci.*, 12.



seven

SUMMARY

NEDERLANDSE SAMENVATTING

DANKWOORD

LIST OF PUBLICATIONS

CV

SUMMARY

Almost all living species, from unicellular to humans, have an endogenous timing system that helps them to adapt to environmental light-dark cycles. In mammals, a central circadian clock, which resides in the suprachiasmatic nucleus (SCN) of the hypothalamus, drives 24 h rhythms in physiology and behavior. The SCN is a bilateral brain structure that consists of about 10,000 neurons in each nucleus and is located on top of the optic chiasm. The SCN neuronal network uses adaptive mechanisms to synchronize the internal rhythms, that have a period length of about 24 h, to the environmental cycles of exactly 24 h. The most important environmental time cue or zeitgeber is light, received by specialized retinal ganglion cells that project directly to the SCN through the retino-hypothalamic tract. Most SCN neurons are autonomous oscillator cells that generate a rhythm in the frequency of action potentials with a peak during the middle of the day. Communication and coupling within the SCN network are important to generate a strong and coherent output signal from the SCN to the periphery, but also to synchronize the SCN to the environmental conditions. Via this manner, the SCN controls the timing of many physiological and behavioral functions and aligns these rhythms to the environmental light-dark cycle.

The SCN's ensemble electrical activity follows a sinusoidal-like pattern that peaks during the day and has a trough during the night. The amplitude of the SCN's electrical activity rhythm can be influenced by external factors, like photoperiod, and is linked to the level of synchronization within the network. For instance, after adaptation to a long photoperiod, the phases of the individual SCN neurons are more dispersed over the 24 h (less synchronized) and the ensemble output in electrical activity has a broadened waveform with a decreased amplitude. Aging is also known to affect the SCN network organization with deterioration in synchronization among the individual SCN neurons and a reduced amplitude. In this thesis, several studies have been conducted to investigate the effects of light exposure and aging on SCN network organization. Specifically, a big part of this work focused on the role of the most abundant neurotransmitter in the SCN, which is GABA, and the GABAergic excitatory/inhibitory (E/I) balance in SCN network plasticity.

The influence of light on SCN network properties and behavior has been convincingly described after adaptation to different day length. But, is reception of the full photoperiod needed for photoperiodic encoding in the SCN, or does exposure to short light pulses at the beginning and end of the day suffice? **Chapter 2** described a series of experiments that examine whether exposure to light for the full length of the day was needed to achieve cellular reorganization within the SCN network as demonstrated after entrainment to long or short photoperiod.

To study this, mice were exposed to "skeleton photoperiods" that mimicked long summer days of 16 hours or short winter days of 8 hours by two brief light exposures of 30 minutes that mark the beginning and end of the day. First, the behavioral phenotypes of entrainment to skeleton and full photoperiod were assessed using locomotor activity recordings. Behavioral entrainment to long and short days were similar under skeleton and full photoperiods, with compressed and expanded durations of the active phase under long and short photoperiods, respectively. Next, light-induced phase shifts were measured in mice after they adapted to either skeleton or full photoperiod, since previous work indicated a reduction in phase shifting capacity under long photoperiod conditions.

Again, skeleton photoperiods were sufficient to diminish the light-induced phase shifts in long photoperiod, similar to results obtained in full photoperiod.

Furthermore, to identify the level of cellular synchronization within the network, electrophysiological and bioluminescence imaging experiments were performed. The ensemble multiunit electrical activity (MUA) of SCN slices from mice entrained to skeleton long photoperiod showed a broader waveform when compared to short photoperiod. This change in waveform shape indicates a lower synchronization level in the SCN network after adaptation to skeleton long photoperiod, which is an important feature to represent and convey day length information. Cellular synchronization was also determined on the basis of the molecular rhythms in slices from mice adapted to skeleton long and short photoperiods by measuring single cell PER2::LUC expression for several consecutive cycles. These bioluminescence experiments showed a higher phase distribution of PER2 peak times in slices from mice entrained to skeleton long photoperiod, compared to skeleton short photoperiod. This confirmed that the SCN of mice adapted to skeleton long photoperiod is less synchronized than the SCN of mice adapted to skeleton short photoperiod, which was similar in mice entrained to full photoperiods.

Lastly, *ex vivo* calcium imaging experiments were used to study the effect of skeleton photoperiods on GABAergic activity and the E/I balance. The percentage of GABAergic inhibitory responses was significantly lower in SCN tissue from mice entrained to skeleton long compared to skeleton short photoperiod. Similar to a full long photoperiod, the E/I balance was remarkably high following a skeleton long photoperiod.

The results of **chapter 2** together showed that exposure to a skeleton photoperiod, and thus the timing of only two brief light pulses, affects the circadian clock in a similar manner as complete light exposure under a full photoperiod. This underscores the powerful, yet potentially harmful effects of even relatively short light exposures during the evening or night for example nocturnal animals.

Photoperiodic phase adjustment in the SCN network is a good example of SCN network plasticity. Research has shown that aging affects the circadian clock at different levels, among which the network level. In the following chapters we further investigated the effect of aging on several cellular, network, and behavioral properties of the circadian system. In **chapter 3**, the plasticity of the circadian clock in old mice was examined, while challenged with different light regimes. Old PER2::LUCIFERASE mice (22-28 months) and young controls were exposed to either an equinoctial (Light-Dark: LD 12:12), long (LD 16:8), or short (LD 8:16) photoperiod. The old mice showed a reduced rhythm strength and a compromised ability to adapt to short photoperiod. After these behavioral assays, PER2::LUC gene expression characteristics were measured in SCN slices of young and old mice adapted to the different photoperiods, in order to investigate seasonal encoding at the molecular level. Surprisingly, the PER2::LUC rhythms were remarkably similar in the SCN of young and old mice under the different photoperiods. Thus, photoperiodic encoding by the SCN, at least at the molecular level, is still intact after aging and the reduced ability to behaviorally adapt to different photoperiods emerges downstream from the core molecular clock.

Chapter 4 aimed to examine the effect of aging on GABAergic function, the concomitant E/I balance, and on Ca²⁺ homeostasis. In this chapter, the polarity of Ca²⁺ transients in response

to exogenous GABA stimulation was determined in SCN slices of old mice (20-24 months) and young controls and from these results, the E/I balance was established. In SCN tissue of old mice, the amount of GABAergic excitation, and concordantly the E/I balance, was higher when compared to young controls. Especially in the posterior part of the SCN, the percentage of excitatory responses increased and the percentage of inhibitory responses decreased significantly, compared to slices of young mice. Moreover, the baseline Ca^{2+} transients were higher in old SCN neurons, when compared to young suggesting an altered calcium homeostasis in the SCN of old mice. With aging, an increased E/I balance due to loss of inhibition has been demonstrated in other brain networks. The stabilization of SCN E/I ratio to a healthy range in aging could benefit SCN network properties and may also diminish age-related diseases provoked by clock dysfunction.

Thus far, the research described in this thesis, and results from other studies, suggest that the balance between GABAergic excitation and inhibition plays a role in synchronization and/or plasticity of the SCN network. However, the exact role or mechanism remains topic for future studies. Pharmacological manipulations of GABAergic signaling are important tools in both in vivo and in vitro research regarding the E/I balance. Besides drugs affecting the GABA receptor itself, manipulation of intracellular Cl^- concentration is used as this affects the amount and polarity of the ion flux through the GABA-controlled channel. In **chapter 5** experiments were conducted to investigate the role of one of the ion co-transporters (KCC2), which regulate the intracellular Cl^- concentration by removing Cl^- from the cytoplasm, on the GABAergic responses in the SCN with a newly developed blocker ML077. By the use of calcium imaging, GABA-induced single cell Ca^{2+} transients were recorded before and after blocking KCC2 with ML077 in SCN slices of mice entrained to different photoperiods (LD 12:12, LD 16:8, LD 8:16). Blocking KCC2 with ML077 caused a shift in the polarity of the GABAergic response by inducing excitatory responses in previously inhibitory responding neurons, suggesting that KCC2 is an essential component in regulating $[\text{Cl}^-]_i$ and the Cl^- equilibrium potential, thereby determining the sign of the GABAergic response. Remarkably, the percentage of excitatory cells increased with a similar degree in slices from mice adapted to long or short photoperiod and LD 12:12 condition. This indicates on the one hand that KCC2 activity is important for maintaining E/I balance under all photoperiods, but also that KCC2 can mimic the transition of network states from short to long photoperiod. The results from this chapter showed that ML077 promises to be a powerful tool in researching the effect of E/I balance on the level of synchronization in the SCN network.

Finally, the results from this thesis were discussed in **chapter 6**. Plasticity and the right balance in the circadian clock organization are needed for adaptation to environmental changes. Here, we showed for the first time that even short light exposures at the beginning and end of the day can cause network changes, including a change in the function of GABA. Artificial prolonged light duration, which is common in our modern 24 h society, has been shown to affect neurotransmitter systems in the brain and also the SCN. Additionally, this work showed that similar changes in GABAergic function are achieved by brief light exposure late in the evening. The seasonal light regime changes annually by nature. However, artificial prolonged light in the evening, and even short exposure to bright light late in the evening or at night, keeps our circadian system in a continuous mode of summer over months and years. It is still unclear how this affects our physiology and behavior,

and whether the induced changes to our clock network are still reversible. Lastly, the (prolonged) light exposure in the evening is something we impose on ourselves, however it also influences, unsolicited, the circadian clock function of nocturnal animals in their natural environment.

While light management is something that can be influenced, the effects of aging are usually irreversible. Also, aging affects to GABAergic function in the SCN network which could contribute to other age-related deficiencies in the clock machinery. Future research into pharmacological manipulation of the GABAergic E/I balance in the SCN, and its effect on the coupling mechanisms within the network, is important as it might be an interesting lead towards restoration of (age-related) deficits in circadian rhythms.

NEDERLANDSE SAMENVATTING

Bijna alle organismen, van eencelligen tot de mens, hebben een intern tijdssysteem ontwikkeld dat hen in staat stelt om zich aan te passen aan de 24-uurs licht-donker cyclus op aarde. Bij zoogdieren bevindt de centrale circadiane (circa = ongeveer, dia = dag) klok zich in de nucleus suprachiasmaticus (SCN) in de hypothalamus. Het signaal dat hier wordt gegenereerd dient als klok-sigitaal voor de rest van het brein en andere organen en zorgt voor 24-uurs ritmes in fysiologie en gedrag. De SCN is een bilaterale hersenstructuur die bestaat uit twee kernen van elk ongeveer 10.000 neuronen en is gesitueerd bovenop het optisch chiasma, de kruising van beide oogzenuwen in de hersenen. Het neuronale netwerk van de SCN kan de intern gegenereerde ritmes van ongeveer 24 uur synchroniseren met de licht-donker cyclus van de omgeving. De belangrijkste tijdsaanduiding uit de omgeving, ook wel zeitgeber genoemd, is licht dat wordt opgevangen en verwerkt door gespecialiseerde ganglion cellen in de retina welke direct naar de SCN projecteren via de zenuwbanen, de tractus retinohypothalamicus. De meeste SCN neuronen zijn zelfstandig oscillerende cellen die een ritme in de frequentie van actiepotentialen genereren met een piek in elektrische activiteit in het midden van de dag. Communicatie en koppeling binnen het SCN netwerk zijn belangrijk om een sterk en coherent output signaal van de SCN naar de periferie te genereren, maar ook om de SCN te synchroniseren met de licht-donker cyclus uit de omgeving. Op deze manier is de SCN in staat om de timing van vele fysiologische- en gedragsfuncties te reguleren en om deze ritmes optimaal af te stemmen met de omgeving.

De neuronen van de SCN produceren gezamenlijk een sinusgolfachtig signaal in elektrische activiteit, die zijn piek bereikt gedurende de dag en minimaal is in de nacht. De amplitude van dit ritme in elektrische activiteit is beïnvloedbaar door externe factoren, zoals daglengte (fotoperiode), en is gekoppeld aan de mate van synchronisatie tussen de neuronen van het netwerk. Aanpassing aan lange fotoperiodes, dus zomerdagen, zorgt er bijvoorbeeld voor dat de piek in elektrische activiteit (de fases) van de individuele SCN neuronen meer verspreid is over de 24 uur en dus dat het netwerk minder gesynchroniseerd is. Tegelijkertijd is de amplitude van het output signaal, dus het signaal dat de SCN neuronen gezamenlijk produceren, lager en met een verbrede golfvorm. Veroudering is een andere factor die ook effect heeft op het SCN netwerk, met een vermindering in synchroniciteit in het netwerk en een verlaagd amplitude van het ritme van elektrische activiteit van de SCN. In dit proefschrift zijn verschillende studies beschreven waarin de effecten van blootstelling aan licht en veroudering op de netwerkorganisatie van SCN zijn onderzocht. In het bijzonder is een groot deel van dit werk gericht op de rol van de meest voorkomende neurotransmitter in de SCN, namelijk GABA, en de GABAerge exciterende/inhiberende (E/I) balans in de plasticiteit van het SCN netwerk.

De invloed van licht op het circadiane ritme en op de netwerk-eigenschappen de SCN is overtuigend beschreven in studies naar adaptatie aan verschillende daglengtes. Het blijft echter de vraag of ontvangst van de volledige fotoperiode nodig is voor de codering van daglengte door de SCN, of dat blootstelling aan korte lichtpulsjes aan het begin en het einde van de dag voldoende is. In **hoofdstuk 2** wordt een reeks experimenten beschreven waarin onderzocht werd of blootstelling aan licht gedurende de hele dag nodig was voor fotoperiode-afhankelijke cellulaire reorganisatie binnen het SCN netwerk, zoals aangetoond na adaptatie aan een lange of korte daglengte.

Om dit te bestuderen werden muizen blootgesteld aan “skeleton fotoperioden” die lange zomerdagen van 16 uur licht of korte winterdagen van 8 uur licht nabootsten. Een skeleton fotoperiode wordt gekenmerkt door twee korte lichtpulsen van 30 minuten die het begin en het einde van de dag aanduiden en waarbij de rest van de 24 uur het licht uit blijft. Eerst werd met behulp van gedragsmetingen beoordeeld of de muizen hun activiteit konden aanpassen aan deze skeleton fotoperioden. Zoals verwacht vertoonden de muizen vergelijkbare gedragsfenotypes als bij aanpassingen aan volledige lange of korte dagen, met gecompriëerde en uitgebreide actieve fases onder respectievelijk lange en korte fotoperioden. Vervolgens werden de dieren, nadat ze zich hadden aangepast aan de skeleton of de volledige fotoperiode, blootgesteld aan een lichtpuls waarmee fase verschuivingen werden geïnduceerd, aangezien eerder werk heeft uitgewezen dat de fase verschuivende effecten van licht in relatie staan tot daglengte. Overeenkomstig met de dieren die zijn aangepast aan volledige fotoperioden, bleek de fase verschuiving na een lichtpuls kleiner bij de muizen die aangepast waren aan een skeleton lange fotoperiode dan bij muizen die aangepast waren aan een skeleton korte fotoperiode.

Om de cellulaire synchronisatie binnen het netwerk van de SCN na adaptatie aan skeleton fotoperioden te onderzoeken, werden aansluitend elektrofysiologische en bioluminescentie-imaging experimenten uitgevoerd. De *ex vivo* ensemble multiunit elektrische activiteit (MUA) in SCN plakjes van muizen die aangepast waren aan een skeleton lange dag had een duidelijk bredere golfvorm in vergelijking met de skeleton korte dag. Deze verandering in de golfvorm van het elektrische output signaal duidt op een lager synchronisatieniveau in het SCN netwerk na aanpassing aan de skeleton lange fotoperiode. Dit laatste is een belangrijk kenmerk van de SCN in de codering en overbrenging van daglengte-informatie. Cellulaire synchronisatie werd ook bepaald op basis van de moleculaire ritmes van de individuele SCN cellen. Hiervoor werden genetisch gemodificeerde muizen gebruikt waarvan met behulp van bioluminescentie technieken in SCN plakjes het klok gen *per2* gedurende opeenvolgende cycli gemonitord kon worden. Deze bioluminescentie-experimenten toonden een bredere fase verspreiding in PER2-piektijden in plakjes van muizen die waren aangepast aan een skeleton lange fotoperiode, vergeleken met een skeleton korte fotoperiode. Deze resultaten bevestigden dat de SCN van muizen die zijn aangepast aan skeleton lange dag minder gesynchroniseerd is dan de SCN van muizen die zijn aangepast aan skeleton korte dag, iets wat vergelijkbaar is bij muizen blootgesteld aan volledige fotoperioden.

Ten slotte werden *ex vivo* calcium imaging experimenten gedaan om het effect van skeleton fotoperioden op de activiteit van de meest voorkomende neurotransmitter in de SCN, GABA, en de GABAerge E/I balans te bestuderen. GABA kan zowel een inhiberende als exciterende reactie geven wanneer het bindt aan de receptor. Het percentage GABAerge inhiberende reacties was significant lager in SCN weefsel van muizen aangepast aan skeleton lange fotoperiode, in vergelijking met de skeleton korte fotoperiode. Net als bij adaptatie aan een volledige lange dag, was de E/I balans opmerkelijk hoog na een skeleton lange dag.

De resultaten van **hoofdstuk 2** lieten zien dat blootstelling en aanpassing aan een skeleton fotoperiode, en dus de timing van slechts twee korte lichtpulsen, de circadiane klok op een vergelijkbare manier beïnvloedt als blootstelling aan licht gedurende een hele dag zoals bij een

volledige fotoperiode. Dit benadrukt nog eens de krachtige, maar potentieel schadelijke effecten van zelfs relatief korte blootstelling aan licht 's avonds of 's nachts voor bijvoorbeeld nachtdieren.

Daglengte-afhankelijke veranderingen in het SCN netwerk zijn een goed voorbeeld van SCN netwerk plasticiteit. Onderzoek heeft aangetoond dat veroudering de circadiane klok beïnvloedt op verschillende niveaus, waaronder ook het netwerk. In de volgende twee hoofdstukken hebben we het effect van veroudering op verschillende cellulaire-, netwerk- en gedragseigenschappen van het circadiane systeem verder onderzocht. In **hoofdstuk 3** werd de plasticiteit van de circadiane klok in oude muizen onderzocht, terwijl ze werden blootgesteld aan verschillende lichtregimes. Oude PER2::LUCIFERASE-muizen (22-28 maanden oud) en jonge controle muizen werden blootgesteld aan een equinoctiale (LD 12:12), lange (LD 16:8) of korte (LD 8:16) fotoperiode. De oude muizen vertoonden een minder sterk ritme in gedrag, met een meer gefragmenteerd activiteitspatroon, en een verminderd vermogen om zich gedragsmatig aan te passen aan een korte fotoperiode. Na deze gedragstesten werd PER2::LUC-genexpressie gemeten in SCN plakjes van jonge en oude muizen die waren blootgesteld aan de verschillende fotoperioden, om zo codering van daglengte op moleculair niveau te onderzoeken. Verrassend genoeg waren de PER2::LUC ritmes opmerkelijk vergelijkbaar in de SCN van jonge en oude muizen onder de verschillende fotoperioden. Dus, codering van daglengte-informatie in de SCN, althans op moleculair niveau, is nog steeds intact na veroudering. Het verminderde vermogen om zich gedragsmatig aan te passen aan verschillende fotoperioden lijkt dus los te staan van de codering van daglengte op moleculair niveau in de SCN.

In **hoofdstuk 4** werd het effect van veroudering op de functie van GABA, de bijbehorende E/I balans en op Ca^{2+} homeostase in de SCN onderzocht. Zoals eerder beschreven is GABA een van de belangrijkste en meest voorkomende neurotransmitters in de SCN en kan GABA zowel inhiberende als exciterende responses teweegbrengen. Deze reacties zijn te bepalen door de intracellulaire calcium te meten terwijl exogeen GABA aan de SCN neuronen wordt toegevoegd. Zo werd de polariteit van Ca^{2+} levels als reactie op exogene GABA-stimulatie bepaald in SCN plakjes van oude muizen (20-24 maanden) en jonge controles en op basis van deze resultaten werd de E/I balans vastgesteld. In SCN weefsel van oude muizen was de hoeveelheid GABAerge excitatie, en daarmee ook de E/I balans, hoger in vergelijking met jonge controles. Vooral in het posterior gedeelte van de SCN nam het percentage exciterende reacties toe en nam het percentage inhiberende reacties significant af, wanneer vergeleken met SCN plakjes van jonge muizen. Bovendien waren de baseline Ca^{2+} levels hoger in oude SCN neuronen, in vergelijking met jonge, wat wijst op een veranderde calciumhomeostase in de SCN van oude muizen. Met ouderdom is ook in andere hersennetwerken een verhoogde E/I balans aangetoond door verlies van inhiberende signalen. De stabilisatie van de E/I balans tot een gezonde ratio zal de eigenschappen van het verouderde SCN netwerk ten goede komen en kan ook ouderdomsgerelateerde ziekten verminderen die worden veroorzaakt door minder goed werkende centrale klok.

De resultaten van het onderzoek beschreven in dit proefschrift, samen met de uitkomsten van andere studies, suggereren dat de balans tussen GABAerge excitatie en inhibitie een rol speelt bij synchronisatie en/of plasticiteit van het SCN netwerk. Het mechanisme hierachter blijft echter onderwerp voor toekomstige studies. Farmacologische manipulatie van GABAerge neurotransmissie is een belangrijk instrument in zowel in vivo als in vitro onderzoek naar de E/I

balans. Hiervoor worden middelen gebruikt die de GABA-receptor zelf beïnvloeden, maar is ook manipulatie van de intracellulaire Cl^- concentratie een aangrijpingspunt, omdat dit de hoeveelheid en polariteit van de ionenstroom door de GABA-receptor beïnvloedt. In **hoofdstuk 5** zijn experimenten uitgevoerd waarin een nieuw ontwikkelde blocker, genaamd ML077, van een van de ion co-transporters (KCC2) werd gebruikt om zo de rol van KCC2 op de GABA responses te onderzoeken. KCC2 is een co-transporter die de intracellulaire Cl^- concentratie reguleert door Cl^- uit het cytoplasma te verwijderen. Door deze transporter te blokkeren wordt de intracellulaire Cl^- concentratie verhoogd en dus de GABA response van de geblokkeerde neuronen beïnvloed. Met behulp van calcium imaging experimenten, werd de polariteit van Ca^{2+} levels als reactie op exogene GABA-stimulatie bepaald voor en na het blokkeren van KCC2 met ML077 in SCN plakjes van muizen die voorafgaand aan het experiment aangepast waren aan verschillende daglengtes (LD 12:12, LD 16:8, LD 8:16). Het blokkeren van KCC2 met ML077 veroorzaakte een verschuiving in de polariteit van de GABAerge responses door exciterende reacties te veroorzaken in voorheen inhiberend reagerende neuronen. Dit suggereert dat KCC2 een essentiële component is in het reguleren van de intracellulaire Cl^- concentratie en het Cl^- evenwichtspotentiaal, en daardoor ook in het bepalen van de polariteit van de GABAerge response. Opmerkelijk is dat het percentage exciterende cellen in een vergelijkbare mate toenam na blokkade van KCC2 in SCN plakjes van muizen die waren aangepast aan lange of korte fotoperiode en LD 12:12 conditie. Dit geeft aan de ene kant aan dat KCC2 activiteit belangrijk is voor het handhaven van de E/I balans onder alle fotoperioden, maar ook dat KCC2 de netwerkveranderingen van korte naar lange fotoperiode kan nabootsen. De resultaten van dit hoofdstuk lieten zien dat ML077 een krachtig hulpmiddel kan zijn voor toekomstig onderzoek naar de effecten van de E/I balans op het synchronisatieniveau in het SCN netwerk.

Tot slot worden in **hoofdstuk 6** alle resultaten van dit proefschrift bediscussieerd. Plasticiteit en de juiste balans in het netwerk van de centrale circadiane klok zijn nodig voor accommodatie aan veranderingen in de omgeving. In dit proefschrift is voor het eerst aangetoond dat zelfs korte blootstelling aan licht aan het begin en het einde van de dag netwerkveranderingen kunnen veroorzaken, waaronder een verandering in de functie van GABA. Het is aangetoond dat langdurige blootstelling aan kunstmatig licht in de avond, iets wat gebruikelijk is in onze moderne 24-uurs samenleving, neurotransmittersystemen in verschillende regionen in de hersenen, waaronder de SCN, beïnvloedt. Bovendien toonde dit werk aan dat vergelijkbare veranderingen in de GABAerge functie worden bereikt door een korte blootstelling aan helder licht laat in de avond. De licht-donker cyclus verandert van nature door het jaar heen. Maar langdurige blootstelling aan kunstmatig licht 's avonds, en zelfs korte blootstelling aan helder licht 's avonds laat, houdt ons circadiane systeem maanden en zelfs jaren in een continue zomer-modus. Het is nog steeds onduidelijk hoe dit onze fysiologie en ons gedrag beïnvloedt en of de veroorzaakte veranderingen in ons kloknetwerk nog omkeerbaar zijn. Ten slotte is de (langdurige) blootstelling aan licht in de avond iets dat we onszelf opleggen, maar het beïnvloedt ook, ongevraagd, de circadiane klokfunctie van nachtdieren in hun natuurlijke omgeving.

Hoewel lichtmanagement kan worden beïnvloed, zijn de effecten van veroudering meestal onomkeerbaar. Net als adaptatie aan een lange dag heeft veroudering ook invloed op de functie

van GABA in het SCN netwerk, iets wat zou kunnen bijdragen aan ouderdomsgerelateerde ziekten waarbij het disfunctioneren van de centrale klok een rol speelt. Toekomstig onderzoek naar farmacologische manipulatie van de GABAerge E/I balans in de SCN, en het effect ervan op de synchronisatie-mechanismen binnen het netwerk, is belangrijk omdat het een interessant aanknopingspunt kan zijn voor het herstel van (ouderdomsgerelateerde) circadiane aandoeningen.

DANKWOORD

Mijn promotietraject was een langdurig, leuk en leerzaam proces. Ik ben blij en trots dat er nu, na 8.5 jaar, definitief een einde aan gaat komen. Dit dankwoord is het laatste wat ik schrijf en waarschijnlijk het eerste wat vele lezen. Bij deze wil ik dan ook iedereen bedanken die direct of indirect betrokken is geweest bij de totstandkoming van dit proefschrift.

Op de eerste plaats wil ik graag mijn promotor en co-promotor bedanken. Prof. Meijer, beste Joke, bedankt voor de steun en het vertrouwen dat je me gaf om vaak zelfstandig te werk te gaan. Je enthousiasme over de wetenschap is inspirerend en aanstekelijk. Dr. Michel, beste Stephan, ik heb jouw wetenschappelijke brein altijd bewonderd. Ik zal onze urenlange sessies missen waarin jouw stromen aan nieuwe ideeën voorbij kwamen en het aan mij de taak was om eruit te halen wat praktisch haalbaar was. Ook de mogelijkheid om altijd aan te kunnen kloppen met vragen en/of problemen, zowel uit het lab als privé, heb ik de afgelopen jaren zeer gewaardeerd. Dank daarvoor.

Dan wil ik iedereen bedanken die het werken op het lab aangenamer heeft gemaakt. Dat zijn mijn vele (oud) collega's en studenten van de neurofysiologie groep, door de jaren heen teveel om hier allemaal op te noemen, maar toch wil ik in het bijzonder Renate, Mayke, Ashna, Laura, Jos, Tom, Hester, Michel, Claudia en Robin benoemen. Bedankt voor alle samenwerkingen en de jaren vol gezelligheid in Leiden.

Dank ook aan alle mensen die indirect mijn tijd in de wetenschap leuker hebben gemaakt. Sporten is zo belangrijk voor een goede (mentale) gezondheid en was voor mij een noodzaak om dit project tot een goed einde te brengen. Beste Herculanen en lieve teamgenootjes, wat is het fijn om wekelijks met jullie te badmintonnen en wedstrijden te spelen. Samen sporten is een heerlijke uitlaatklep, maar onze derde helft is minstens net zo fijn. En wat ben ik blij dat ik nu eindelijk ook aan de belachelijk hoge standaard van het eerste team voldoe, met een PhD op zak doe ik niet meer onder voor de rest.

Lieve Neurobuddies, wat ontzettend leuk dat we elkaar hebben gevonden tijdens de master. Jullie cognitieve dissonantietheorie, positieve kijk op alles en ongekend enthousiasme hebben me er doorheen geholpen. Bedankt voor alle briljante en epische uitjes, lunches, dinertjes en weekendjes weg.

Lieve Lijn, ik hoop dat je weet hoeveel ik onze vriendschap waardeer. Bedankt dat ik al 22 jaar alle lief en leed met je mag delen.

Dan Sietske en Michelle, dierbare vriendinnen, bedankt dat jullie mijn paranimfen willen zijn. Ik heb jullie bewonderd tijdens jullie eigen promotietrajecten en ben trots dat jullie nu mij willen bijstaan. Jullie zijn voor mij voorbeelden in hoe je je knap staande kunt houden binnen de wetenschapswereld.

Dan was er nog alle steun van mijn grote (schoon) familie. Lieve Kees, Mieke en Kim, ondanks dat we veel genen delen, zijn we toch allemaal iets anders gaan doen. Bedankt voor al jullie dappere pogingen om mijn onderzoek te begrijpen. Speciale dank aan Rudolf (en ook Sanneke). Jullie stonden me bij in de moeilijke, laatste fase van dit traject en hebben me geholpen het mogelijk te maken dat ik dit proefschrift tot een goed einde kon brengen. Lieve pap en mam, bedankt voor jullie onvoorwaardelijke steun en vertrouwen, en mijn onbezorgde school- en studietijd. Het 'altijd zelf blijven nadenken' en 'zeggen wat je denkt' hebben me veel gebracht in dit promotietraject.

Lieve Ruben, je bent mijn grote voorbeeld. Ik ken niemand die zoveel discipline heeft om thuis te werken, zichzelf leert programmeren en ook nog eens het geduld heeft om mij te helpen met statistiek. Zonder dat je het misschien zelf doorhad heb je me enorm geïnspireerd. Bedankt dat je er altijd voor me bent, zonder jou was dit proefschrift er nooit geweest.

Tot slot, lieve Sven en Lise, toen ik aan dit proces begon waren jullie er nog niet. Sven, jij kwam tijdens mijn tijd als promovendus, en Lise, jij in de jaren daarna waarin ik dit proefschrift af probeerde te maken. Die combinatie was niet altijd makkelijk, maar ik had het nooit anders gewild. Jullie altijd opgewekte gezichtjes en vrolijke babbels zorgden ervoor dat ik beter kon relativeren en efficiënter ging werken. Dit proefschrift is er alleen maar beter van geworden.

LIST OF PUBLICATIONS

Olde Engberink, A.H.O., Huisman, J., Rohling, J.H., Michel, S.H.*, Meijer, J.H.*. (2020) Brief light exposure at dawn and dusk can encode day length in the neuronal network of the mammalian circadian pacemaker. *FASEB*, 34(10), 13685-13695.

Buijink, M.R.*, **Olde Engberink, A.H.O.***, Wit, C.B., Meijer, J.H., Rohling, J.H., Michel, S. (2020) Aging affects the capacity of photoperiodic adaptation downstream from the central molecular clock. *J Biol Rhythms*, 35(2), 167-179.

Olde Engberink, A.H.O., Meijer, J.H. & Michel, S. (2018) Chloride cotransporter KCC2 is essential for GABAergic inhibition in the SCN. *Neuropharmacology*, 138, 80-86.

Olde Engberink, A.H.O., Hernandez, R., de Graan, P., Gruol, D.L. (2017) Rapamycin-sensitive late-LTP is enhanced in the hippocampus of IL-6 transgenic mice. *Neuroscience*, 367, 200-210.

Buijink, M.R., Almog, A., Wit, C.B., Roethler, O., **Olde Engberink, A.H.O.**, Meijer, J.H., Garlaschelli, D., Rohling, J.H., Michel, S. (2016) Evidence for weakened intercellular coupling in the mammalian circadian clock under long photoperiod. *PLoS One*, 11, e0168954.

Jongbloets, B.C., van Gassen, K.L.I., Kan, A.A., **Olde Engberink, A.H.O.**, de Wit, M., Wolterink-Donselaar, I.G., Groot Koerkamp, M.J.A., van Nieuwenhuizen, O., Holstege, F.C.P., De Graan, P.N.E. (2015) Expression profiling after prolonged experimental febrile seizures in mice suggests structural remodeling in the hippocampus. *PLoS One*, 10, e0145247.

Nelson, T.E., **Olde Engberink, A.H.O.**, Hernandez, R., Puro, A., Huitron-Resendiz, S., Hao, C., De Graan, P.N., Gruol, D.L. (2012) Altered synaptic transmission in the hippocampus of transgenic mice with enhanced central nervous systems expression of interleukin-6. *Brain. Behav. Immun.*, 26, 959-971.

CURRICULUM VITAE

Anneke Hermina Octavia Olde Engberink werd geboren op 5 oktober 1986 in Eindhoven. In 2005 behaalde zij haar VWO diploma met de profielen 'Natuur & Gezondheid' en 'Natuur & Techniek' aan het Were Di College te Valkenswaard. In datzelfde jaar startte zij met de studie Biomedische Wetenschappen aan de Universiteit Utrecht, waarvan zij in 2009 het Bachelor of Science diploma haalde. Vervolgens werd Anneke toegelaten tot de researchmaster Neuroscience and Cognition, track Experimental and Clinical Neuroscience, ook aan de UU. Het eerste jaar van de master heeft zij 10 maanden stage gelopen in de onderzoeksgroep van Pierre de Graan. Hier heeft zij de invloeden van koortsstuipen op de ontwikkeling van temporaalkwabepilepsie op latere leeftijd bestudeerd in muizen. Haar tweede onderzoeksstage voerde zij uit in San Diego, in het lab van Donna Gruol. Gedurende 6 maanden heeft zij onderzoek gedaan naar de effecten van een immuun factor op LTP in hippocampus plakjes en deze stage afgesloten met een perfecte score. In september 2011 behaalde zij haar Master of Science diploma.

Na een jaar gewerkt te hebben bij het Nationaal Vergiftigingen Informatie Centrum, startte zij haar promotieonderzoek bij de sectie Neurofysiologie in het Leids Universitair Medisch Centrum onder supervisie van Prof. Dr. J.H. Meijer en Dr. S. Michel. Haar onderzoek richtte zich op de invloed van licht en ouderdom op het neuronale netwerk van de centrale biologische klok. Hierbij lag de focus op de rol van de neurotransmitter GABA en de GABAerge excitatie/inhibitie balans in netwerk plasticiteit. De resultaten van dat onderzoek zijn beschreven in dit proefschrift. Na haar tijd als promovendus heeft zij nog een paar jaar doorgewerkt als Postdoctoraal onderzoeker in dezelfde onderzoeksgroep.

Momenteel werkt Anneke in het onderzoeksveld van dementie als Adviseur Wetenschappelijk Onderzoek bij Alzheimer Nederland.

